ROLES OF miRNAs DURING EARLY ZEBRAFISH DEVELOPMENT

By

Chunyao Wei

Dissertation

Submitted to the Faculty of the

Graduate School of Vanderbilt University

In partial fulfillment of the requirements

For the degree of

DOCTOR OF PHILOSOPHY

In

Biological Sciences

August, 2013

Nashville, Tennessee

Approved:

Wenbiao Chen, PhD

James G. Patton, PhD

Antonis Rokas, PhD

Charles K Singleton, PhD

Lilianna Solnica-Krezel, PhD

ACKNOWLEDGEMENTS

During my graduate studies, I received instructions and assistance from a lot of wonderful people. First of all, I want to thank my mentor, Dr. James Patton, for introducing me into the noncoding RNA world and allowing me to participate in several projects I really enjoyed. He is a great mentor and I feel very lucky being his student during my graduate trainings. All the people he recruited into the Patton Lab are very smart, nice and collaborative, and I am very grateful for the opportunity to learn from such talented individuals. Specifically, I want to thank Dr. Elizabeth Thatcher and Dr. Nan Li, who have never hesitated to offer their help to me since the first day when I entered the Patton Lab as a rotation student. Being with them, I was truly motivated and inspired to devote myself into research careers. I also want to thank the fish community and program of developmental biology that consistently assist me in data analysis and Stevenson Center fish facility that maintains and feeds my fish.

I thank my thesis committee members, Dr. Wenbiao Chen, Dr. Antonis Rokas, Dr. Charles Singleton and Dr. Lilianna Solnica-Krezel for their exceptional support and valuable suggestions in all the research I have been working on. I really appreciate the time they spent meeting with me every year to give me professional instructions from the perspectives of their expertise and the way they trained me to be a best scientist I could ever be.

I want to thank my parents, who never stop caring me in every aspect of my life. They always respect and understand my choice throughout my studies and encourage me to pursue the goal for the final success.

There are also many friends in Department of Biological Sciences and in Nashville Chinese Community who helped me in the last 6 years. I'd like to thank Rosalind Johnson and Leslie Maxwell, the former and current graduate program coordinator respectively, for their assistance in processing my course registration and financial support. Among all my Chinese friends in Nashville, I would like to specifically thank Dr. Zhaoying Han for giving me a lot of support and help in my everyday life when I first moved to Nashville for my graduate studies, and Ms. Heng Dai and Ms. Xuan Huang for being very supportive in the last 3 months and always bringing happiness and confidence into my heart on those very hard days.

This work reported below was mainly supported by NIH grant GM075790 and EY019759 to JGP and a Discovery Grant from Vanderbilt University.

5/24/2013

TABLE OF CONTENTS

LIST OF FIGURES

LIST OF ABBREVIATIONS

AChR……...……..…..…Acetylcholine Receptor

AGO……...……...…..…..…Argonaute

BrdU……...……. 5-bromo-2'-deoxyuridine

BoNT A..…….……...…..…..….Botulinum Neurotoxin protease type A

cDNA…….…..…complementary DNA

CNC cells…….…Craniofacial Neural Crest cells

CNS……..……...…..…..…Central Nervous System

DCV……....…..…..…Dense Core Vesicle

Dpf…….…..…..Days post fertilization

dsRNA……...…..…..……Double Strand RNA

ECM…….Extracellular Matrix

ELISA……..……Enzyme-Linked Immuno-Sorbent Assay

ESCC miRNA…….……...…..…..…ES cell-specific cell cycle-regulating miRNA

ES cells……..…Embryonic Stem cells

FACS……..……Fluorescence-Activated Cell Sorting

GFP……....….Green Fluorescent Protein

Hpf……...……Hours post fertilization

iPS cells……..……..……induced Pluripotent Stem cells

mES cells……...…Mouse Embryonic Stem cells

MO……..Morpholino

miRNA……..…microRNA

MMP……...…….Matrix Metalloproteinase

MRE...……...……miRNA Recognition Elements

MZT……..…..…….Maternal-Zygotic Transition

NMJ…….....….…..…Neuromuscular Junction

NIC……...…….……Non-Injected Control

PGCs……...…….....…Primordial Germ Cells

piRNA……...….Piwi interacting RNA

PTGS……...…Post Transcriptional Gene Silencing

PTK2.2…….……Protein Tyrosine Kinase 2.2

RISC……..……..…RNA Induced Silencing Complex

RNAi……RNA interfering

RPKM……..……Reads Per Kilobase per Million

siRNA……...…….small interfering RNA

SNAP-25……..Synaptosomal Associated Protein 25KDa

SNARE……..……Soluble N-ethylmaleimide-sensitive factor attachment protein receptor

ssRNA……..……single strand RNA

SV…….……..……Synaptic Vesicle

TMM value……...…..…Trimmed Mean of M value

tRF…….……tRNA-derived Fragments

TUNEL…….……..……Terminal deoxynucleotidyl transferase dUTP Nick End Labeling

UTR……...……Untranslated Region

CHAPTER 1:

Introduction

In 1993, the first microRNA (miRNA) *lin-4* was discovered as a gene regulator in *C. elegans* from a series of forward genetic screens (Lee et al., 1993). Later on, a second miRNA *let-7* that is highly conserved among species was identified in *C. elegans*, raising the possibility that small non-coding RNAs may regulate global gene expression in diverse organisms (Pasquinelli et al., 2000; Reinhart et al., 2000). These discoveries thrust miRNAs into the limelight and opened a new window for people to interpret the functional importance of non-coding portions of the genome. In the past 10 years, multiple studies have been dedicated to identifying more miRNAs in genome-wide transcriptome analyses and characterizing miRNA functions in multiple biological processes impacting development, disease and metabolism. So far, several hundred miRNAs are encoded in the genomes of vertebrates and more than 2200 mature miRNAs have been identified in the human genome. miRNAs are emerging as important regulators at almost every level of gene expression.

miRNAs are small non-coding RNAs that regulate gene expression at the post-transcriptional level. By specific binding to recognition elements in the 3' untranslated regions (UTRs) of target mRNAs, miRNAs inhibit gene expression in a sequence-dependent manner via destabilizing target mRNAs and/or blocking translation. miRNAs recognize 3'UTR binding sites based on imperfect base-pairing, therefore it is very challenging to directly predict miRNA target genes based on computational analyses alone. Some rules have been developed but constant refinement of these prediction

algorithms is needed. It is generally accepted that although miRNAs in animals recognize transcripts through imperfect base-pairing to their target mRNAs, nucleotides 2-7 at the 5'end of the miRNA, a region termed the 'seed region', usually pair with high complementarity, often perfect pairing (although with many exceptions) (Bartel, 2009). Computational analyses as well as experimental evidence suggest that each miRNA regulates more than one target and each target can be regulated by multiple miRNAs, suggesting that a large portion of the transcriptome is subject to miRNA regulation. In fact, computational evaluation predicted that over one third of human genes are regulated by miRNAs (Lewis et al., 2005; Lewis et al., 2003).

In vertebrate embryonic development, miRNAs coordinately interact with many target transcripts to fine-tune overall gene expression. In order to understand miRNA expression and function, I first characterized the temporal expression of all miRNAs during very early zebrafish embryonic development using high-throughput sequencing and identified 8 novel miRNAs. I also identified an unexpected abundance of piRNAs during early development. To analyze specific targets and understand the rationale for miRNA regulation, I focused on mRNA targets for *miR-153* and *miR-27*. I show that *miR-153* regulates *snap25* during synaptic transmission and motor neuron development. In addition, I also show that *miR-27* targets *ptk2.2* to regulate pharyngeal arch morphogenesis.

miRNA Biogenesis

In vertebrate genomes, approximately 50% of miRNAs are located close to other miRNAs, often transcribed as polycistronic RNAs. Some miRNA genes localize to

regions of the genome distinct from annotated genes, indicating that they are expressed as their own transcription units (Corcoran et al., 2009; Kim and Nam, 2006; Rodriguez et al., 2004). In contrast, other miRNAs (70% in mammalian genomes, but less than 15% in zebrafish) are encoded in the introns of other genes (Kim and Nam, 2006; Rodriguez et al., 2004; Thatcher et al., 2008), indicating that they share the same transcription regulation as their host genes, though some recent data has suggested the possibility of independent transcription for some intronic miRNAs (Corcoran et al., 2009; Thatcher et al., 2008). The remaining miRNAs overlap with the exons of either non-coding RNAs or protein coding RNAs (Kim, 2005; Kim and Nam, 2006; Rodriguez et al., 2004).

As discussed above, most vertebrate miRNAs are transcribed by RNA polymerase II as long primary transcripts called pri-miRNAs, either as independent genes or from the intron/exon of a protein-coding gene. The initial long RNA primary transcripts (pri-miRNAs) contain one or several clustered miRNA coding sequences that form characteristic stem-loop structures with bulges in the stem area (Cai et al., 2004; Kim and Nam, 2006; Lagos-Quintana et al., 2003; Lee et al., 2004). In the nucleus, pri-miRNA transcripts are cleaved at the base of the stem-loop to release hairpin structured precursor miRNAs (pre-miRNAs) by the Microprocessor Complex consisting of the RNase III-like enzyme Drosha and its cofactor DGCR8 (Denli et al., 2004; Gregory et al., 2004; Han et al., 2004; Lee et al., 2003). After cleavage, pre-miRNAs are transported by Exportin-5 into the cytoplasm (Lund, 2004; Yi et al., 2003), where the loop regions are further processed by another RNase III-like enzyme Dicer and its cofactor TRBP or PACT to generate an imperfect small RNA duplex of approximately 22nt (Bernstein et al., 2001; Hammond, 2000; Hutvagner et al., 2001; Ketting, 2001; Knight, 2001). After cleavage,

one strand of the duplex is incorporated into the RNA-Induced Silencing Complex (RISC) to serve as a mature, active miRNA (Khvorova et al., 2003; Schwarz, 2003). The other strand (called the passenger strand or miRNA*) is either quickly degraded or can sometimes be loaded into the RISC as a functional miRNA (Rand et al., 2005; Shin, 2008). Mature miRNAs guide the RISC to specific mRNA targets, where AGO and GW182 protein families collaborate to mediate mRNA repression or mRNA destabilization (Braun et al., 2011; Chekulaeva et al., 2011; Fabian et al., 2011; Hutvagner and Simard, 2008; Lian et al., 2009; Miyoshi et al., 2005; Rivas et al., 2005; Takimoto et al., 2009; Yao et al., 2011). An overview of miRNA biogenesis is shown in Figure 1.

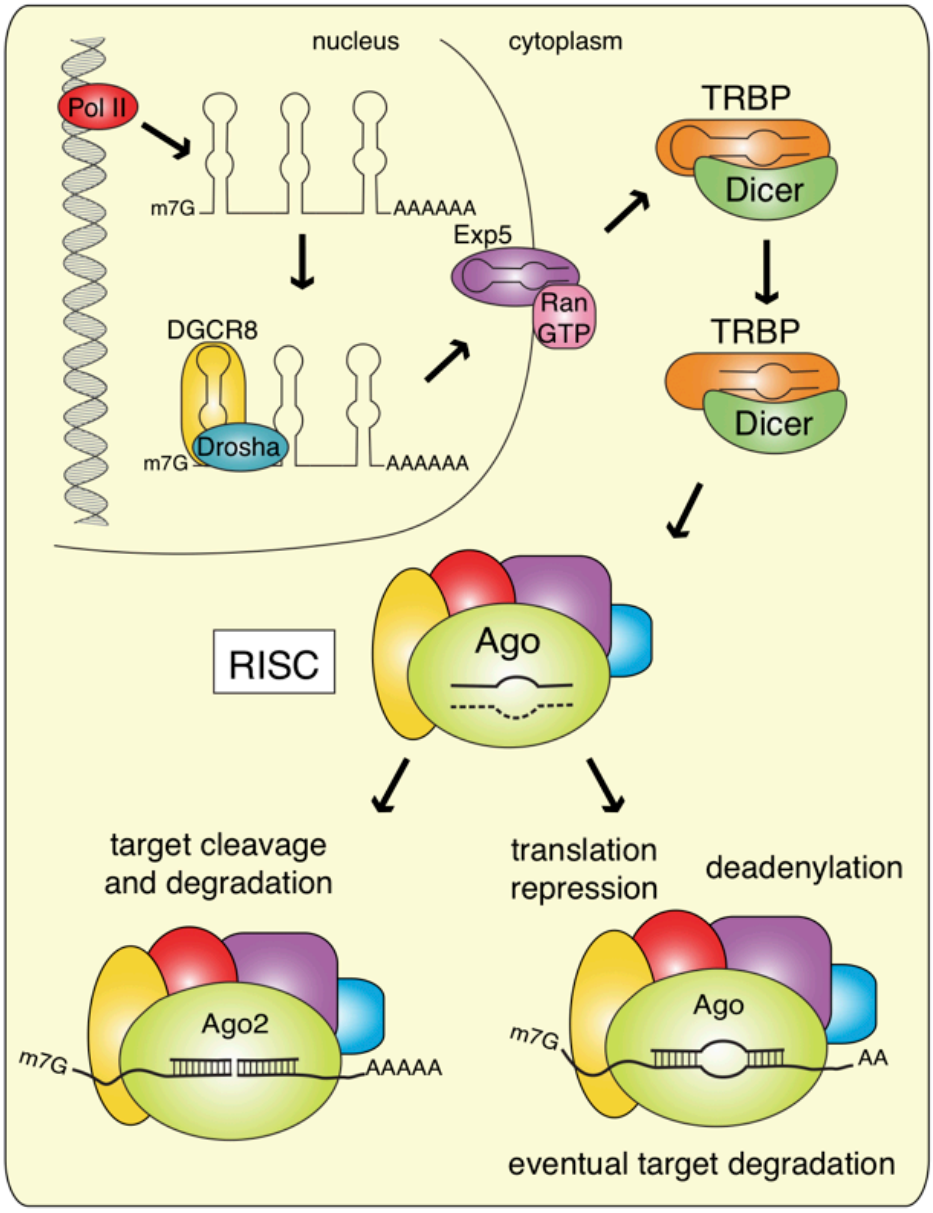

Figure 1. miRNA biogenesis pathway.
miRNA biogenesis begins with transcription by RNA polymerase II to generate pri-miRNAs. Hairpin structures are then excised by the Drosha-DGCR8 complex and pre-miRNAs are transported into cytoplasm by Exportin5 in a Ran-GTP dependent process. Dicer recognizes and further processes the precursors by cleaving the loop sequences, generating small RNA duplexes that are incorporated into RISC complexes. In RISC, one or both strands are selected as mature miRNAs and guide RISC to target 3' UTRs of target mRNAs. miRNAs bind their targets with either perfect complementarity, followed by mRNA cleavage, or partial complementarity, followed by translation repression with subsequent degradation. Figure by Abby Olena.

miRNA expression analysis using high throughput sequencing

High-throughput sequencing (also called Deep-sequencing or Next-generation sequencing) is a newly developed technology that uses massively parallel sequencing reactions to produce millions of short reads from libraries derived from small RNA or DNA fragments. Initial deep-sequencing used "454 sequencing" with *emulsion* PCR or "Illumina sequencing" using *bridge* PCR (Bentley et al., 2008; Wheeler et al., 2008), but, to date, new sequencing platforms have been developed such as SOLiD (ABI). Illumina sequencing technology developed rapidly leading to much higher coverage and a term switch from "deep" to "ultra-deep" (Ajay et al., 2011). For Illumina sequencing, small DNA molecules (converted from RNAs or directly from Genomic DNA) are physically bound to a flow cell and sequenced in parallel via "sequencing by synthesis". DNA polymerase is used to determine the sequence base by base with the addition of reversible versions of dye-terminators. One nucleotide is added at a time followed by the detection of fluorescent signals at each specific position in real time. With repeated removal of blocking groups on the first base, the next base is then detected in a similar manner (Bentley et al., 2008). To overcome possible bias and artifacts introduced during RNA conversion into cDNA (Landgraf et al., 2007), single molecule direct RNA sequencing technology is under development by Helicos.

When successful, high throughput sequencing results in the generation of huge data sets containing several hundred million short reads per sample. Compared with microarray-based gene expression analyses, high throughput sequencing is able to measure absolute abundance of RNA species without suffering from potential background and cross-hybridization issues (Harbers and Carninci, 2005; Irizarry et al.,

2005). High throughput sequencing provides a major advance in robustness, comparability, and richness of expression profiling data (Mooney et al., 2013; t Hoen et al., 2008). At present, the utilization of high-throughput sequencing technologies has revolutionized our ability to dissect transcriptomes, even for RNAs expressed at extremely low levels.

This technology is ideal for the discovery of miRNAs since the sequences are small and reads can encompass the entire sequence (Bar et al., 2008; Soares et al., 2009; Sunkar et al., 2008). High throughput sequencing allows verification of the existence of all small miRNA transcripts, the ability to discover new miRNAs, and the ability to quantitatively analyze precise levels of all miRNAs. To date, high throughput sequencing has been applied to the analyses of miRNA expression in various systems (Berezikov et al., 2011; Chiang et al., 2010; Friedlander et al., 2009; Ladewig et al., 2012; Landgraf et al., 2007; Ruby et al., 2007; Wang et al., 2011; Wei et al., 2012). At the same time, deep-sequencing technologies have also allowed a sharp rise in the rate of novel miRNA discovery (Kozomara and Griffiths-Jones, 2011). In addition to miRNAs, a number of small non-coding RNAs have been identified in studies using high throughput sequencing including piwi-interacting RNAs (piRNAs), transcription initiation RNAs (tiRNAs) and tRNAs-derived small RNAs (tRF) (Aravin et al., 2006; Girard et al., 2006; Lee et al., 2009; Taft et al., 2009).

miRNA 3' termini sequence heterogeneity

Accumulating evidence from deep-sequencing analysis of miRNAs demonstrated that in plants and animals, miRNAs exhibit post-transcriptionally modified heterogeneous

3’ ends, typically by the addition of non-genomic-template uridines or adenines (Ameres et al., 2010; Berezikov et al., 2011; Burroughs et al., 2010; Fernandez-Valverde et al., 2010; Kamminga et al., 2010; Landgraf et al., 2007; Lehrbach et al., 2009; Morin et al., 2008; Wyman et al., 2011). An example of *miR-203b* sequence heterogeneity is shown in Figure 2. Although the affect of these tailed nucleotides on miRNA function is largely unknown, existing evidence supports the idea that extra non-template uridines at the miRNA 3’ termini can regulate their half-life by promoting degradation. Many of the miRNAs that have been shown to contain extra 3' uridines have these nucleotides added to 3’ arm of the precursor miRNA, implying that addition of uridines may occur before Dicer cleavage. Supporting this hypothesis is *let-7* whose degradation before Dicer processing is triggered by 3’end polyuridylation mediated by TUT4 in mammalian cells (Heo et al., 2009). Thus, detection of mature transcripts containing non-template addition of uridines at the 3’ termini could be interpreted as the products of surviving precursors whose uridine tail is not long enough to trigger degradation or those that are actively in the process of degradation (Burroughs et al., 2010). In mouse and humans, mature *miR-26a* derived from the 5’arm of precursor transcripts have also been reported to be degraded upon the addition of uridines at the 3’termini of the mature miRNAs, suggesting an underlying novel mechanism by which uridylation can also be applied after Dicer processing and directly to the mature miRNAs to promote degradation (Jones et al., 2009).

In contrast to uridine addition, the biological significance of adenine addition is still in debate. Studies of adenylated *miR-122* in human and mouse liver suggested that addition of A residues stabilizes miRNAs, similar to findings in plants (Ji and Chen,

2012; Katoh et al., 2009). However, analysis of deep-sequencing of miRNAs following knockdown of PAPD4, a nucleotidyltransferase enzyme that is thought to adenylate miRNAs and other noncoding RNAs (Martin and Keller, 2007), showed that adenylation did not appear to affect miRNA stability. Instead, adenine addition appeared to reduce the effectiveness of miRNA targeting, possibly through interfering with incorporation into RISC, a regulatory role that would complement the role of miRNA uridylation in blocking DICER processing (Burroughs et al., 2010). Further work is needed to determine the effects of adenine and uridine addition on the stability of individual miRNAs.

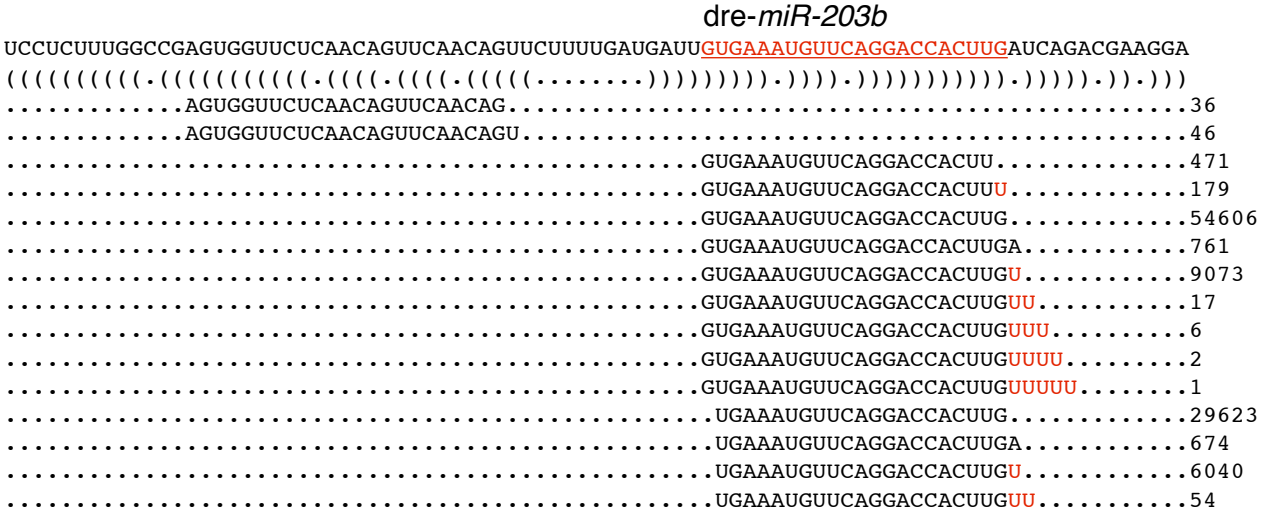

Figure 2. 3' terminal sequence heterogeneity of *miR-203b*.
The *miR-203b* precursor sequence is shown on the top, with mature *miR-203b* labeled in red and underlined. The sequences of mature *miR-203b* reads and its star strand reads at 1 dpf embryos are aligned below, with corresponding abundance presented on the right. The additions of non-genomic template uridines are labeled in red.

microRNAs in vertebrate embryonic development

Overall effects of miRNAs on embryonic development

Given the fact that most miRNAs are produced in the same biogenesis pathway, mutants in this pathway have provided a unique opportunity to study the general influence of miRNA function during embryonic development. Since Dicer is the exclusive step required for processing pre-miRNAs into mature miRNAs, abolition of Dicer function blocks the production of all miRNAs. In zebrafish, maternal-zygotic *dicer* mutants (MZ*dicer* mutants) die early in development but remarkably display intact axis formation and mostly correct early embryonic patterning. However, These animals subsequently undergo abnormal morphogenesis during neural development and organogenesis. Defects in MZ*dicer* mutants led to the identification of a large microRNA family: the *miR-430* family which is highly expressed during early zebrafish development. Most of the defects in MZ*dicer* mutant fish can be rescued simply by expression of *miR-430* (Giraldez et al., 2005b).

In mice, loss of Dicer leads to lethality during early embryogenesis. Dicer-null mutant embryos die prior to embryonic day (E) 7.5, possibly due to the failure to maintain stem cell populations, as indicated by the strongly reduced expression of Oct4, a key regulator of embryonic stem cell maintenance and proliferation (Bernstein, 2003). Considering that Dicer processes both endogenous small interfering RNAs (endo-siRNAs) and miRNAs, the phenotypes observed in Dicer-deficient mice may result in part from the functional absence not only of miRNAs, but also endo-siRNAs. In the canonical biogenesis pathway, the generation of miRNAs, but not siRNAs, specifically requires DGCR8, an RNA-binding protein that assists Drosha in producing pre-miRNAs

(Han et al., 2004; Han et al., 2006; Landthaler et al., 2004; Tomari and Zamore, 2005). Similar to Dicer mutants, zygotic Dgcr8 knockout embryos arrest early in development (prior to E6.5), although both zygotic and maternal-zygotic Dgcr8 knockout embryos develop through the blastocyst stage with normal-appearance (Suh et al., 2010). Dgcr8 knockout embryonic stem cells (ES cells) fail to efficiently turn off the stem cell program upon the introduction of differentiation, although some differentiation markers are still expressed (Wang et al., 2007).

Unlike ES cells, however, Dgcr8 knockout oocytes develop normally and their mRNAs profiles are surprisingly almost identical to that of wild-type oocytes (Ma et al., 2010; Suh et al., 2010). In sharp contrast, Dicer mutant oocytes show severe defects in oocyte maturation with hundreds of misregulated mRNAs (Murchison et al., 2007; Tang et al., 2007). These findings, together with the known functions of endo-siRNAs (Babiarz et al., 2008), suggest that endo-siRNAs, but not miRNAs are essential for oocyte maturation in mice. Both, however, are required for normal progression during mouse embryonic development.

miRNAs during the maternal-zygotic transition (MZT)

After fertilization, embryos undergo rapid and largely synchronous cell cycles during early development (O'Farrell et al., 2004). At the very beginning, the overall amount of cytoplasm in the embryo remains relatively constant while the number of nuclei and the amount of DNA increase exponentially. During this period, mRNAs and proteins provided by the mother drive development, the embryonic genome is thought to be transcriptionally silent until later stages (Kane and Kimmel, 1993; Newport and

Kirschner, 1982). Activation of zygotic transcription coincides with the elimination of many maternal mRNAs. The transition from a maternal to a zygotic expression profile in development is called the midblastula or maternal-zygotic transition (MZT) (Schier, 2007). Although the expression of many miRNAs can be detected before the MZT, the earliest stage when miRNAs are thought to function is during the MZT (Wei et al., 2012). In zebrafish, the *miR-430* cluster starts to be expressed at 2.5 hours post fertilization (hpf) with mature forms detectable around 4 hpf (Giraldez et al., 2006a). Gene expression microarray analyses performed in the presence or absence of *miR-430*, coupled to in silico identification of sequences complementary to the seed region of *miR-430,* suggested that more than 300 mRNAs are directly regulated by *miR-430* during early zebrafish development. These mRNAs, whose target sites, interestingly, are not generally conserved in orthologous genes of two other teleosts, were further investigated for their common features and it was discovered that a large portion of these target mRNAs are deposited at high levels into embryos before fertilization. They remain at high levels before zygotic transcription but are rapidly downregulated thereafter. In addition, the predicted *miR-430* target sites were also significantly enriched in a large number of maternal mRNAs (Giraldez et al., 2006a). Taken together, these results suggested that *miR-430* directly targets and clears many maternal mRNAs in zebrafish embryos during the MZT (Figure 3).

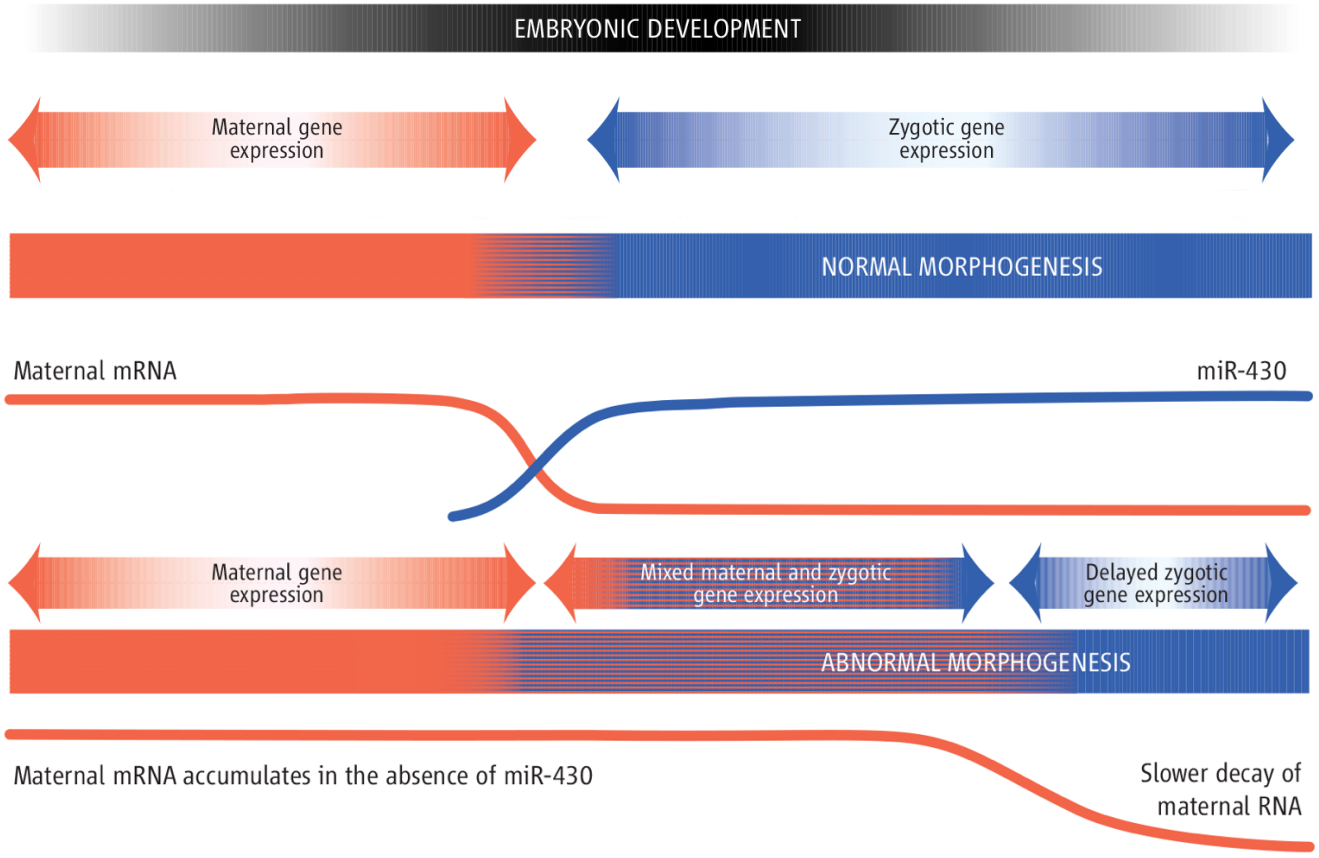

Figure 3. *miR-430* mediates maternal mRNA clearance during embryonic development.
In early zebrafish embryogenesis, *miR-430* regulates the transition from maternal to zygotic transcription and normal morphogenesis by targeting many maternal mRNAs for degradation. In the absence of *miR-430*, maternal mRNAs accumulate and zygotic genome activation are delayed, therefore interfering with morphogenesis. (Adapted from Cohen *et al*., *Science* (2006))

miRNAs and ES Cells

miRNAs and embryonic stem cell self-renewal

The necessity of miRNAs in ES cells has been clearly demonstrated by the phenotypes of DGCR8 null ES cells, where the deletion of DGCR8 depletes most active miRNAs (Wang et al., 2007). Unlike Dicer deficient ES cells, which show a complete proliferation block, DGCR8-null ES cells do not show a complete initial proliferation block but fail to efficiently differentiate and display altered cell cycle properties. Upon the depletion of both Dgcr8 alleles, ES cells accumulate in G1, suggesting a defect in the transition from G1 to S (Wang et al., 2007). Reintroduction of individual miRNAs in the background of Dgcr8 knockout ES cells resulted in the identification of 14 miRNAs that are able to markedly rescue proliferation defects. These miRNAs share similar seed sequences and function redundantly at saturating levels. Two large miRNA clusters (*miR-290* and *miR-302*) are highly expressed in undifferentiated ES cells and directly target *Cdkn1a* (also known as *p21*), *Rbl2* and *Lats2*, all of which are inhibitors of cyclinE-Cdk2 complexes that regulate the G1-S transition in ES cells. Cells overexpressing *Cdkn1a* showed an increased G1 fraction very similar to that seen in Dgcr8 knockout cells, consistent with miRNA dependent regulation of the cell cycle. These ES cell-specific miRNAs promote ES cell proliferation, and are therefore called ES cell-specific cell cycle-regulating miRNAs (ESCC miRNAs) (Wang et al., 2008). Notably, overexpression of ESCC miRNAs clusters (*miR-302/367*) in mouse and human somatic cells can even cause de-differentiation and rapidly reprogram to an iPS cell state without a requirement for exogenous transcription factors (Anokye-Danso et al., 2011).

Several other miRNAs were also reported to regulate ES cell proliferation. *miR-*

106, an ESCC member, and *miR-372* target *Cdkn1a*; *miR-92b* targets *p57*, another inhibitor of G1/S progression, and *miR-195* has been shown to down-regulate WEE1, an inhibitory kinase of the G2 cyclin B-CdK complex. These results suggest that in ES cells, miRNAs function redundantly to regulate the cell cycle, leading to the establishment and maintenance of ES cell self-renewal.

miRNAs in embryonic stem cell differentiation

The switch of ES cells from a pluripotent state to lineage-specified differentiation is marked by efficient silencing of pluripotent marks and decreased cell proliferation, coinciding with activation of lineage-specific gene expression. The expression of many miRNAs is increased upon differentiation of human ES cells (Bar et al., 2008). In a condition that normally promotes differentiation, DGCR8 null ES cells, where most active miRNAs are depleted, fail to fully downregulate pluripotent genes and express limited lineage-specific genes (Wang et al., 2007). This reveals that besides regulating cell proliferation, miRNAs are also necessary for ES cell differentiation. Rbl2, a transcriptional repressor, was reported to be a direct target of the *miR-290* family. The repression of Rbl2 by *miR-290* family leads to increased levels of the DNA methyltransferases Dnmt3a and Dnmt3b, and consequently up-regulation of de novo DNA methylation, which is required for the silencing of pluripotency markers and differentiation (Benetti et al., 2008; Sinkkonen et al., 2008). During retinoic acid induced differentiation, mES cells up-regulate *miR-134*, *miR-296* and *miR-470* to coordinately down-regulate Nanog, Oct4 and Sox2, leading to transcriptional and morphological changes characteristic of differentiating mouse embryonic stem cells (Tay et al., 2008). Moreover, *miR-200c*, *miR-203* and *miR-183* also cooperate to suppress expression of

stem cell factors such as Sox2 and Klf4 in mouse embryonic stem cells (Wellner et al., 2009). Similarly, *miR-145* is repressed by OCT4 in hES cells but is highly expressed upon differentiation to target Oct4, Sox2 and Klf4, therefore repressing self-renewal and promoting the differentiation of the 3 germ layers (Xu et al., 2009). Thus, whereas most promoters of ES cells-specific miRNAs are occupied and controlled by the pluripotency factors Oct4, Sox2, Nanog and Tcf3 (Chen et al., 2008; Marson et al., 2008), these key factors are also inhibited at the posttranscriptional level by miRNAs that promote differentiation.

Another miRNA family that is broadly expressed across differentiated tissues is the *let-7* family. In mouse embryos, mature *let-7* miRNAs are not present in ES cells until differentiation starts, although primary *let-7* transcripts are produced in ES cells (Thomson et al., 2006; Wulczyn et al., 2007). These discoveries suggest the expression of *let-7* family is subject to precise regulation during the switch from pluripotency to differentiation. Indeed, introduction of *let-7* family miRNAs into DGCR8 null ES cells silenced self-renewal, but co-introduction of one ESCC miRNA member (*miR-294*) was able to counteract the inhibitory activity of *let-7*, indicating that the *let-7* and ESCC miRNAs have opposing roles in the maintenance of ESC self-renewal (Melton et al., 2010). It has been demonstrated that *let-7* shuts down mES cell self-renewal not only by directly targeting specific mRNAs, but also by negative effects on the transcription factors c-Myc and N-Myc, consequently down-regulating Myc-dependent mRNAs and miRNAs, such as the *miR-290* cluster, *miR-141*, *miR-200*, and *miR-429* (Chen et al., 2008; Lin et al., 2009; Melton et al., 2010). These genes are crucial for ES cell identity, including genes that that promote cell cycle progression and stem cell identity (Johnson et

al., 2007; Melton et al., 2010; Rybak et al., 2009). In particular, Lin28 and Sall4, two well-known pluripotency factors, contain *let-7* binding sites and are direct targets of *let-7*. Interestingly, these factors are also indirectly regulated in an opposite fashion by *miR-294*, showing that *let-7* and ESCC families antagonistically regulate many of the same target genes with roles in ES cell self-renewal (Melton et al., 2010).

miRNAs in Neurogenesis

Neurogenesis, a fundamental process for embryonic neurodevelopment, is initiated from neuroectoderm progenitor cells resulting in the formation of functional neurons. In vertebrates, the expression of many miRNAs is highly regulated in the nervous system and in individual neurons (Kapsimali et al., 2007), leading to speculation that miRNAs are key players during neural differentiation from ES cells and in the embryos. Gain- and loss-of function approaches delineated the roles for a variety of neural-specific miRNAs in vertebrates, including *miR-184*, *let-7*, *miR-137*, *miR-9*, *miR-124*, *miR-134*, *miR-133*, *miR-26b* and *miR-153* (Sun et al., 2013; Wei et al., 2013). Among these neural-specific miRNAs, *miR-9* and *miR-124* are the best characterized examples. These two miRNAs are expressed during differentiation of neural progenitor cells and highly enriched in the brain (Kapsimali et al., 2007; Wienholds et al., 2005a). They are thought to limit the expression of genes supporting progenitor self-renewal. *miR-9* directly targets TLX, a highly conserved orphan nuclear receptor that is critical for neural stem cell self-renewal. *miR-9* therefore promotes neuronal progenitor cell differentiation, and elaborate feedback loop exists whereby TLX also represses *miR-9* transcription (Zhao et al., 2009). Many other genes are also regulated by *miR-9* (e.g. NEFH, TLX, Foxg1, Gsh2, SIRT1 and REST/NRSF) to promote neuronal progenitor cell

differentiation (Conaco et al., 2006; Laneve et al., 2010; Packer et al., 2008; Saunders et al., 2010; Shibata et al., 2008). In addition, *miR-9* mediated inhibition of Foxp1 in the chick spinal cord and Map1b in mouse cortical neurons are also reported to establish motor neuron identity and axon length/branching, respectively (Dajas-Bailador et al., 2012; Otaegi et al., 2011).

miR-124 has been studied extensively in multiple organisms, with distinct expression patterns and functional activity in different species. Although *miR-124* is dispensable for neural differentiation in *Drosophila* (Sun et al., 2012; Weng and Cohen, 2012), it has been repeatedly shown in vertebrates to promote cell cycle exit and neuronal differentiation. Besides the CNS, *miR-124a* is also expressed in the eye, mostly in cells of the neural retina but not in the pigmented epithelium (RPE) (Deo et al., 2006). In the subventricular zone of mice, *miR-124* physiologically targets the transcription factor Dlx2, Notch ligand Jag1 and Sox9 (Scott et al., 2010), important regulators of neurogenesis, to maintain the proper progression from the subventricular zone stem cell lineage to neurons (Cheng et al., 2009). Many other targets of *miR-124* have been reported, such as BAF53a, SCP1, Ephrin-B1, and PTBP1 (Arvanitis et al., 2010; Cheng et al., 2009; Makeyev et al., 2007; Visvanathan et al., 2007; Yoo et al., 2009). These factors are involved in multiple biological processes related to neuronal development and repression of their expression is essential for the establishment of neuronal differentiation. Interestingly, during neuronal differentiation, *miR-124* and *miR-9** function synergistically to target *baf53a* in neural progenitors to allow BAF53b to be expressed in postmitotic neurons (Yoo et al., 2009). This facilitates the switch from neural progenitor-specific BAF complexs to neuron-specific BAF complexes (Lessard et al., 2007; Wu et al., 2007). In addition, *miR-124a*

also represses Lhx2 in mice to regulate hippocampal axonogenesis and retinal cone survival (Sanuki et al., 2011).

As key regulators of mitotic exit of neural progenitors and the onset of neuronal differentiation, *miR-124* and *miR-9/9**are regulated by the REST/NRSF protein complex (Akerblom et al., 2012; Conaco et al., 2006). In zebrafish, the REST/NRSF complex is also regulated by miRNAs. *miR-26b* directly targets CTDSP2, a phosphatase component of the REST/NRSF complex that activates genes required for neuronal cell differentiation in vivo (Dill et al., 2012). Intriguingly, *miR-26b* is encoded in an intron of the Ctdsp2 gene and *pre-miR-26b* is co-expressed with *ctdsp2* mRNAs. This intrinsic negative feedback loop is inactive in neural stem cells due to the inhibited biogenesis of mature *miR-26b*, but active during neurogenesis, where mature *miR-26b* is produced to down-regulate CTDSP2. Besides neuronal fate determination, an increasing number of miRNAs have been implicated in dendritic morphogenesis, axonal pathfinding, and synaptic development. For example, my work described in this thesis revealed that *miR-153* regulates SNAP25, a core component of the SNARE complex to regulate synaptic release at neuromuscular junctions as well to maintain proper axonal outgrowth and dendritic branching of motor neurons in zebrafish (Wei et al., 2013). *miR-134* is expressed in dendrites and synapses in rat hippocampal neurons and negatively regulates the size of dendritic spines—postsynaptic sites of excitatory synaptic transmission. This is consistent with a purported role in generating rapid and local responses in an activity dependent manner (Schratt et al., 2006).

miRNAs in craniofacial development

Molecular mechanisms governing the formation of different components of craniofacial complexes during zebrafish craniofacial development are conserved in higher vertebrates (Yelick and Schilling, 2002). Using lineage-tracing and fate map analysis in zebrafish and avians, it appears that craniofacial mesenchyme is derived from both migratory neural crest and paraxial mesoderm (Kontges and Lumsden, 1996; Schilling and Kimmel, 1994). The neurocranium is derived from both craniofacial neural crest (CNC) cells and mesoderm, while the pharyngeal skeleton originates solely from CNC cells (Yelick and Schilling, 2002). Currently, several miRNAs have been extensively studied for their roles in CNC cell proliferation and differentiation during pharyngeal cartilage formation (*miR-140, miR-92* and *miR-196*). Vertebrate *miR-140* resides in an intron of the Wwp2 gene and is co-transcribed with its host gene in chondrogenic cells where it is transcriptionally regulated by a master regulator of cartilage development, Sox9 (Eberhart et al., 2008; He et al., 2011a; Wienholds et al., 2005a). In CNC cells, Sox9 attenuates platelet-derived growth factor (Pdgf) signaling during palate development by directly inhibiting the PDGF receptor (Pdgfra), therefore diminishing PDGF-mediated attraction of CNC cells to ensure migration toward the oral ectoderm for appropriate palatogenesis (Eberhart et al., 2008). *miR-92a*, is highly enriched in chondrogenic progenitors and reported to positively regulate Bmp signaling to promote cell proliferation and differentiation during pharyngeal cartilage formation by targeting the Bmp antagonist *noggin3*. Dysregulation of *miR-92a* disrupts Bmp signaling resulting in a loss of all pharyngeal cartilage elements (Ning et al., 2013). In addition, perturbation of *miR-196*, a miRNA encoded in Hox clusters, was shown to affect the number of posterior branchial arches and the initiation of pectoral appendages (He et al., 2011b). Recently, *miR-27* has also been identified as a regulator of CNC cells at the post-

migration stage. The loss of this miRNA also abolished the formation of pharyngeal arches and the outgrowth of pectoral fins (see Chapter 4).

Consistent with discoveries in zebrafish, deletion of murine Dicer leads to a loss of CNC cell derived craniofacial bones due to CNC cell development arrest and massive apoptosis, suggesting that miRNAs are required for craniofacial organogenesis and pharyngeal arch morphogenesis (Nie et al., 2011; Zehir et al., 2010). For example, murine *miR-452* is enriched in neural crest cells and is necessary for the expression of Dlx2, a transcriptional regulator of pharyngeal arch development. By targeting Wnt5a in the first pharyngeal arch, *miR-452* regulates signaling networks involving Wnt, Shh and Fgf8, an epithelial-mesenchymal signaling cascade that converges on *Dlx2* expression (Sheehy et al., 2010).

miRNAs in cilia formation and left-right asymmetry

Cilia are microtubule-based organelles that are present on the surface of specialized cells in protozoa and metazoan. They generally function to propel fluid for movement (motile cilia) or sense extracellular signals (motile and immotile cilia), ranging from one cilium to several hundred per cell (Berbari et al., 2009; Fliegauf et al., 2007; Goetz and Anderson, 2010; Shah et al., 2009). Defects in cilia formation and function have been linked with a variety of human diseases, such as chronic airway disease, neurosensory impairment, and Bardet-Biedl syndrome (Fliegauf et al., 2007; Nigg and Raff, 2009). During embryogenesis, evidence gathered from both zebrafish and mouse embryos suggests a strong connection between proper left-right asymmetry and the flow-generating function of cilia (Amack et al., 2007; Amack and Yost, 2004; Kreiling et al.,

2008; Marszalek et al., 1999; Nonaka et al., 1998; Okada et al., 1999; Schneider et al., 2008; Supp et al., 1999; Takeda et al., 1999).

Recently, several lines of evidence suggest a novel mechanism of ciliogenesis and subsequent embryonic left-right asymmetry through miRNA-mediated post-transcriptional regulation. In cultured cells, *miR-129-3p*, a conserved vertebrate miRNA, was found to control cilia biogenesis by downregulating CP110 and repressing branched F-actin formation. Using DNA microarray-based methods, Cao *et al*. (2012) identified many cilia and actin dynamics-related targets of this miRNA including ARP2, TOCA1, ABLIM1 and ABLIM3 (Cao et al., 2012). Moreover, inhibition of *miR-129-3p* in zebrafish embryos suppressed cilia formation in Kupffer's vesicle and the pronephros, causing defective left-right asymmetry during organogenesis (Cao et al., 2012). Instead of directly regulating cilia formation, zebrafish *miR-92* targets the transcription factor GATA5 to regulate endoderm formation during embryogenesis, which in turn affects Kupffer's vesicle development and cilia length (Li et al., 2011). Overexpression or depletion of this *miR-92* causes cardia and viscera bifida or abnormal Kupffer's vesicles followed by left-right patterning defects in different organs, respectively (Li et al., 2011).

Another example of miRNA-mediated ciliogenesis is in human airway epithelium and *Xenopus laevis* embryonic epidermis, where *miR-449* is highly expressed in multiciliated cells to repress the Delta/Notch pathway. By directly inhibiting Notch1 and its ligand Delta-like1 (DLL1) in both systems, *miR-449* facilitates multiciliogenesis, unraveling a conserved mechanism by which Notch signaling undergos miRNA-mediated inhibition to allow ciliated cell progenitors to differentiate during embryonic development (Marcet et al., 2011).

siRNAs and piRNAs

Besides miRNAs, two other classes of small non-coding RNAs that play important roles in regulating gene expression are small interfering RNAs (siRNAs) and piwi-interacting RNAs (piRNAs). The term "siRNAs" is correlated with the discovery and application of RNA interference (RNAi) in post-transcriptional gene silencing (PTGS), which was first reported by Napoli and Jorgenesen in 1990 during a study in petunias (Napoli et al., 1990). Later the PTGS events of *par-1* were observed in *C. elegans* via the introduction of both sense and antisense RNAs (Guo and Kemphues, 1995). In 1998, Fire and Mello demonstrated that dsRNAs were much more efficient than ssRNAs in gene silencing in worms and suggested that silencing observed in earlier cases was due to dsRNA contamination. They named this phenomenon RNA interference (RNAi) (Fire, 1998). Subsequent studies in plants and the creation of an *in vitro Drosophila* system refined the RNAi mechanism and showed that silencing requires the production of 21-23 nucleotide species of dsRNAs (Hammond, 2000; Tuschl et al., 1999; Zamore et al., 2000). It is now known that these small RNAs are derived by cleavage with Dicer resulting in 2-nt overhangs at the 3'end of small RNA duplexes. For mammalian RNAi, long RNAs cannot be delivered to cells because of interferon responses but for worms and flies, long dsRNAs can be introduced that are then cleaved by Dicer into 21-23nt dsRNAs. When one of the strands pairs with an mRNA target, the mRNA is cleaved by the RISC component Argonaute2 (Ago2 or slicer) in the middle of the perfectly paired region (Ketting et al., 2001; Liu et al., 2004; Rand et al., 2005; Tabara et al., 1999; Tomari et al., 2004) (Matranga et al., 2005). Although the introduction of synthesized siRNA duplexes has been widely used for efficient knockdown of endogenous genes, endogenous siRNAs have also been identified in many

species that function to maintain proper gene expression patterns (Ghildiyal et al., 2008; Okamura and Lai, 2008; Ruby et al., 2006; Tam et al., 2008). Recently, siRNAs have also been reported to function in the nucleus of yeast and mammalian cells, mediating heterochromatin formation on the promoter sequences of their target genes, serving as a novel mechanism for targeted gene silencing (Castel and Martienssen, 2013; Gullerova et al., 2011; Gullerova and Proudfoot, 2012; Verdel et al., 2004).

In contrast to miRNAs, piRNAs (piwi-interacting RNAs) are slightly larger (25-31 nt) and were initially discovered to bind Piwi proteins—a subgroup of the Argonaute family of proteins in mammalian testes essential for gametogenesis (Aravin et al., 2006; Girard et al., 2006; Grivna et al., 2006; Lau et al., 2006). These small RNAs are produced from discrete genomic loci, generally spanning 50-100kb, and comprising mainly defective transposon sequences. Later studies in flies, zebrafish, and mouse indicated that piRNAs interact with potentially active, euchromatic transposons to form a defense system for transposon control and maintenance of genome integrity. Deletion of Piwi-family proteins in animals leads to derepression of transposable elements, germ cell apoptosis, and sterility (Aravin et al., 2007; Brennecke et al., 2007; Houwing et al., 2007; Vagin et al., 2006). The biogenesis of piRNAs was first determined in the *Drosophila* female germline by Greg Hannon's Group, later work showed a similar pathway is used in mouse and zebrafish. Briefly, piRNAs are generated from a reciprocal amplification loop in which primary piRNAs associate with Piwi proteins to direct cleavage of transposable element mRNAs (Aravin et al., 2007; Brennecke et al., 2007; Houwing et al., 2008). The initial cleavage products then serve to promote production of sense strand secondary piRNAs that in turn bind Ago3 to generate more primary piRNAs by pairing

with and directing cleavage of antisense RNAs derived from discrete repetitive genomic loci, referred to as piRNA clusters (Brennecke et al., 2007; Malone et al., 2009). This model of biogenesis is referred to as the Ping-Pong model because the production of piRNAs from one strand drives the generation of piRNAs from the other strand (Brennecke et al., 2007). An overview of piRNA biogenesis is shown in Figure 4.

Although originally identified as germline-specific, recent studies showed that piRNAs are also expressed in some somatic cells (ovarian follicle cells) in flies with a secondary biogenesis pathway independent of Ago3 (Lau et al., 2009; Li et al., 2009; Malone et al., 2009). In addition, deep sequencing of small RNAs in early zebrafish embryos also showed robust expression of piRNAs at the onset of gastrulation, when the germline is not fully differentiated, implying that piRNA expression may not be restricted to the germline and might have novel functions during embryogenesis (Wei et al., 2012). Consistent with this speculation, it was reported that piRNAs induce deadenylation and decay of *nanos*, a maternal mRNA in *Drosophila* embryos (Rouget et al., 2010). In *Aplysia*, piRNAs were surprisingly discovered in the brain, where they facilitate serotonin-dependent methylation of a conserved CpG island in the promoter of CREB2, the major inhibitory constraint of memory in *Aplysia*, leading to enhanced long-term synaptic facilitation. This reveals a novel role of piRNAs in the establishment of stable long-term changes in neurons for the persistence of memory (Rajasethupathy et al., 2012).

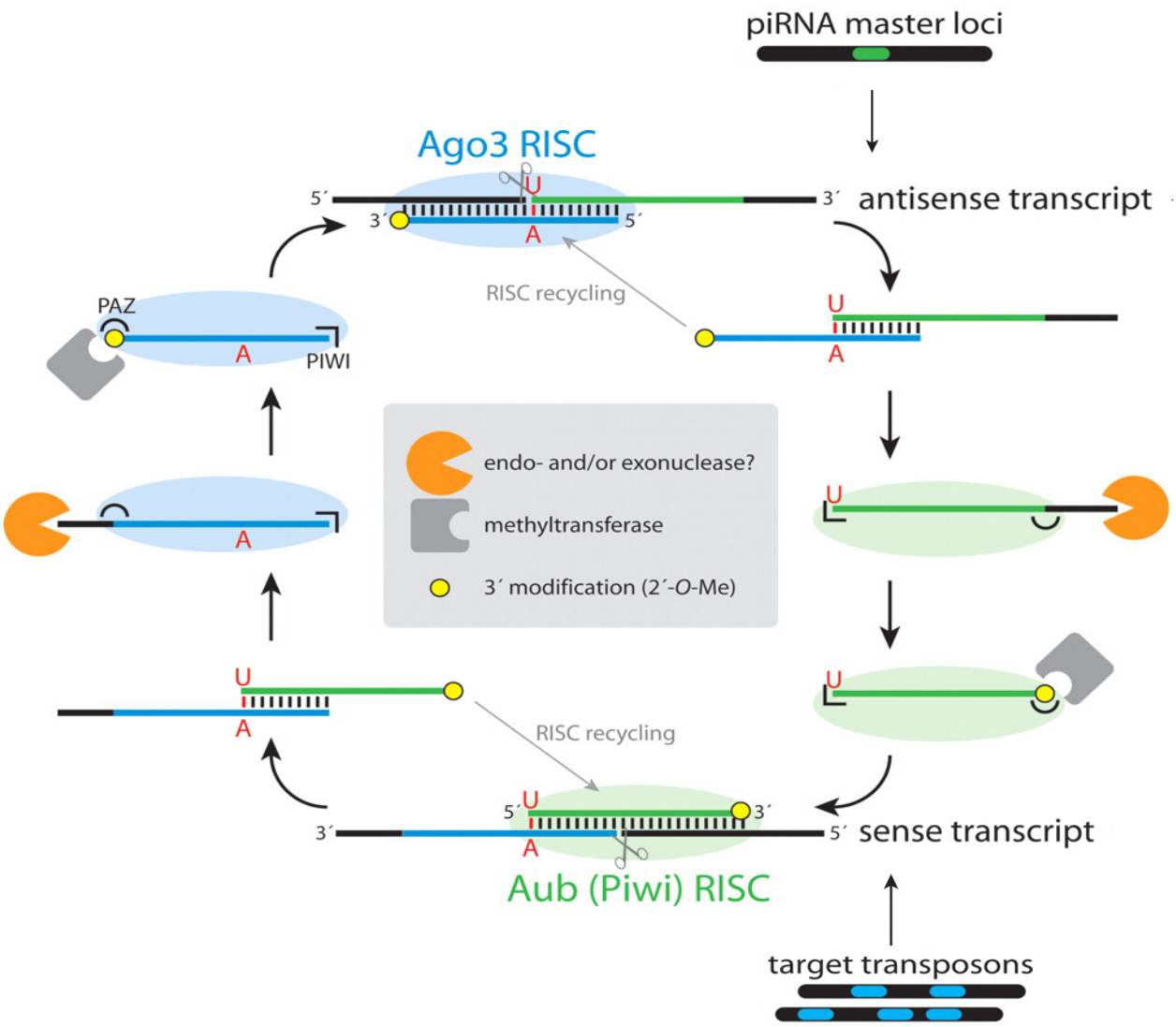

Figure 4. Ping-pong model of piRNA biogenesis pathway in *Drosophila*.
Pre-existing or maternally deposited piRNAs (primary piRNAs) associate with Piwi proteins to direct cleavage of transposon sense transcripts (*bottom*). The cleaved sense transcripts are not degraded but are processed into secondary piRNAs. These piRNAs are incorporated into Ago3 RISC complexes, which in turn pair with and cleave antisense transcripts derived from the piRNA master loci to generate more primary piRNAs (*top*). These piRNAs guide Piwi complexes to continue to target transposon transcripts. Thus, piRNAs are generated from a reciprocal amplification loop in which the 5′ ends of piRNAs are defined by RISC cleavage. The 3′ end is subsequently 2′-*O*-Me-modified by a methyltransferase, Pimet/DmHen1 in *Drosophila*. (Adapted from Hartig *et al*., *Gene&Dev*, (2007))

Summary

miRNAs represent a major class of small regulatory molecules that are involved into almost every aspect of gene expression, including embryonic development, immune response, long-term learning and memory, and disease. Although much progress has been achieved during the last 10 years to determine the regulatory mechanisms controlling miRNAs biogenesis and function, many questions remain to be answered. A key question is post-transcriptional regulation of miRNAs. Emerging evidence derived from multiple cancer and development studies has suggested that miRNAs are subject to precise control during almost every step of biogenesis. Another challenging question is to completely decipher the rules governing miRNA recognition of mRNA targets. Although several criteria are known to facilitate target identification, existing algorithms still have a very high false-positive rate indicating that more work is needed to understand the possible involvement of other regulatory determinants during miRNA-mRNA pairing.

The work presented in this thesis focuses on characterizing the expression and function of zebrafisfh miRNAs during early embryonic development. The data included here are part of a wide range of efforts from many labs to try to fully understand the role and biological significance of miRNA control of gene expression. The abundance and conservation of miRNAs and piRNAs suggests important roles for these RNAs in multiple biological settings. Understanding the targets of these RNAs is needed to fully comprehend their roles in overall regulation of gene expression.

CHAPTER 2:

Transcriptome-wide analysis of small RNA expression in early zebrafish development[1]

Chunyao Wei, Leonidas Salichos, Carli M. Wittgrove, Antonis Rokas,

and James G. Patton[2]

Department of Biological Sciences, Vanderbilt University, Nashville, TN 37235 USA

[1] This work has been published. Wei, C., Salichos, L., Wittgrove, C.M., Rokas, A., and Patton, J.G. (2012). "Transcriptome-wide analysis of small RNA expression in early zebrafish development." RNA *18*, 915-929.

[2] CW and JGP conceived and designed the experiments. CW and CMW performed the experiments. CW, LS, AR and JGP analyzed the data. CW, AR and JGP wrote the paper.

Abstract

During early vertebrate development, a large number of noncoding RNAs are maternally inherited or expressed upon activation of zygotic transcription. The exact identity, expression levels, and function for most of these noncoding RNAs remain largely unknown. miRNAs (microRNAs) and piRNAs (piwi-interacting RNAs) are two classes of small non-coding RNAs that play important roles in gene regulation during early embryonic development. Here, we utilized next generation sequencing technology to determine temporal expression patterns for both miRNAs and piRNAs during four distinct stages of early vertebrate development using zebrafish as a model system. For miRNAs, the expression patterns for 192 known miRNAs within 122 different miRNA families and 9 novel miRNAs were determined. Significant sequence variation was observed at the 5' and 3'ends of miRNAs with most extra nucleotides added at the 3' end in a non-template directed manner. For the *miR-430* family, the addition of adenosine and uracil residues is developmentally regulated and may play a role in miRNA stability during the maternal zygotic transition. Similar modification at the 3' ends of a large number of miRNAs suggests widespread regulation of stability during early development. Besides miRNAs, we also identified a large and unexpectedly diverse set of piRNAs expressed during early development.

Introduction

The importance of small RNA-mediated gene regulation has been increasingly recognized in recent years, playing multiple roles during development (Pauli et al., 2011). miRNAs and endogenous siRNAs have been shown to regulate gene expression by silencing specific genes whereas piRNAs have been implicated mainly in genome protection and/or maintenance in germ cells via silencing of transposable elements (Aravin et al., 2007; Bartel and Chen, 2004; Brennecke et al., 2007; Czech et al., 2008; Flynt and Lai, 2008; Houwing et al., 2007; Tam et al., 2008). miRNAs have been identified in organisms as diverse as viruses, unicellular algae, plants, worms, flies, fish and mammals (Bartel, 2004; Skalsky and Cullen, 2010; Zhao et al., 2007). For those miRNAs thus far analyzed, expression patterns are highly regulated, both temporally and spatially (Landgraf et al., 2007; Ruby et al., 2007; Wienholds et al., 2005a). miRNAs mainly exert their effects by blocking translation and/or destabilizing mRNAs (Baek et al., 2008; Giraldez et al., 2006b; Guo et al., 2010; Lim et al., 2005). piRNA expression is thought to be mostly restricted to germ cells and some somatic cells in flies (Haase et al., 2010; Halic and Moazed, 2009; Malone et al., 2009).

Mature miRNAs are 22-23 nucleotides (nt) in length. They are derived from longer primary transcripts (pri-miRNAs) that contain multiple stem-loop structures which undergo two sequential cleavages by the enzymes Drosha and Dicer to produce mature small RNA duplexes (Cai et al., 2004; Hutvagner et al., 2001; Ketting et al., 2001; Lee et al., 2003; Lee et al., 2002). Generally, one of the two strands is then incorporated into an RNA Induced Silencing Complex (RISC) with one or more Argonaute proteins (Schwarz, 2003). In contrast to miRNAs, piRNAs are slightly larger (25-30 nt) and, at least in flies

and fish, derived from a reciprocal amplification loop in which primary piRNAs associate with Piwi proteins to direct cleavage of transposable element mRNAs (Brennecke et al., 2007; Houwing et al., 2008). The initial cleavage products then serve to promote production of sense strand secondary piRNAs that in turn generate more primary piRNAs by pairing with and directing cleavage of antisense RNAs derived from discrete repetitive genomic loci referred to as piRNA clusters (Brennecke et al., 2007; Malone et al., 2009). This model of biogenesis is referred to as the Ping-Pong model because the production of piRNAs from one strand drives the generation of piRNAs from the other strand (Brennecke et al., 2007).

Zebrafish is widely used as a model system to study early vertebrate development (Kimmel et al., 1995). Previous work has shown that miRNAs play important functional roles during cell specification and differentiation (Flynt et al., 2007; Giraldez et al., 2005a; Mishima et al., 2009). In zebrafish, miRNA expression patterns have been extensively examined using direct cloning and microarray analyses (Giraldez et al., 2005a; Thatcher et al., 2007; Wienholds et al., 2005a). These studies have shown that most miRNAs are not highly expressed during the first 12 hours of zebrafish development but that the overall pattern becomes increasingly diverse and complex as development proceeds (Chen et al., 2005; Thatcher et al., 2007; Wienholds et al., 2005a). Despite the seeming lack of diversity during the earliest stages of development, miRNA function is clearly essential as maternal-zygotic Dicer mutant fish show severe defects and die by 7 dpf (Giraldez et al., 2005a). One of the most abundant early expressed families of miRNAs is the *miR-430* family which functions to induce deadenylation, degradation, and clearance of maternal mRNAs, facilitating the maternal-zygotic

transition (Giraldez et al., 2006a). A similar phenomenon occurs in *Xenopus laevis* through the action of the *miR-427* family (Lund et al., 2009).

In zebrafish, piRNAs are mainly expressed in ovaries and testes (Houwing et al., 2008; Houwing et al., 2007). Ziwi-mutant fish, which lack the zebrafish PIWI protein, exhibit extensive apoptosis in adult germ cells and are sterile (Houwing et al., 2007). This suggests an essential role in genome maintenance but the exact role and mechanism of action for these small RNAs remains mostly unknown.

Recently, the utilization of next generation sequencing technologies has revolutionized our ability to dissect transcriptomes, even for RNAs expressed at low levels. Here, we used RNA-Seq to examine the expression of miRNAs and piRNAs across four stages of early zebrafish development. We discovered the presence of large numbers of miRNAs, both maternally deposited and zygotically transcribed. Many miRNAs show widespread variation at their 3' ends, mostly by the addition of non-template directed nucleotides that are added in a developmental stage-specific manner. We also show that piRNAs are extensively expressed throughout early embryonic development suggesting a broad role during the earliest cell divisions.

Results

Small RNA Sequencing

We isolated total RNA from zebrafish embryos at four different stages of early development (256-cell, sphere, shield and 1dpf) representing 2.5, 4, 6, and 24 hours post fertilization (hpf), respectively. We chose these stages because they coincide with key gene expression changes during early vertebrate development. At the 256-cell stage, the

majority of RNAs are maternally deposited. The sphere stage represents the time during which the embryo shifts from utilization of many maternally deposited RNAs and initiates zygotic transcription. During the shield stage, gastrulation continues to generate and shape the 3 germ layers. By 1 dpf, the major organ systems have formed and hearts are beating. To examine gene expression patterns during these specific stages, small RNA libraries (15-30 nt) were prepared for high-throughput sequencing using the Illumina platform (Hafner et al., 2008). We constructed independent libraries for each stage, and generated a total of 29,963,921 sequence reads. In order to validate the reliability of the different high throughput sequencing runs, experimental duplicates of small RNA libraries were prepared from sphere stage RNA and independently sequenced. A significant correlation was observed between the results from the two independent libraries (R^2=0.89; Figure 5). In addition, the miRNA profiles revealed by our sequencing data across all four stages were largely consistent with prior miRNA expression analyses (Chen et al., 2005; Thatcher et al., 2007; Wienholds et al., 2005a).

Analysis of the size distribution of all reads within each library revealed at least three classes between 18-30 nt. The major size class peaked at 22-23 nt (Figure 6A). Based on the sequences and genomic positions of these reads, this class represents miRNAs. From all 4 stages, ~55% of the total reads were identified as miRNAs, representing 198 distinct miRNAs (based on sequence alignment with miRBase Release 16 (Griffiths-Jones, 2004; Griffiths-Jones et al., 2006; Griffiths-Jones et al., 2008)). At the sphere stage, 99% of the miRNA reads were derived from just one family, the *miR-430* family. To better examine the diversity of non-coding reads, we grouped identical sequences which showed that a wide diversity of small RNAs were recovered (Figure

6B,C). Examination of the reads after such grouping revealed a second size class peaking at 26-28 nt (Figure 6A; Figure 15A,B). Based on RNA sequences and genomic mapping, these RNAs are derived primarily from repetitive elements. The smallest size class peaked at 18 nt and consists almost entirely of tRNA-derived small RNAs (see below) and rRNA-related small RNAs (data not shown).

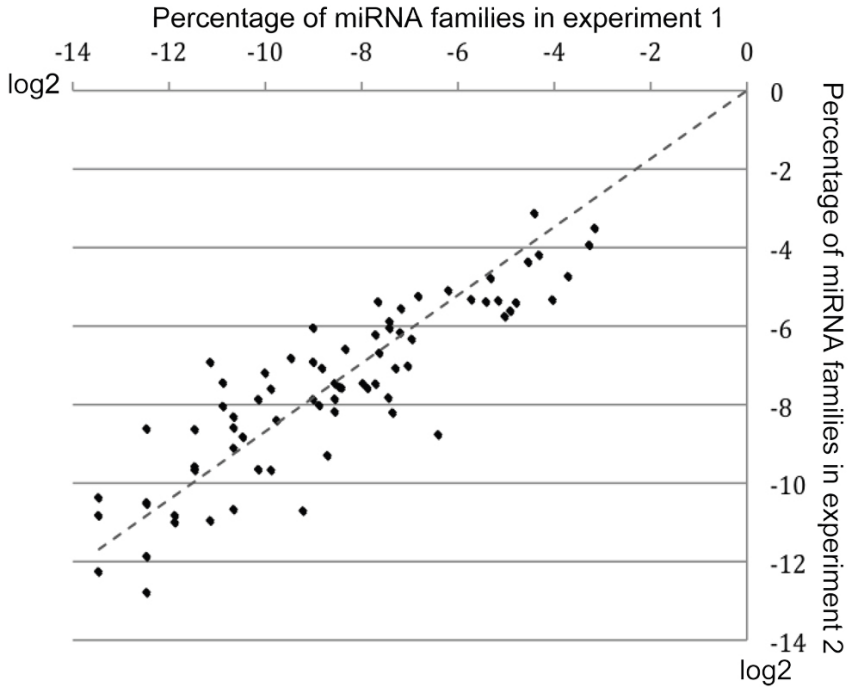

Figure 5. Reliability of library preparation and sequencing.
Total miRNA read numbers from sequencing of independent libraries prepared from sphere stage RNA were quantified, normalized, transformed into log 2 values, and plotted as shown.

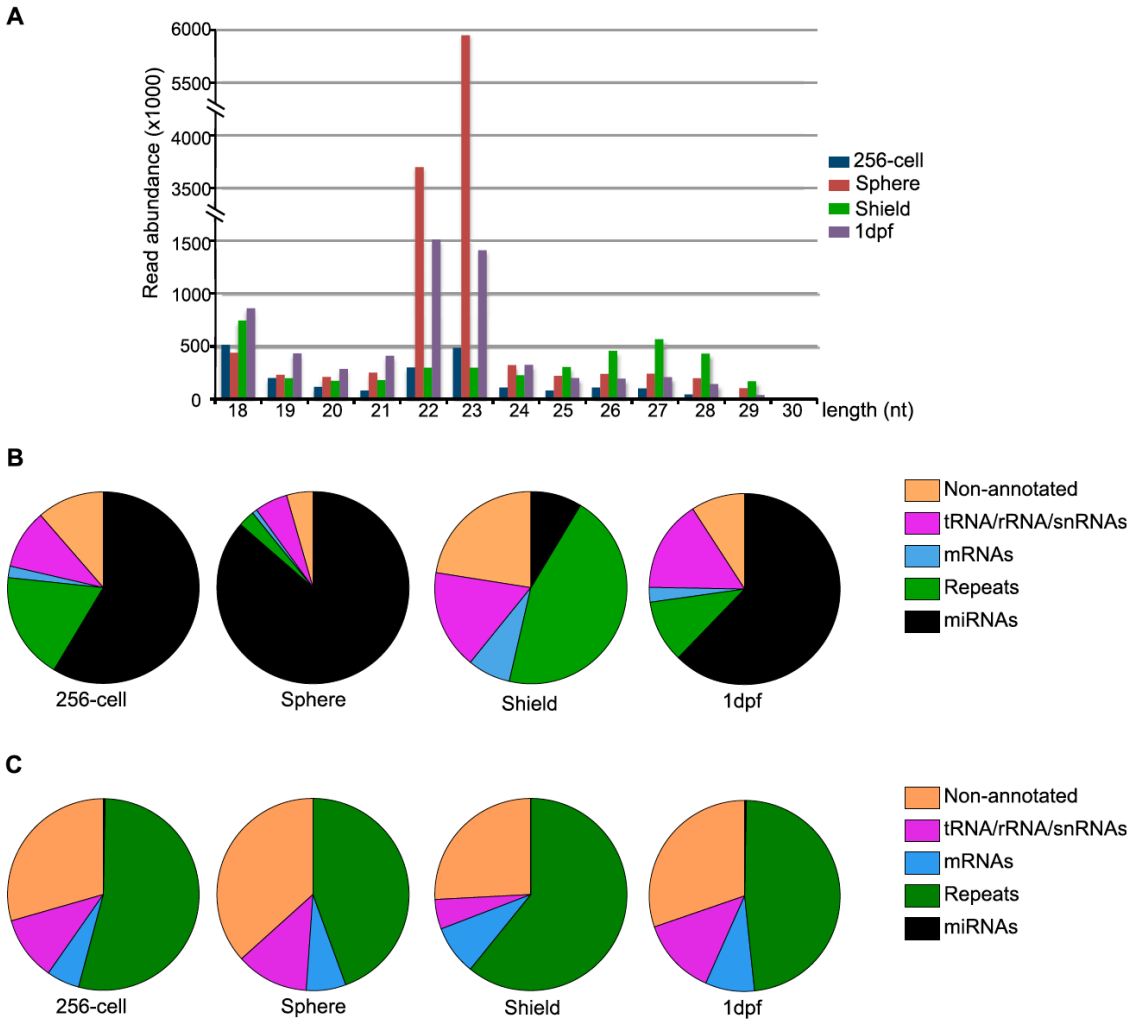

Figure 6. Sequencing Summary

(A) Size distribution of all sequencing reads between 18 and 30 nucleotides. RNA reads derived from four developmental stages are indicated in different colors. The size distribution and abundance of the reads from each stage are as indicated. (B) Read frequency for all sequences. The identity and frequency of small RNAs reads from different developmental time points are as indicated. (C) Read frequency for unique sequences. In contrast to B where the total read frequencies were charted, small RNA reads derived from the same miRNA were grouped together as a single subset. This analysis shows a large number of unique reads are derived from distinct genomic elements, mostly repetitive elements.

miRNA Expression Analysis

Analysis of the sequencing reads showed that 198 known miRNAs were detected that could be grouped into 122 families. Most of the miRNA reads were derived from just one arm of the hairpin structures that constitute each precursor miRNA. Short reads corresponding to the loop and the other precursor arm (star sequence arm) were also detected but at much lower frequencies, consistent with proposed miRNA biogenesis models (Kim et al., 2009). However, we also found exceptions in which the star reads were much more prevalent than the mature reads (e.g. *miR-735* and *miR-135b*; see Supplemental Table 1 for full list). An extreme example of diverse read lengths with different 5' and 3' ends was detected for reads derived from *miR-2190*, one of the most recently annotated zebrafish miRNAs (Soares et al., 2009). We found multiple small RNAs derived from this locus with different ends, suggesting random cleavage at multiple sites across the proposed precursor hairpin (Supplemental Table 1). The *miR-2190* putative hairpin overlaps with two rRNA genes in the zebrafish genome and that fact, together with the observed sequence heterogeneity, suggests that *miR-2190* is more likely to be a product of rRNA degradation rather than an authentic miRNA.

Quantitation of miRNA expression patterns was determined based on the read frequency for each mature miRNA. Previous work demonstrated a significant correlation between read numbers and miRNA levels with the caveat that bias cannot be completely eliminated due to secondary structures or other variables (Landgraf et al., 2007). Nevertheless, normalization between developmental stages has usually been performed using miRNA read numbers divided by the total number of genome matching reads in each library (Ameres et al., 2010; Chen et al., 2005). We initially analyzed expression

patterns in this manner (Figure 7). We found that this method was not perfect as overall transcriptional activity significantly changes as development proceeds resulting in a large increase in the size of the small RNA libraries. Also, there is a large increase in the total number of reads generated largely by a huge increase in reads derived from the *miR-430* family which increased from 25% of the total miRNA reads at the 256-cell stage to 99% at the sphere stage. If the libraries are normalized using individual miRNA read numbers divided by the total number of genome matching reads in each library, changes in the expression of individual miRNAs can become obscured by overall transcription levels as development proceeds, as well as the extreme abundance of reads derived from just the *miR-430* family. Thus, we also normalized the values from each library based on the levels of two miRNAs that are present at moderate levels in all libraries (*let-7a* and *miR-9*). For this, we performed RT-qPCR to determine the levels of these miRNAs relative to U6 snRNA (Figure 8). We then used the relative values of *let-7a* and *miR-9* to normalize the read frequencies for each library (Friedlander et al., 2009) (Figure 9 and Figure 7B). Reassuringly, the expression patterns were similar, whether normalized to *miR-9* levels or *let-7a* levels, even though the RT-qPCR levels for these miRNAs differ by an order of magnitude and despite the fact that *let-7a* levels can be biased using deep sequencing approaches (Linsen et al., 2009). As expected, normalization based on *miR-9* or *let-7* resulted in very different heat maps compared to that obtained when total genome matching reads are used for normalization (Figure 7).

Figure 7. miRNA Expression Heat Maps.
(A) Heat map generated by dividing the read numbers for individual miRNAs by the total genome matching reads. (B) Heat map based on normalization of miRNA levels relative to the expression level of *miR-9*. (C) Heat map generated by a scaling normalization method, TMM (Robinson and Oshlack, 2010). For TMM, Mg values (log fold changes) were trimmed by 30% and Ag values (absolute intensity) by 5%.

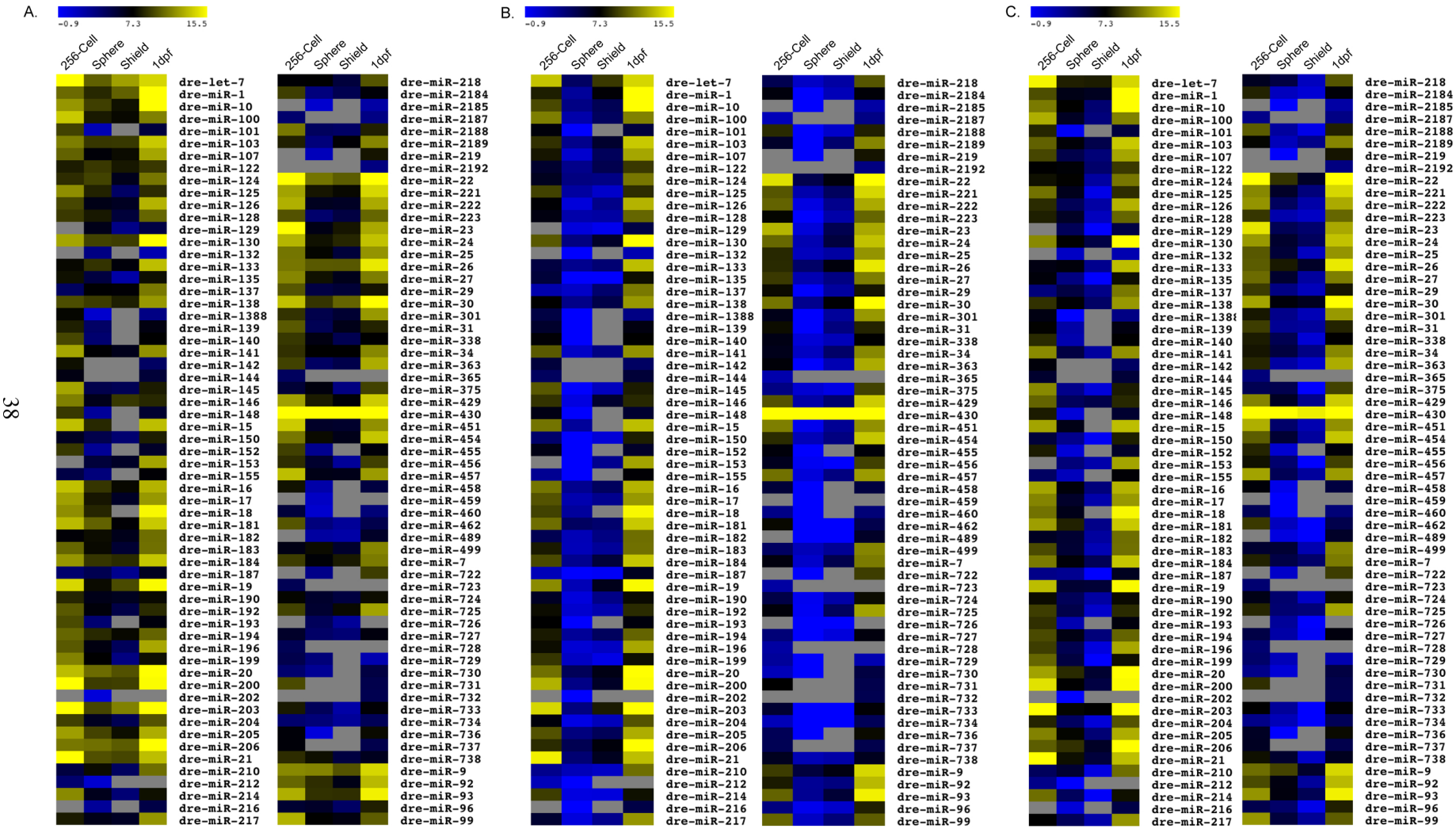
A.
B.
C.
-0.9
7.3
15.5
256-Cell
Sphere
Shield
1dpf
dre-let-7
dre-miR-1
dre-miR-10
dre-miR-100
dre-miR-101
dre-miR-103
dre-miR-107
dre-miR-122
dre-miR-124
dre-miR-125
dre-miR-126
dre-miR-128
dre-miR-129
dre-miR-130
dre-miR-132
dre-miR-133
dre-miR-135
dre-miR-137
dre-miR-138
dre-miR-1388
dre-miR-139
dre-miR-140
dre-miR-141
dre-miR-142
dre-miR-144
dre-miR-145
dre-miR-146
dre-miR-148
dre-miR-15
dre-miR-150
dre-miR-152
dre-miR-153
dre-miR-155
dre-miR-16
dre-miR-17
dre-miR-18
dre-miR-181
dre-miR-182
dre-miR-183
dre-miR-184
dre-miR-187
dre-miR-19
dre-miR-190
dre-miR-192
dre-miR-193
dre-miR-194
dre-miR-196
dre-miR-199
dre-miR-20
dre-miR-200
dre-miR-202
dre-miR-203
dre-miR-204
dre-miR-205
dre-miR-206
dre-miR-21
dre-miR-210
dre-miR-212
dre-miR-214
dre-miR-216
dre-miR-217
dre-miR-218
dre-miR-2184
dre-miR-2185
dre-miR-2187
dre-miR-2188
dre-miR-2189
dre-miR-219
dre-miR-2192
dre-miR-22
dre-miR-221
dre-miR-222
dre-miR-223
dre-miR-23
dre-miR-24
dre-miR-25
dre-miR-26
dre-miR-27
dre-miR-29
dre-miR-30
dre-miR-301
dre-miR-31
dre-miR-338
dre-miR-34
dre-miR-363
dre-miR-365
dre-miR-375
dre-miR-429
dre-miR-430
dre-miR-451
dre-miR-454
dre-miR-455
dre-miR-456
dre-miR-457
dre-miR-458
dre-miR-459
dre-miR-460
dre-miR-462
dre-miR-489
dre-miR-499
dre-miR-7
dre-miR-722
dre-miR-723
dre-miR-724
dre-miR-725
dre-miR-726
dre-miR-727
dre-miR-728
dre-miR-729
dre-miR-730
dre-miR-731
dre-miR-732
dre-miR-733
dre-miR-734
dre-miR-736
dre-miR-737
dre-miR-738
dre-miR-9
dre-miR-92
dre-miR-93
dre-miR-96
dre-miR-99

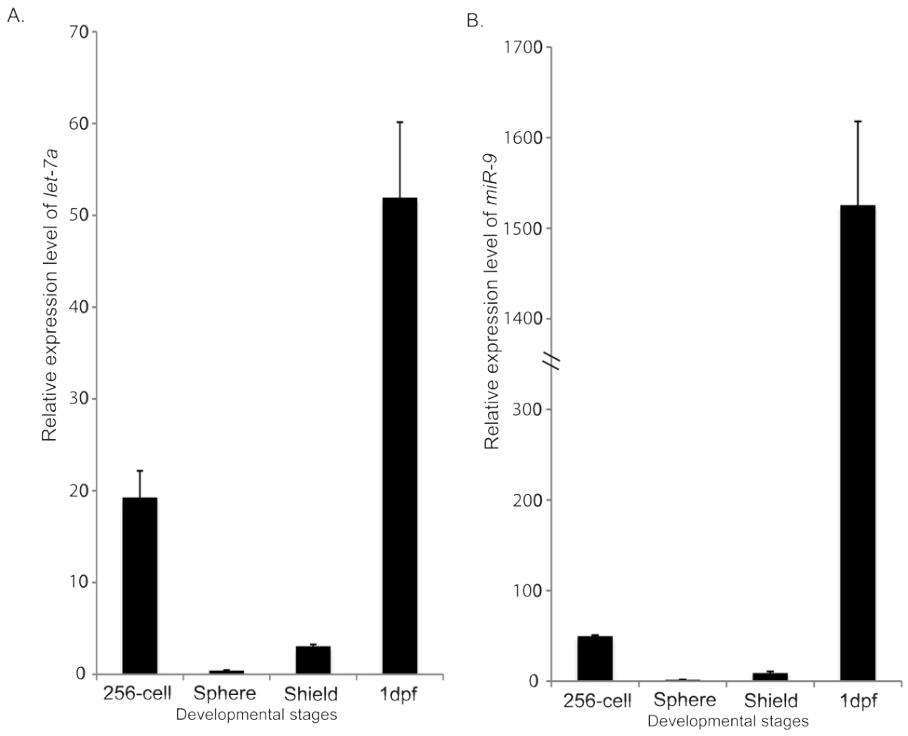

Figure 8. Quantitative RT/PCR of *let-7a* and *miR-9* expression.
RT/qPCR was conducted with primers specific for either *let-7a* (A) or *miR-9* (B) on RNA preparations from the indicated developmental stage. These RNAs are expressed at mid-range levels via Illumina sequencing and their levels, as determined via RT/qPCR at the different stages, are as shown relative to U6 snRNA. Error bars represent s.e.m.

Quantitation and normalization of sequencing data to analyze gene expression patterns is not trivial and subject to ongoing research and debate (Meyer et al. 2010). Thus, as a further test of whether normalization based on *miR-9* or *let-7* is valid, we used the trimmed mean of M values (TMM) to normalize the data (Robinson and Oshlack, 2010). TMM uses raw data to estimate appropriate scaling factors that facilitates analysis of differential expression patterns. When we used TMM normalization, we reassuringly found that the derived heat maps were very similar to those obtained after normalization with either *miR-9* or *let-7* (Figure 7). Finally, we used northern blots on 6 miRNAs with

differing raw read numbers to confirm our normalization method and the resulting heat maps (Figure 9).

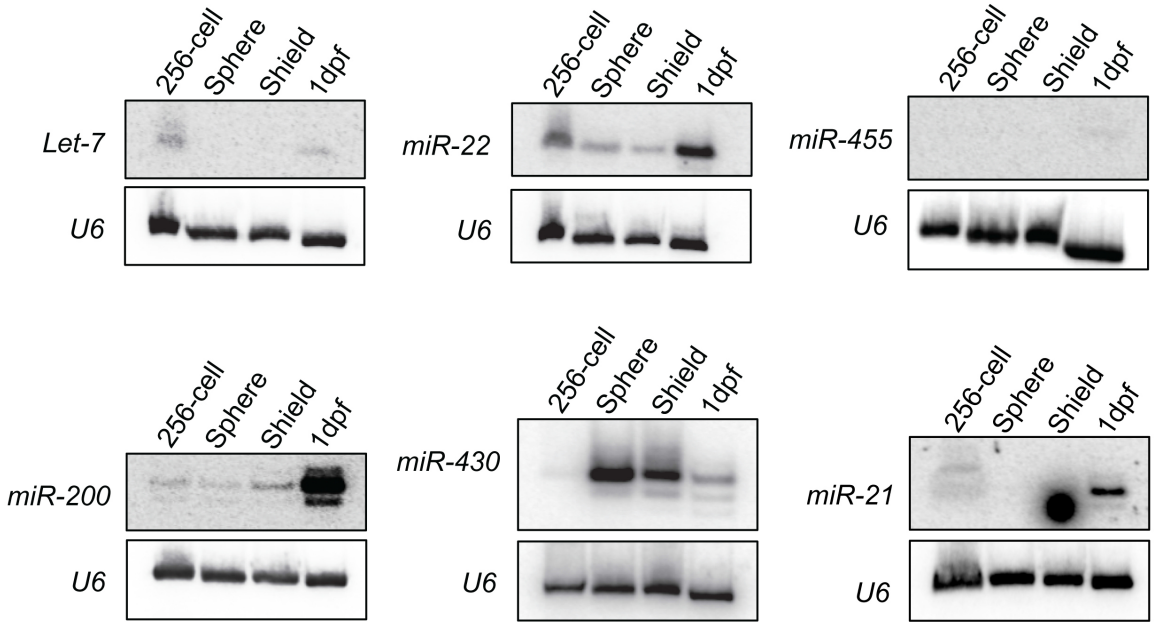

Figure 9. Northern verifications of miRNA expression.
A subset of miRNAs were selected and northern blots used to validate the expression levels indicated in the heat maps shown in Fig. 2. Note that *miR-430* is highly expressed compared to other miRNAs but the levels of expression change during development. The round spot in miR-21 panel is non-specific.

Developmentally, we found that 178 miRNAs belonging to 109 different families are present at the 256-cell stage. Because this is before the onset of zygotic transcription, these miRNAs are maternally deposited and, interestingly, are present at relatively high levels, suggesting an important role during the earliest stages of development (Newport and Kirschner, 1982; Schier, 2007). 88 out of the 109 miRNA families that are expressed at the 256-cell stage are down regulated at least 2-fold as development and zygotic

transcription proceeds. The 10 most abundant miRNAs expressed at this stage and their subsequent changes in expression are listed in Table 1. For the sphere state, a total of 180 different miRNAs were detected. Many of the maternally inherited miRNAs that were detected at the 256-cell stage were not observed by the sphere stage. From the sphere stage onward, miRNAs can be roughly divided into 2 distinct groups based on their expression patterns during early development. The first group is composed of 60 miRNA families that are expressed at low levels across all 4 stages, while the second group is composed of 48 miRNAs that show decreased expression at the sphere stage followed by at least a 2-fold increase in expression as development proceeds (Figure 10). The miRNAs in the second group appear to be more broadly expressed.

Table 1. Abundantly expressed miRNAs at 256-cell stage.

miRNA family	Seed sequence	Raw read number at 256-cell[a]	Fold change from 256-cell to sphere	Other members
miR-430	AAGUGCU	62,555	12.0	-
miR-21	AGCUUAU	40,599	−178.1	-
miR-22	AGCUGCC	28,085	−55.6	-
miR-203	UGAAAUG	22,723	−128.1	-
let-7	GAGGUAG	15,332	−46.3	-
miR-23	UCACAUU	10,829	−462.3	-
miR-200	AACACUG	9,969	−67.6	*miR-8*
miR-19	GUGCAAA	4,288	−86.7	-
miR-451	AACCGUU	3,170	−216.0	-
miR-100	ACCCGUA	4,899	−46.5	*miR-99*

[a]Also includes miRNA reads with 3′ end heterogeneity that does not match the genomic loci (see Supplemental Table 2).

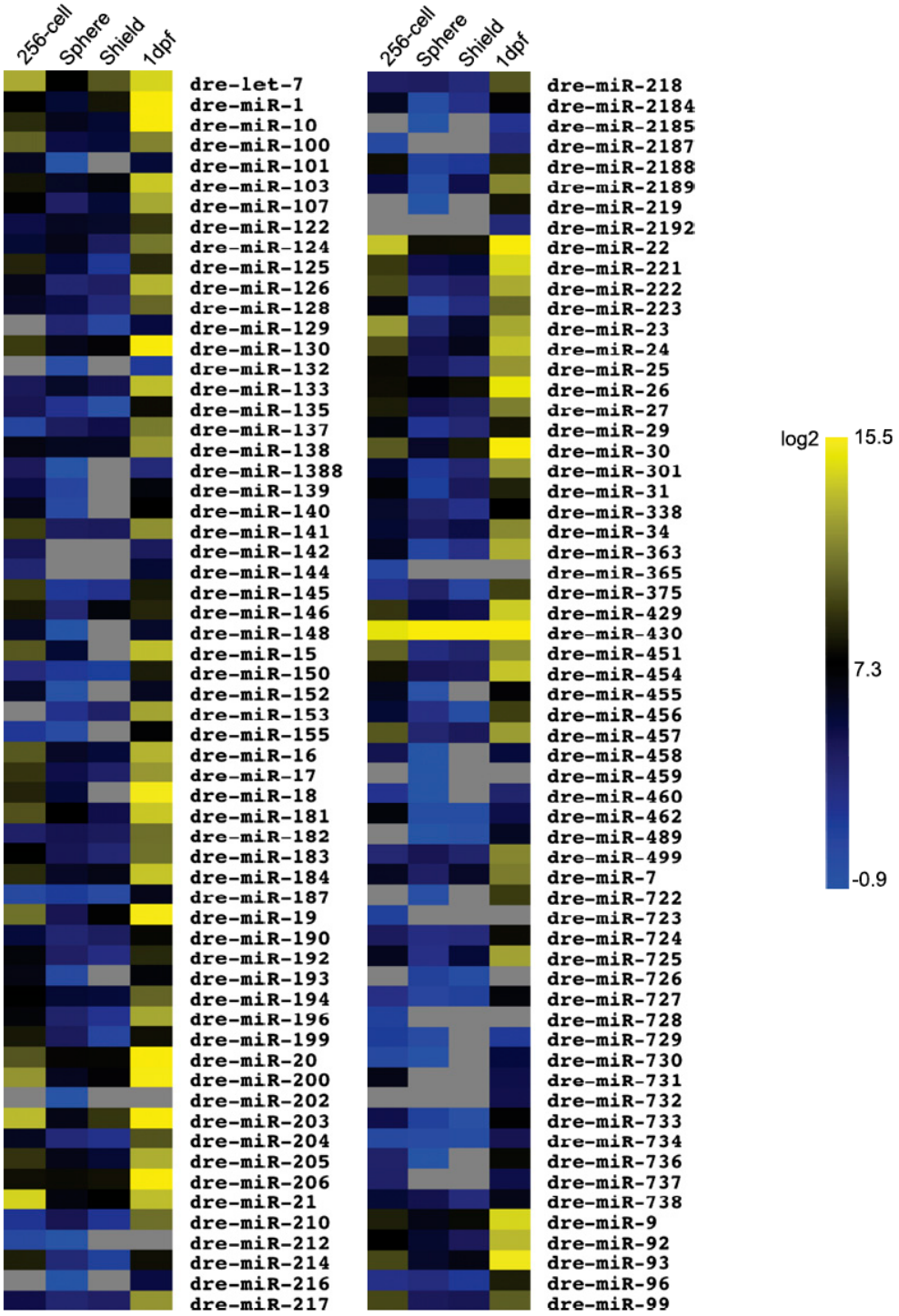

Figure 10. miRNA family expression profiles.

miRNA family read frequency was normalized (see Material and Methods) and compared across four developmental stages. Yellow indicates high expression and blue indicates low expression. Gray indicates undetectable levels of expression.

Identification of Novel miRNAs

Analysis of all sequencing reads during early zebrafish development resulted in the identification of 8 miRNAs that had not been previously reported in the zebrafish genome (Table 2). For this, we analyzed all small RNA reads from the four developmental stages using the miRDeep algorithm (Friedlander et al., 2008). Following this pipeline, predicted miRNAs were filtered for novel miRNA identification by comparison to sequences deposited in the miRNA Registry. To increase accuracy, miRDeep-predicted novel miRNAs that genomically overlap with tRNA, rRNA, or transposable elements, were eliminated and our analyses were restricted to only those that were identified in at least two different developmental stages and/or two independent libraries. With this restriction, 5 novel candidate miRNAs were identified, 2 of which are conserved across vertebrates whereas the other 3 appear to be zebrafish specific (Figure 11). The remaining 3 were discovered independent of miRDeep and match miRNA sequences reported for other species. For these three, we aligned small RNAs to known miRNA hairpin sequences of other species in conjunction with secondary structure analyses of the corresponding zebrafish genomic loci. Of the three, 2 show conservation of the mature miRNA strand while 1 shows conservation of the passenger strand. For all 8 new zebrafish miRNAs, we validated their presence by examining and ensuring that their flanking sequences and corresponding genomic loci fit existing models of miRNA biogenesis (see Supplementary Material, Novel miRNA Sequences). To independently confirm the expression of these miRNAs, we performed northern blots on total RNA from the same four stages of development as used for deep sequencing. As expected, these miRNAs were expressed at low levels but we were still able to detect bands of the appropriate size for the mature sequences for 6 out the 8 novel miRNAs and bands

corresponding to pre-miRNAs for 5 of the 8 (Figure 12). We could not detect signals for the two remaining novel miRNAs, presumably due to expression at levels below the limits of detection. Nevertheless, based on the criteria used to identify these miRNAs, we believe they constitute newly reported miRNAs.

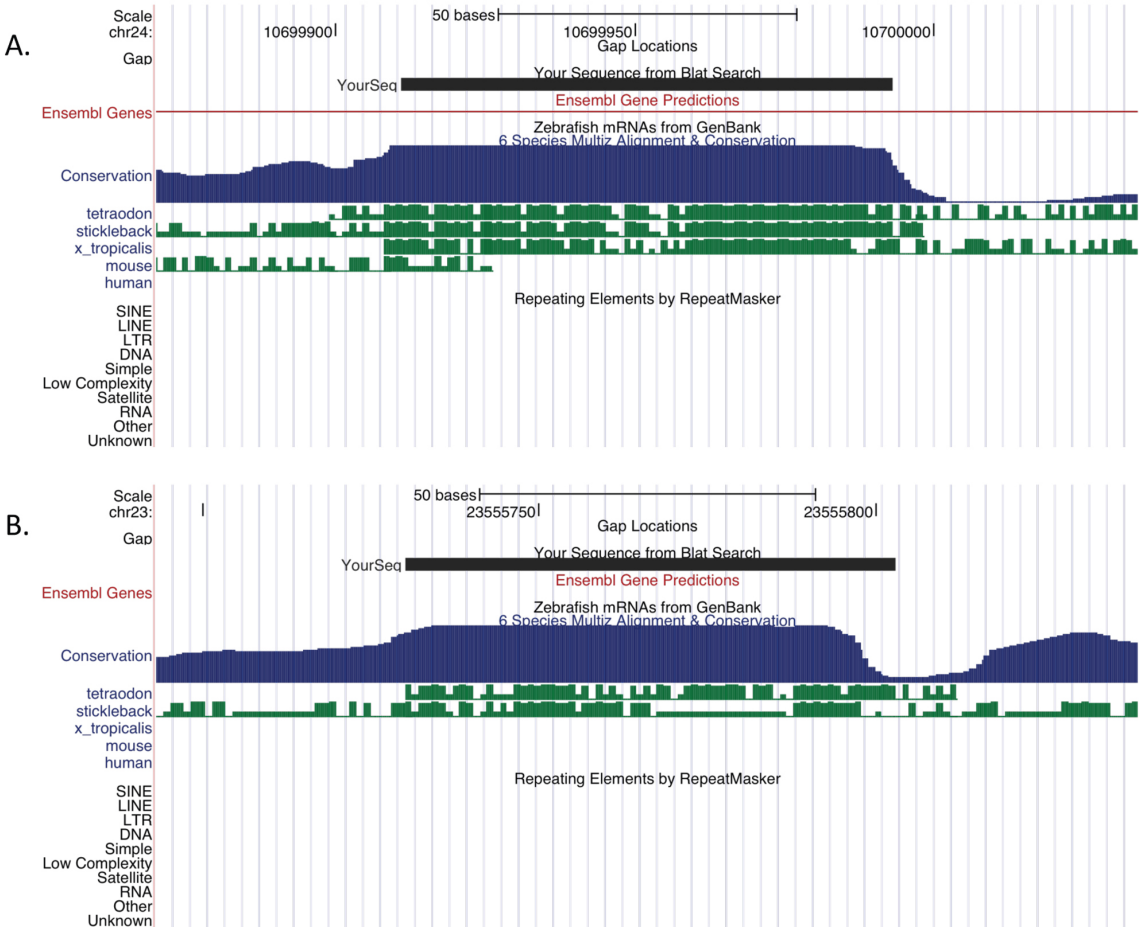

Figure 11. Novel conserved miRNAs.

The genomic location and conservation of two novel miRNAs are shown as a snap shot from the UCSC genome browser. Predicted pre-miRNA sequences were used to conduct blast searches with the results as shown.

Panel A miRNA: 5'-UGUACCAUGCUGGUAGCCAGU-3'

Panel B miRNA: 5'-UGUGAAUCCUACACUGGAAGG-3'

Table 2. Novel miRNAs

Sequences	Reads at 1 dpf	Seed	Star strand detected	Stages with expression	Conservation?
ACAAUGGAAGCCAAUGGUUACC	231	CAAUGGA	No	256-cell	No
UGAAGGUCAAUGGUUACCAGUU	102	GAAGGUC	Yes	shield	No
UGUACCAUGCUGGUAGCCAGU	26	GUACCAU	No	sphere	Yes[a]
AUGGAAAUACUCGCUGAUACUG	80	UGGAAAU	Yes	256-cell/sphere	No
UGUGAAUCCUACACUGGAAGG	41	GUGAAUC	Yes	shield	Yes[a]
GUGGGAUCGCGCCUGUGAAU	23	UGGGAUC	No	256-cell/sphere	ssc-*miR-1285*
CCACCUCCCCUGCAAACGUCCA	7	CACCUCC	No	256-cell/sphere	bta-*miR-1306*
GGCCGAAGUGGAGAAGGGU	335	GCCGAAG	Yes	256-cell/sphere	mdo-*miR-739*

[a] Conservation was determined by sequence similarity indicated in the UCSC genome browser. See Figure 11.

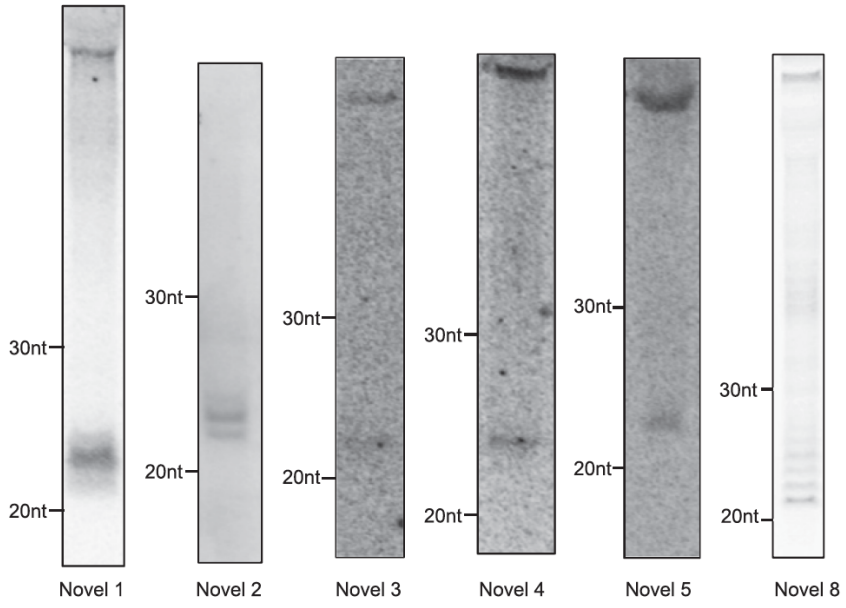

Figure 12. Northern blot of novel miRNAs

Northern blots were performed to verify the expression of predicted novel miRNAs. Mature miRNAs were detected for 6 of the 8 predicted miRNAs and miRNA precursors were detected for 5 of the 6 miRNAs.

miRNA Sequence Variation

Sequence variation at the 5' and 3' ends of mature miRNA sequences has been reported following deep sequencing analyses (Burroughs et al., 2010; Fernandez-Valverde et al., 2010; Kamminga et al., 2010; Landgraf et al., 2007; Lehrbach et al., 2009; Morin et al., 2008). Such variation is due to mismatches between the reads and their corresponding genomic loci with most mismatches detected at the 3' ends. We also observed significant sequence variation, mostly nucleotide additions at the 3' ends (Figure 13A, Supplemental Table 2). Within the mature miRNA sequences, less than 1% of the reads differed from their genomic loci. In contrast, ~40% of the total reads were 1-2 nucleotides longer at the 3' end than the mature sequence reported in miRBase, whereas much less 5' end variation was detected. In some cases, the additional nucleotides matched the sequence of the pre-miRNA, suggesting that cleavage events during miRNA processing are not always precise. In the case of *miR-2190*, sequence heterogeneity was observed at both the 5' and 3' ends with no clear preference for specific precursor cleavage sites, again arguing against this being a *bona fide* miRNA.

We also detected significant 3' sequence variation (~10% of reads) due to the addition of non-genomically encoded nucleotides, mostly adenine, uracil, or both (Figure 14A). Rarely, did we detect addition of cytosine or guanosine although *miR-181* had reads with guanosine addition and *miR-738* had reads with cytosine addition. Among miRNA families, the composition and extent of sequence variation was nearly identical between family members (Figure 12B). Additions at the 3' end in this manner (tailing) have been reported previously with proposals that the extra adenine nucleotides might stabilize miRNA half-life (Burns et al., 2011; Fernandez-Valverde et al., 2010; Katoh et

al., 2009). Our data are consistent with this idea but also support the hypothesis that tailing with U residues may be a mechanism to target miRNAs for degradation. Support for this hypothesis is based on variation at the 3' end of *miR-430* family members. As above, this family is the most abundant miRNA at the sphere stage where it constitutes 97% of the reads and functions to target maternal mRNAs for degradation (Giraldez et al., 2005a; Giraldez et al., 2006a). We found that 3' non-template directed uracil addition among *miR-430* family members is relatively low until the sphere stage after which time increasing addition of U residues was observed. In contrast, the extent of modification by the addition of A residues was not significantly different across these stages. Increasing modification by the addition of U residues coincided with declining levels of detectable *miR-430* from the sphere stage onward (Figure 13C).

To further examine the effects of nucleotide addition on the levels of *miR-430*, we also analyzed the 3' ends of *miR-430* reads that lacked the last guanosine from the mature miRNA. These reads are likely to be derived from mature *miR-430* RNAs that have undergone trimming and subsequent tailing at the time of library preparation. For these RNAs, we found a significant increase in adenosine addition at the sphere stage (Figure 13D). In contrast, uracil addition for these reads was lowest at the sphere stage. Together with the modifications described above for mature *miR-430* family members, the sequencing data are consistent with the hypothesis that U and A additions are associated with miRNA destabilization and stabilization, respectively (Figure 13D).

To more broadly assess the dynamics of nucleotide addition between stages, we next examined the subset of modified miRNAs whose expression overlaps both the 256-cell stage and the sphere stage. For these miRNAs, we calculated the percentage of reads

that showed U addition compared to all tailed reads. For each miRNA shown in Figure 13E, we show the extent of U modification at the 256 cell stage (red) compared to U modification at the sphere stage (blue). Increased levels of U modification were observed for the majority of miRNAs as the embryo proceeds from the 256-cell stage through the sphere stage. Interestingly, if all modifications on all miRNAs are examined across stages of development, we see a similar phenomenon with the majority of modifications detected at the 256-cell stage followed by the sphere stage and then decreasing levels of 3' modification thereafter. This is shown by the extent and amounts of black lines above the X axis in Figure 14B. The data are consistent with the idea that there is active stabilization/destabilization prior to and through the beginning of the maternal zygotic transition after which multiple mechanisms are in play to control the expression and stability of a given miRNA.

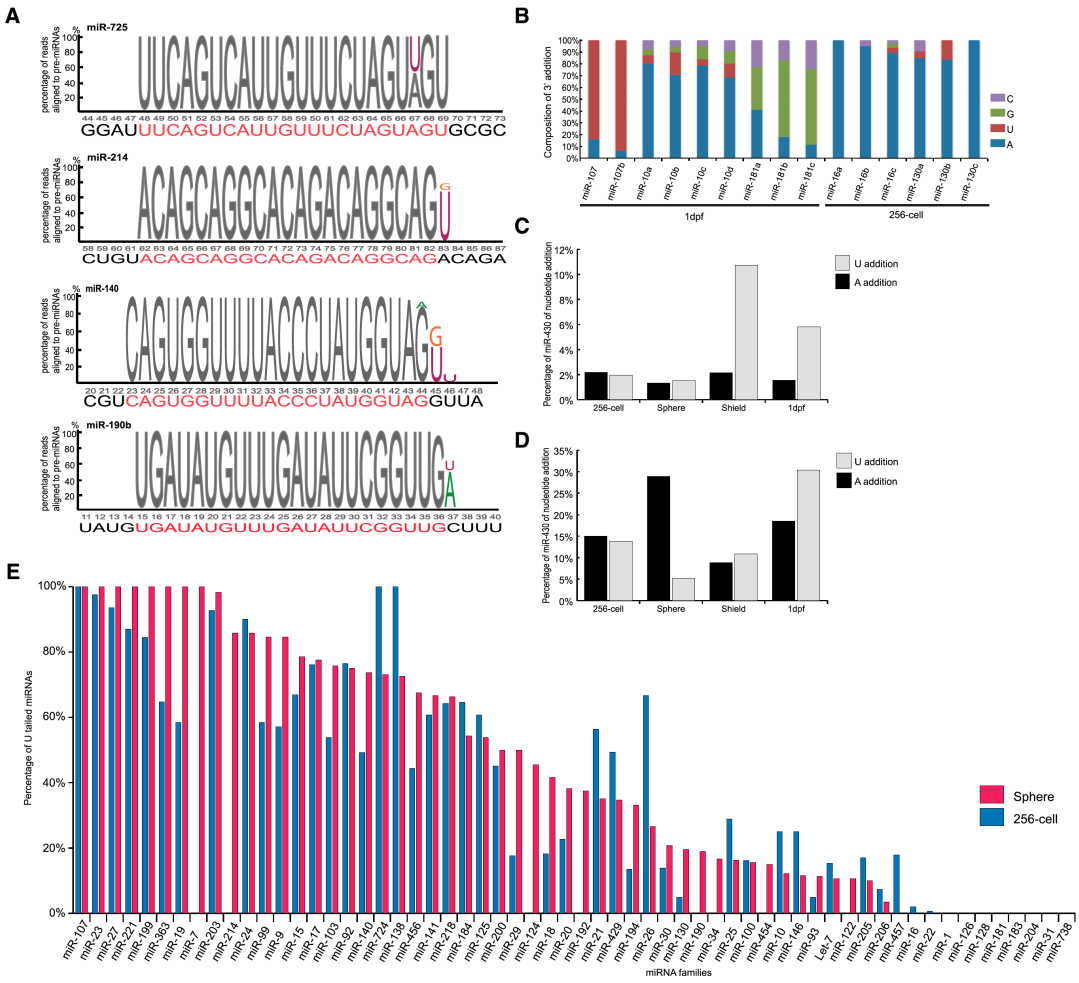

Figure 13. miRNA sequence heterogeneity.

(A) Significant sequence variation was detected among mature miRNA reads, especially at 3' ends. Shown are compilations from four different miRNAs with the extent of variation at any particular nucleotide indicated by the size of the font. Below in red is the mature miRNA sequence with adjacent genomic sequence in black. Non-template directed 3' additions are shown in color. (B) Similar composition of 3' addition among different miRNAs of the same family. The extent and base composition of miRNA tailing is indicated for a representative subset of miRNA families at the indicated stages of development. The percentage of reads with different nucleotide 3' ends is shown in different colors. (C) Modification of mature *miR-430* reads. The ratio of both A or U tailed mature *miR-430* family reads to total mature *miR-430* reads is shown across four developmental stages. (D) Modification of *miR-430* reads subject to trimming. A large number of *miR-430* reads did not contain the normal terminal guanosine. For this subset, the ratio of A or U tailed RNAs *miR-430* reads is shown across four developmental stages. (E) The percentage of U tailed miRNA reads for all tailed miRNA reads in both 256-cell and sphere stage embryos. All miRNAs with 3' additions of non-template-directed U residues are shown for the 256-cell and sphere stage. The percentage of U addition increased from the 256-cell stage to the sphere stage.

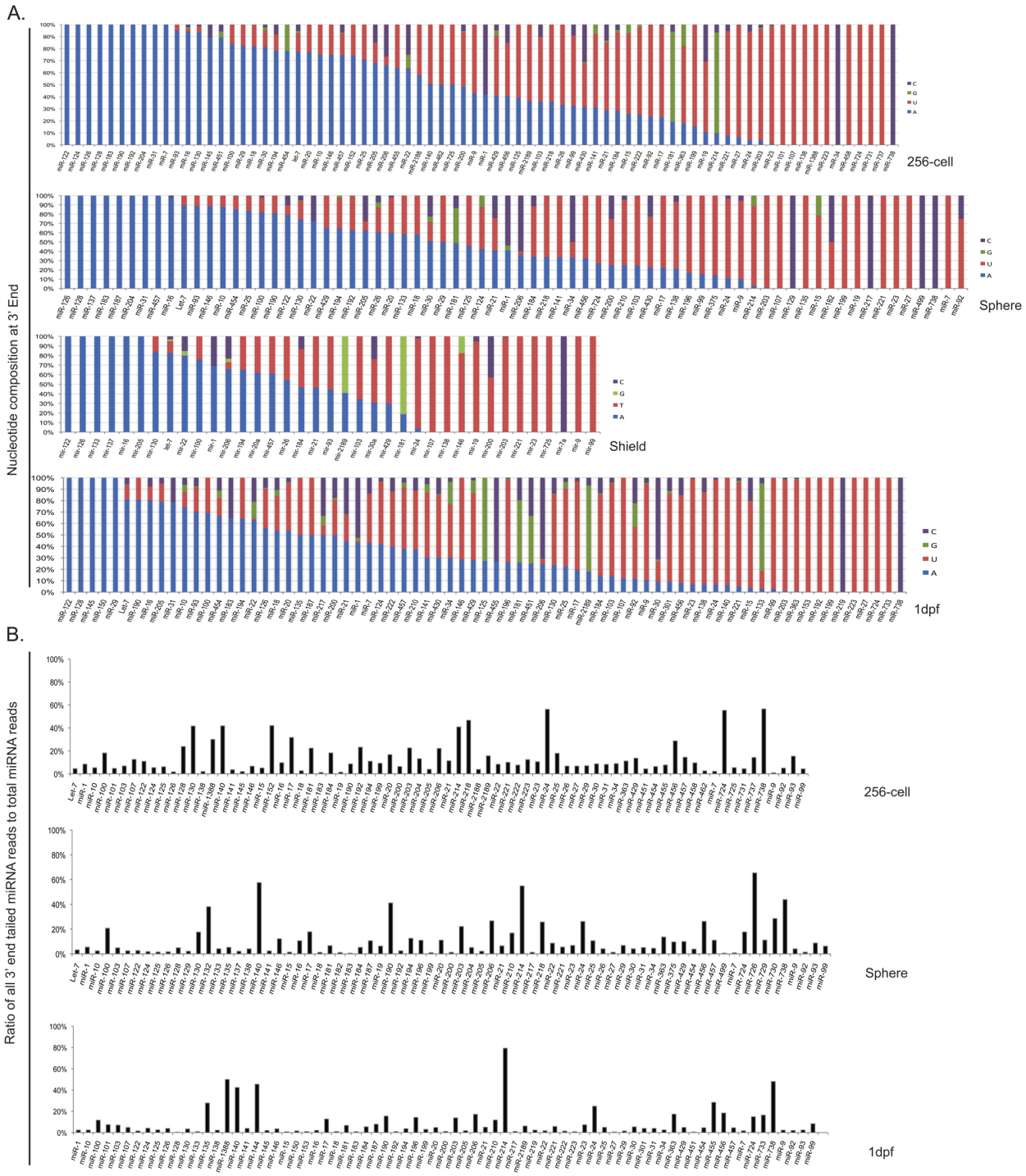

Figure 14. Analysis of non-template directed addition of nucleotides to miRNA 3' ends.

(A) All miRNA reads with 3' additions were quantified and the percentage of different nucleotide additions are as shown in different colors at the indicated developmental stages. (B) The percentage of miRNA reads containing any of the 4 possible nucleotide additions was calculated for each miRNA family at the indicated developmental stages.

Zebrafish piRNA Expression

When we examined the total reads from all four developmental time points, a distinct subset of small RNAs was detected that derive from genomic regions that do not encode miRNA genes (Figure 6). These RNAs represent a diverse array of sequences with a peak size distribution of ~26-28 nt and they map to either repetitive or unique genomic sequences (Figure 6). Their overall detection was clearly not saturated as more than 80% were detected only once. Based on size, they most likely represent piRNAs (Figure 15A,B). Three additional criteria suggest that these RNAs are *bona fide* piRNAs. First, 10,892 reads matched sequences previously reported to be piRNAs in zebrafish (Houwing et al., 2007). Second, in genome wide, a much, much larger number of reads (674,777 sequences from 1,068,353 reads from shield stage) mapped to transposable elements with a strong bias toward the antisense strand (Figure 15C and Figure 16). Finally, for those reads that mapped to the sense strands of transposable elements, there was a strong preference for an A at position 10 while those derived from antisense strands showed a preference for a U at position 1. This is completely consistent with the Ping-Pong model of piRNA biogenesis (Figure 17). The full list of these small RNAs is deposited at http://www.ncbi.nlm.nih.gov/geo with number GSE27722 (See Materials and Methods).

Over 65% of the piRNA reads that originated from repetitive elements were derived from the LTRs of transposable elements (Figure 18). A different subset mapped back to unique genomic loci, primarily intergenic regions of the zebrafish genome. For both, the reads showed a periodicity and strand preference. Based on the genomic loci of both types of piRNAs, it appears that the majority of the piRNA reads are derived from

long transcripts that are then subsequently processed into smaller RNAs. The genomic regions that give rise to these long transcripts are referred to as piRNA clusters (Brennecke et al., 2007; Houwing et al., 2007). We defined piRNA clusters as genomic fragments encoding at least 10 unique piRNAs with gaps no greater than 1kb (Supplemental Table 3). By grouping reads into defined piRNA clusters, we were able to quantify expression patterns based on the abundance of clusters instead of absolute piRNA reads, allowing examination of the expression of piRNAs during early zebrafish development. Previous work reported piRNA expression in adult ovaries and testes (Houwing et al., 2007) but we detected widespread embryonic piRNA expression across all 4 developmental stages (Figure 15D, E). Beginning at the sphere stage and becoming much more prevalent at the shield stage, we detected increased piRNA expression (Figure 15D-G). The increase was not due to a decrease in other small RNAs because the sequencing runs were not saturated and, for example, we detected a robust increase in piRNA reads between 256-cell and sphere stage embryos, coincident with the large increase in *miR-430* reads. This suggests enhanced transcriptional activity of piRNA clusters and transposable elements with a resultant increase in piRNA production that likely functions to maintain genome integrity during early cell divisions and as germ cells are set aside. Compared to piRNA expression data from adult ovaries and testes (GEO: GSE7131; http://www.ncbi.nlm.nih.gov/geo/ under series number GSE7131) (Houwing et al., 2007), there is a significant reduction in piRNA expression in adult tissues compared to the early developmental stages we examined. At least for ovaries and testes, the expression patterns in adult tissues most closely resemble those observed at the 256-cell stage. This is consistent with maternally contributed piRNAs being most similar in pattern to those detected in ovaries and testes.

Previous analysis of piRNAs in zebrafish showed that in adult ovaries and testes, the majority of piRNAs are derived from the plus strands of genome (Houwing et al., 2007). In contrast, during early development, we observed a preference for piRNAs from minus strands (Figure 15F, G). Given the fact that zebrafish piRNAs have a strong bias toward the antisense strand of transposons, this suggests that the expressed transposable or repetitive elements that are associated with piRNAs at very early developmental stages are, at least partially, different from those expressed in adult ovaries and testes. It is not clear why such strand preferences exist at the different times of development. Regardless of strand of origin, the data suggest that piRNAs have important functions not only in adult ovaries and testes but also at multiple stages of early development.

Figure 15. Zebrafish piRNA expression.
(A, B) After filtering out miRNA reads, the size distribution and abundance of reads mapping to unique (A) or repetitive (B) genomic loci is shown. Different colors represent reads from different developmental stages.
(C) Correlation between the abundance of reads derived from shield stage small RNAs and the density of transposable elements along chromosome 11. At the top, small RNAs that map to chromosome 11 are indicated either as unweighted (gray), meaning the total number of reads irrespective of how many positions (copies) along a chromosome that might encode this RNA, or weighted (orange line), meaning the total number of reads divided by the number of positions or copies within the zebrafish genome. Transposable elements and transposons were divided into DNA/LTR (blue) and LINE/SINE (red) based on the origin of the small RNA reads. The density of repetitive elements (ratio) was determined by the percentage of nucleotides mapping to transposable elements per 50kb.
(D, E) Genomic localization of piRNA clusters. Vertical lines represent piRNA clusters from 4 developmental time points and also from data generated from adult ovaries and testes across either chromosome 4 or 5. Red lines indicate plus strands while the blue lines indicate minus strands.
(F, G) Quantification of expression of piRNA clusters from total reads (F) or reads derived from unique genomic loci (G). Black and white columns represent the strands from which the reads originated.

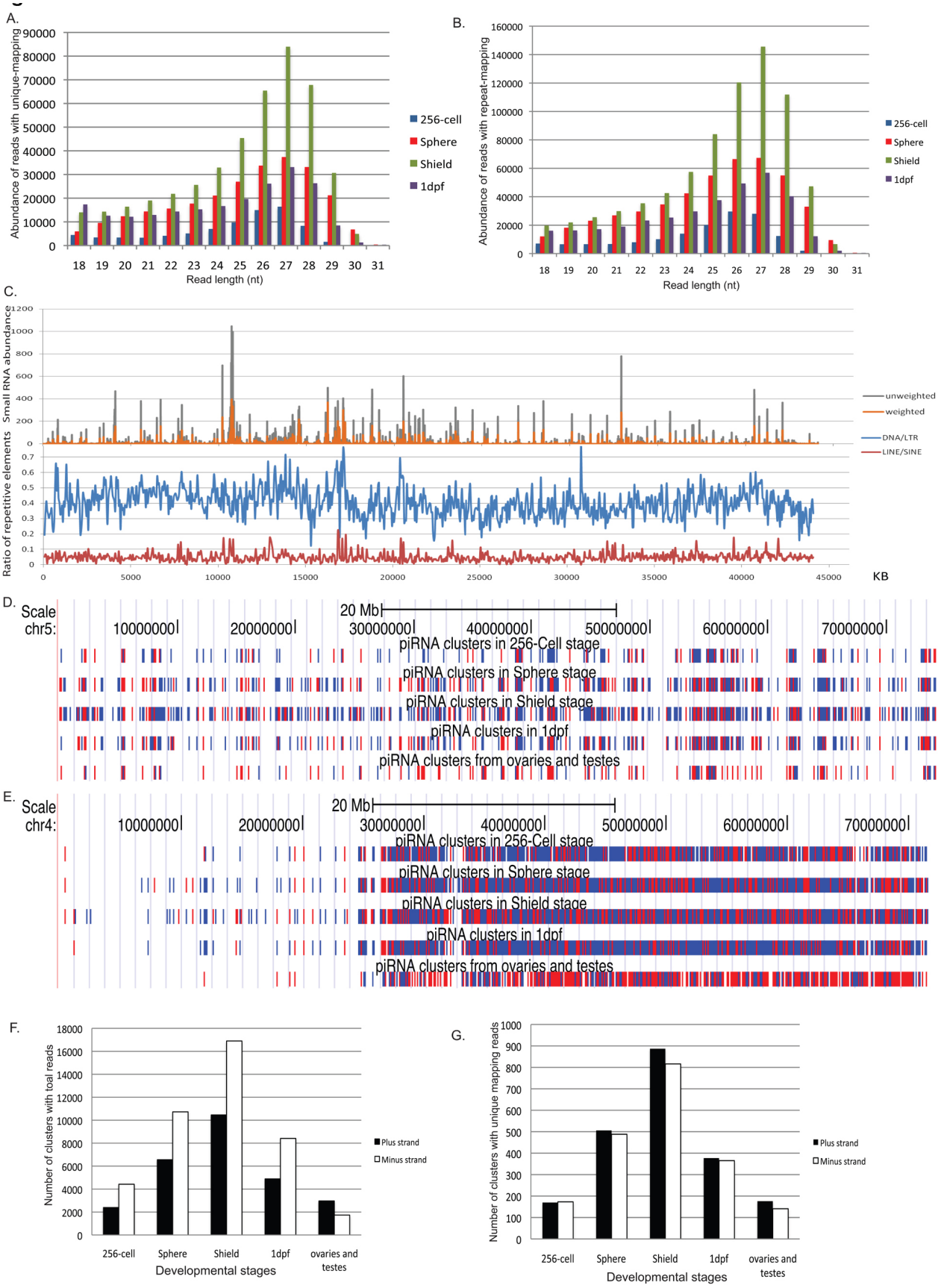
A.
Abundance of reads with unique-mapping
Read length (nt)
256-cell
Sphere
Shield
1dpf
B.
Abundance of reads with repeat-mapping
Read length (nt)
256-cell
Sphere
Shield
1dpf
C.
Small RNA abundance
Ratio of repetitive elements
unweighted
weighted
DNA/LTR
LINE/SINE
KB
D.
Scale
chr5:
20 Mb
piRNA clusters in 256-Cell stage
piRNA clusters in Sphere stage
piRNA clusters in Shield stage
piRNA clusters in 1dpf
piRNA clusters from ovaries and testes
E.
Scale
chr4:
20 Mb
piRNA clusters in 256-Cell stage
piRNA clusters in Sphere stage
piRNA clusters in Shield stage
piRNA clusters in 1dpf
piRNA clusters from ovaries and testes
F.
Number of clusters with toal reads
Plus strand
Minus strand
256-cell
Sphere
Shield
1dpf
ovaries and testes
Developmental stages
G.
Number of clusters with unique mapping reads
Plus strand
Minus strand
256-cell
Sphere
Shield
1dpf
ovaries and testes
Developmental stages

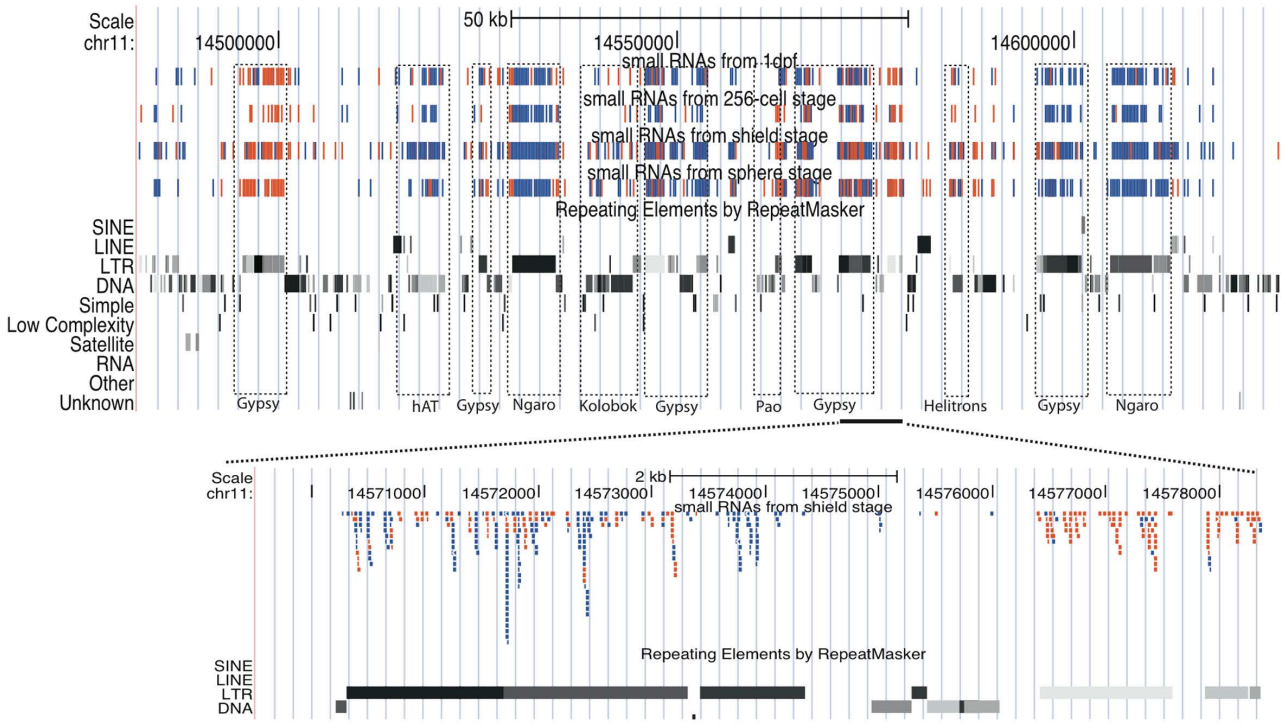

Figure 16. Genomic organization of piRNA reads.
Small RNA reads were mapped to transposable elements along chromosome 11. Each short vertical line represents a small RNA read with red indicating the plus strand and blue indicating the minus strand. Reads from 4 developmental stages were mapped, as indicated. The different classes of repeats along chromosome 11 were annotated by RepeatMasker and are as marked in the lower half of the figure as are the positions of transposable elements. At bottom, an enlarged window of RNA reads from the shield stage were mapped with blue and red indicating strand origin, as above, and the number of the dots indicating read frequency.

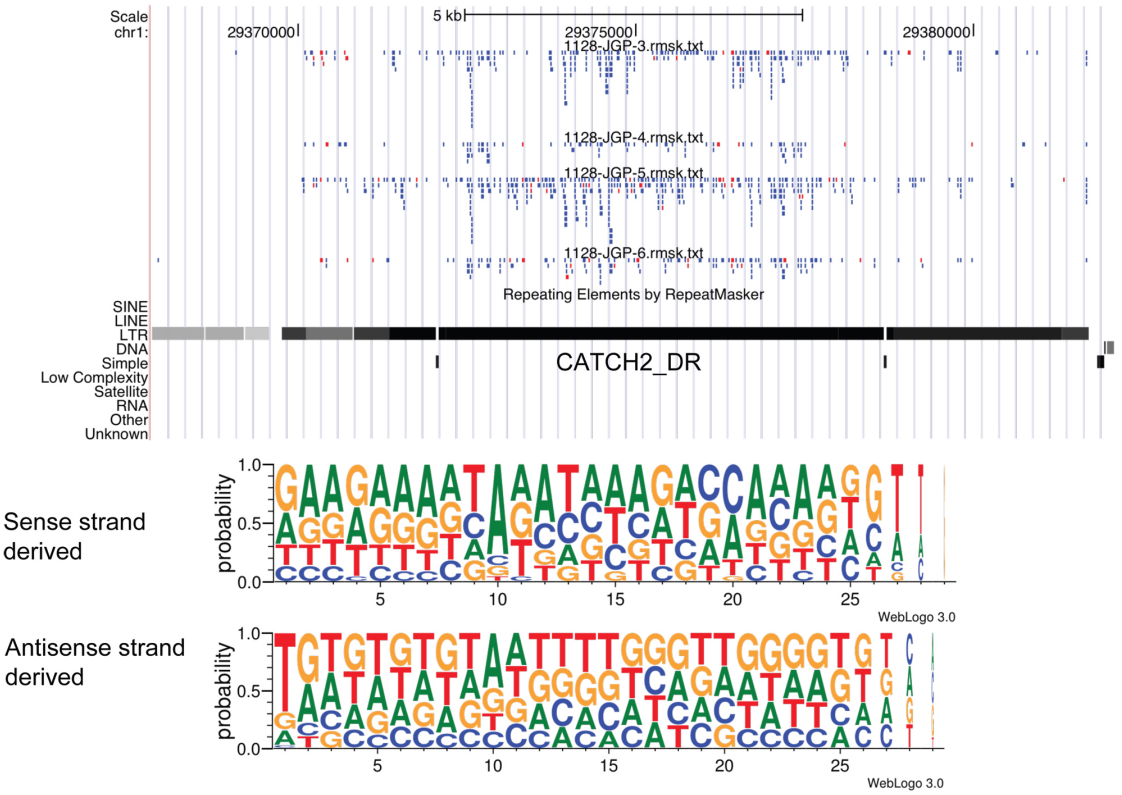

Figure 17. Small RNA reads derived from transposable elements.
Small RNA reads derived from CATCH2, an LTR-containing transposable element, were split into those derived from the sense strand (red) and those from the antisense strand (blue). The average size of these RNAs is 25.4 nucleotides. Below is shown the sequence composition of these RNAs with the size of each letter indicating the frequency of detection. Sequence logos were generated using WebLogo (http://weblogo.threeplusone.com/) (Crooks et al., 2004; Schneider and Stephens, 1990).

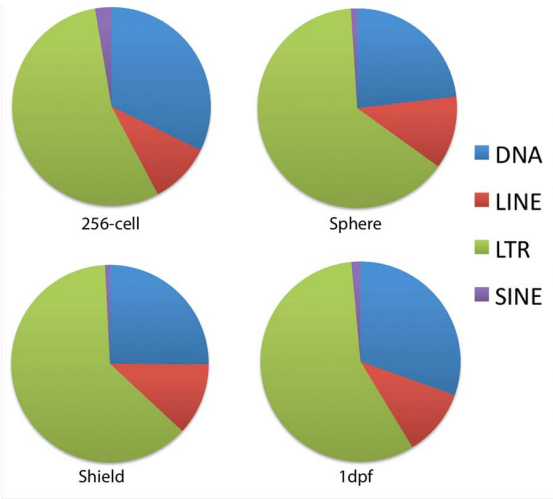

Figure 18. Origin of RNAs derived from repetitive genomic elements.
The read frequency of small RNAs derived from the indicated genomic origin are shown across four developmental stages.

tRNA-derived small RNAs in zebrafish

In addition to miRNAs and piRNAs, we also detected a large number of other small noncoding RNAs. One particularly interesting subset (~225 different sequences; 56,311 total reads) was derived from tRNAs (Figure 19). These RNAs matched the 5' and 3' ends of tRNAs with a size range between 18-28 nt (Figure 19A, B and Supplemental table 4). The 3' end reads contained the universal 3' CCA sequence that is added post-transcriptionally indicating that these RNAs are derived from mature tRNAs, consistent with previous reports (Cole et al., 2009; Haussecker et al., 2010; Lee et al., 2009). Interestingly, the sizes of the 3' tRNA reads are mainly 18 nt, while the 5' tRNA reads are distributed more widely, suggesting they might be under different selection mechanisms or have different functions (Figure 19B). Given the non-random accumulation of these small RNAs from just the 5' and 3' ends, it is hard to argue that these RNAs are degradation products. Indeed, other reads across the entire mature tRNA sequence were observed at much, much lower frequencies (17-fold less at 256-cell and 1dpf, Figure 19C). We note that the tRNA-derived fragments we detect are likely different from angiogenin-mediated tRNA fragments found in stress-induced cells because the cleavage sites we detect are different from those reported (Emara et al., 2010; Thompson et al., 2008; Yamasaki et al., 2009).

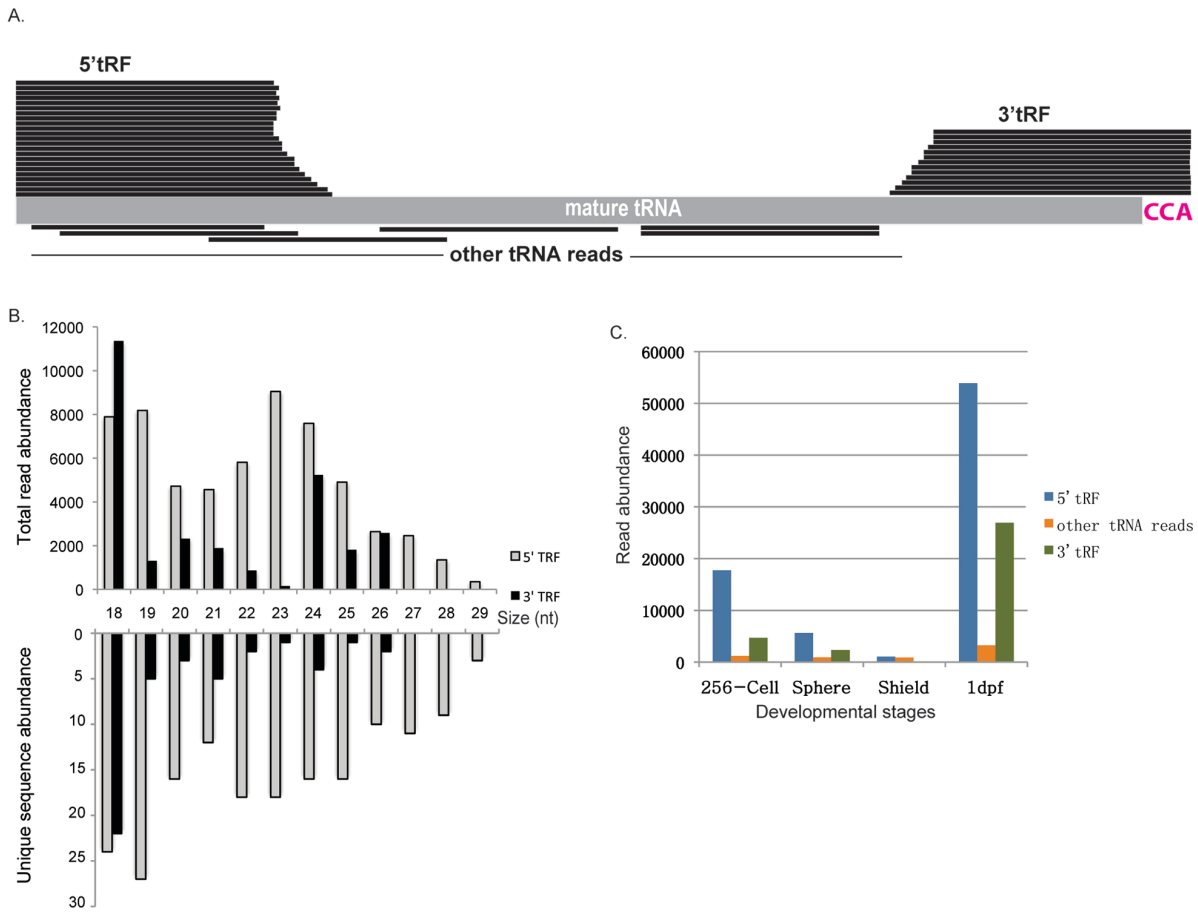

Figure 19. Zebrafish tRNA-derived Fragments (tRF).

(A) Graphic representation of tRF alignments to zebrafish tRNAs. Most reads mapped to the 5'and 3' ends or mature tRNAs. (B) Size distribution of all identified tRF reads from 4 developmental stages in terms of either unique read sequence abundance or total read abundance. (C) The raw abundance of the 5' tRF and 3' tRF reads at 4 developmental stages, as indicated.

Discussion

miRNA Expression

miRNAs are postulated to play important roles during the maternal-zygotic transition, when embryos reshape and reprogram the transcriptional landscape (Giraldez, 2010). Using deep-sequencing, we determined the expression patterns for 198 distinct miRNAs and we identified 5 novel miRNAs and 3 new conserved zebrafish miRNAs expressed during early development. Maternally inherited miRNAs and a subset of miRNAs that are expressed very early in development are important for zebrafish embryogenesis (Giraldez et al., 2005a; Giraldez et al., 2006a). Compared to prior approaches involving direct cloning or microarrays, the increased sensitivity of miRNA detection with deep sequencing affords the opportunity to more completely define the expression patterns, and ultimately the function, of small noncoding RNAs during early vertebrate development, including those expressed in single cells or specific tissues (Thatcher et al., 2007; Wienholds et al., 2005b). The 198 miRNAs that we identified and profiled can be classified into 122 miRNA families. 70% of these families are expressed at or below the limits of detection using microarrays. Fortunately, for those miRNAs expressed at detectable levels using microarrays, there was a strong correlation between the data sets lending confidence that data generated from our sequencing libraries are accurate (Thatcher et al., 2007; Wienholds et al., 2005b).

Previous studies showed that zebrafish miRNA expression patterns become increasingly complex as development proceeds (Thatcher et al., 2007; Wienholds et al., 2005b). Our results revealed more widespread miRNA expression at earlier stages of development than previously observed. Beginning at the 256-cell stage, a large number

(178 out of 216 currently known zebrafish miRNAs) of miRNAs are detectable with several expressed at relatively high levels. These miRNAs are likely maternally deposited and may either regulate initial development or function similar to the *miR-430* family to target maternally inherited mRNAs for degradation during the maternal-zygotic transition (Giraldez et al., 2005a; Newport and Kirschner, 1982; Schier, 2007). We found that fully 99% of the miRNA reads detected during the sphere stage are derived from *miR-430* family members. Interestingly, maternally inherited miRNAs appear to be rapidly down-regulated during the maternal-zygotic transition raising the possibility that they are subject to similar forms of regulation as maternally inherited mRNAs. Beyond maternally inherited miRNAs, our analyses are also consistent with important early roles for a number of miRNAs including *miR-203*, *miR-1*, and *miR-133*, which function to balance proliferation and differentiation during early development (Mishima et al., 2009; Yi et al., 2008). In contrast to previous results, we detected significant levels of *let-7,* raising the question as to its exact role in early development (Kloosterman et al., 2004; Wienholds and Plasterk, 2005).

Normalization of miRNA Sequencing Data

Often, total genome matching reads are used to account for differences in the sequencing depth of individual libraries when normalizing small RNA sequencing data. This certainly applies when biological replicates are being sequenced, for example, when comparing two independent libraries from the same developmental stage. However, if the overall transcriptome changes dramatically between samples, normalization based solely on total genome matching reads can obscure important biology (Robinson and Oshlack, 2010). During early development, cell numbers are increasing dramatically

concomitant with extraordinary changes in gene expression. This creates a unique set of problems when normalizing the data. We chose to normalize based on the relative expression levels of either *miR-9* or *let-7*. These miRNAs were chosen because they are expressed at moderate levels across the four stages of early development that we examined. The resulting heat maps were very similar, whether using *miR-9* or *let-7* and northern blots of 6 miRNAs were completely consistent with the derived heat maps. Interestingly, when we normalized using TMM, the resulting heat maps were also very similar to those obtained with either *miR-9* or *let-7*. Thus, we believe that the strategy we adopted to normalize small RNA sequencing data during early development is appropriate. Nevertheless, we realize that under conditions where differential gene expression patterns are changing dramatically, every available method has certain limitations and that other methods can certainly be used to quantitatively analyze small RNA sequencing data.

Sequence Variation

miRNA 3' tailing and trimming were previously reported in worms, flies, mouse, and human cells (Ameres et al., 2010; Burroughs et al., 2010; Fernandez-Valverde et al., 2010; Katoh et al., 2009; Landgraf et al., 2007; Lehrbach et al., 2009). We detected many tailed miRNAs containing additional non-template directed nucleotides, mostly A and U, primarily at 3' ends (Fig 13A). The extent of 3' variation may actually be higher than that reported here since in some cases (e.g. *let-7*) the extra A and U residues match the pre-miRNA flanking sequence so their origin is not clear. The temporal pattern of A versus U tailing suggests that the addition of A residues might stabilize miRNA half life whereas U addition may promote degradation. This seems to hold true for the *miR-430*

family but may apply more broadly since we detected a large percentage of tailed miRNAs during very early development with decreasing modification at the later stages. It is possible that different mechanisms regulate miRNA half life during the maternal zygotic transition compared to later stages but our data suggest a common mechanism.

piRNA Expression

piRNAs have been reported to be specifically expressed in the germline to maintain genome integrity (Halic and Moazed, 2009). We identified many piRNAs in 256-cell stage embryos, consistent with maternal inheritance. We also found a peak of piRNA expression at the shield stage with readily detectable levels out to 1 dpf. Except for the shield stage, the pattern is similar to that reported in mouse embryos (Ohnishi et al., 2010). However, the robust expression levels at the shield stage, when the germ layers are forming, may indicate an important function for piRNAs during early development. Previous work has reported that piRNAs can induce deadenylation and decay of *nanos*, a maternal mRNA in *Drosophila* embryos (Rouget et al., 2010). In zebrafish, primordial germ cells (PGCs) are first specified before sphere stage during embryogenesis and give rise to germ cells after proper migration and further differentiation (Knaut et al., 2000). Zebrafish PGCs show maximal migration activity amongst a far larger number of somatic cells at the beginning of gastrulation (5.5-6 hpf) (Blaser et al., 2005; Raz, 2003). The shield stage coincides with gastrulation suggesting that the widespread expression of piRNAs that we detect at this time may play an important role in the maintenance and proper migration of PGCs. Only a very limited number of PGCs have formed or are forming during this time raising the possibility of piRNAs originating from other cells besides PGCs in embryos. Consistent with a

requirement for piRNAs during these early stages, morpholino mediated knockdown of Ziwi protein inhibited and/or blocked proper germ cell migration (H. Dai, C. Wei, and JG Patton, unpublished). Future studies are needed to understand the temporal and spatial manner of piRNA expression and their specific functions during early embryonic development.

tRNA derived small RNAs

Small tRNA-derived fragments were previously reported in different cell lines (Cole et al., 2009; Haussecker et al., 2010; Lee et al., 2009). Our sequencing analyses expand the number of species that express this class of small RNA, indicating that the biogenesis and function of tRNA-derived small RNAs is conserved, suggesting an important role. Several lines of evidence raise the possibility that these small RNAs function in gene silencing in a Dicer-independent manner (Cole et al., 2009; Haussecker et al., 2010). It will be important to determine how or whether these RNAs regulate gene expression, especially in light of the fact that these RNAs are themselves temporally regulated during development.

Materials and Methods

Sequence libraries availability

Sequencing data have been deposited into http://www.ncbi.nlm.nih.gov/geo under the series number GSE27722, and public data with series number GSE7131 are available at http://www.ncbi.nlm.nih.gov/geo/.

Small RNA purification, cloning, and sequencing

Zebrafish embryos were collected at the 256-cell stage, sphere stage, shield stage, and 1 day post fertilization (dpf). Total RNA was isolated from embryos using Trizol. RNAs were fractionated on 15% denaturing polyacrylamide gels and small RNAs between 15-30 nucleotides were excised and purified. cDNA libraries were generated using specific linkers and RT/PCR, as previously described (Hafner et al., 2008). Libraries were sequenced in the Genome Technology Core of Vanderbilt University using the Illumina sequencing platform. The numbers of sequencing reads from the 4 developmental stages are listed in Supplemental table 5.

3' ligation adaptor: AMP-5'pCTGTAGGCACCATCAATdideoxyC-3'.

5' ligation adaptor: 5'-ACACUCUUUCCCUACACGACGCUCUUCCGAUC-3'.

RT primer: ATTGATGGTGCCTACAG.

PCR forward primer:

5'AATGATACGGCGACCACCGAACACTCTTTCCCTACACGACG-3'.

PCR reverse primer:

5'-CAAGCAGAAGACGGCATACGATTGATGGTGCCTACAG-3'.

Small RNA identification

Initial reads were processed to remove the linker sequences using an in-house dynamic alignment algorithm, which allows one mismatch and a minimal 5 starting nucleotides in the linker sequences. Small RNAs matching the zebrafish genome (Zv8) from Ensembl (http://www.ensembl.org) were retrieved with Bowtie, a short read alignment algorithm widely used for aligning short DNA sequences, using the default

parameters which allow at most 2 mismatches in the "seed of 28 nt" with maximum quality values of 70 (Langmead et al., 2009). After elimination of reads derived from known mRNAs, tRNAs, rRNAs and snRNAs, miRNAs were next annotated based on a perfect match to miRNA hairpin sequences as reported in miRbase (http://www.miRbase.org) with further filtering to remove reads derived from miRNA passenger strand and loops. To identify miRNA reads with non-template-directed nucleotide additions, reads with exactly one mismatch at the very 3' end were specifically retrieved form the original data set. For analysis of known miRNAs, sequencing frequencies of less than 2 reads per library were discarded. For quantitation of expression levels, miRNA reads with non-templated addition of 3' nucleotides were included in the counts.

To identify piRNAs, consensus sequences from zebrafish repetitive elements were retrieved from Repbase (Kohany et al., 2006) (http://www.girinst.org/repbase/index.html) and Repeat Maskers using the UCSC genome browser (http://genome.ucsc.edu). Small RNAs perfectly mapping to these consensus sequences and their genomic flanking regions were sorted into piRNA libraries. piRNAs with unique mapping positions in the genome were isolated and analyzed independently. For piRNAs with multiple mapping positions, the abundance of each piRNA was weighted by the number of the piRNA reads divided by the number of its genomic mapping positions, assuming all genomic loci contribute equally to overall read numbers. piRNA clusters were manually defined as genomic loci when at least 10 different piRNAs mapped to positions with less than 1kb between the reads, as previously described (Brennecke et al., 2007; Houwing et al., 2007).

miRNA prediction

We prepared libraries from RNAs between 15-30 nucleotides but only analyzed genome-derived small RNAs of 18 nt or longer that aligned to known hairpin sequences from other species listed in miRbase (http://www.mirbase.org/ftp.shtml). Small reads either perfectly matching the stem regions of these hairpins or overlapping with known mature or passenger miRNAs were then retrieved using Bowtie with default parameters. The dynamic stability of secondary structures of flanking genomic sequences for all retrieved RNAs and their relative localization in the zebrafish genome were further analyzed using RNAfold (Hofacker, 2003) (http://rna.tbi.univie.ac.at/cgi-bin/RNAfold.cgi). Predicted hairpin sequences sharing high similarity with known hairpins from other species were further screened focusing on the small RNAs on the stem regions to identify putative zebrafish miRNA homologs. For prediction analyses, RNAs whose sequencing frequency was less than 5 reads per library were discarded. The 5' ends of novel miRNAs were determined by the starting position of the most abundant small RNA reads mapping to the stem of putative hairpin sequences. Predicted miRNAs were further validated in Ensembl using RFAM and miRBase. Also, miRDeep was independently utilized to predict novel miRNAs from raw sequence data (Friedlander et al., 2008). To identify novel miRNAs, samples from the 4 different stages were subjected to miRDeep analysis with a cutoff score of 2. Predicted miRNAs by miRDeep were further filtered by aligning to the databases of known miRNAs (miRBase), transposable elements, rRNAs, tRNAs, snRNAs and other known small RNAs (UCSC genome browsers). To ensure the authenticity of this predicted miRNAs, only small RNAs that appeared in at least 2 developmental stages were retained. From among the

327 novel miRNAs predicted by miRDeep, 5 were finally recognized as authentic novel miRNAs.

qRT-PCR

qRT-PCR assays (Taqman RT kit and Taqman miRNA custom assays, ABI) were performed to measure the expression levels of *let-7a* and *miR-9*. Relative levels were normalized to U6 snRNA. cDNAs were synthesized from 10ng of total RNA extracted from zebrafish embryos. Products of RT reactions without reverse transcriptase served as a negative control and each measurement was derived from three biological replicates. Expression levels were determined based on the threshold cycle values (C_t) of each miRNA relative to that of U6 and assigned as $2^{-\Delta\Delta Ct}$.

Northern blots

18-23mg of total RNA was extracted from zebrafish embryos at different developmental stages, separated on 15-20% denaturing polyacrylamide gels, and transferred to membranes for northern blot analysis of known miRNAs following procedures as previously described ((Thatcher et al., 2007; Wienholds et al., 2005b). For novel miRNA detection, 13-15μg of small RNAs (less than 200nt) were enriched from 220-250μg total RNA extracted from 1dpf zebrafish embryos using mirVana miRNA isolation kits (Applied Biosystems). The sequences of miRNA northern probes (miRNA StarFire probes, IDT) were complementary to the mature sequences for as *let-7a, miR-455, miR-21, miR-22a, miR-200b, and miR-430b*. For the novel miRNAs, the probes were as follows:

novel miRNA 1: GGTAACCATTGGCTTCCATTGT;

novel miRNA 2: AACTGGTAACCATTGACCTTCA;

novel miRNA 3: ACTGGCTACCAGCATGGTACA;

novel miRNA 4: CAGTATCAGCGAGTATTTCCAT;

novel miRNA 5: CCTTCCAGTGTAGGATTCACA;

novel miRNA 7: TGGACGTTTGCAGGGGAGGTGG;

novel miRNA 8: GGAACCCTTCTCCACTTC.

miRNA Expression Profiles

Absolute read numbers were collected and sorted into miRNA families based on sequence records in miRbase. We defined miRNA families as those miRNAs sharing the same seed sequence along with high sequence similarity toward the 3' end. We also normalized expression levels across four developmental stages relative to *let-7a* and *miR-9* levels, as determined using qRT-PCR. Read numbers were transformed into log2 values and displayed with MultiExperiment Viewer (Saeed et al., 2006; Saeed et al., 2003) (http://www.tm4.org/mev/). The raw log2 value of all single miRNAs and miRNA families throughout development are listed in Supplemental Table 6.

Acknowledgements

We thank Elizabeth Thatcher, Nan Li, and Stacey Lawrence for their assistance in preparing the small RNA libraries. This work was conducted in part using the resources of the Advanced Computing Center for Research and Education at Vanderbilt University and was supported by grants from the National Institutes of Health to JGP (GM 075790 and EY019759), the Searle Scholars Program (AR), and the National Science Foundation

(DEB-0844968 to AR). CW was supported in part by a Discovery Grant from Vanderbilt University.

CHAPTER 3:

miR-153 Regulates SNAP-25, Synaptic Transmission, and Neuronal Development[1]

Chunyao Wei, Elizabeth J. Thatcher, Abigail F. Olena, Diana J. Cha, Ana L. Perdigoto, Andrew F. Marshall, Bruce D. Carter, Kendal Broadie, and James G. Patton[2]

Department of Biological Sciences and Department of Biochemistry, Vanderbilt University and Medical School, Nashville, TN 37235 USA

[1] This work has been published. Wei, C., Thatcher, E.J., Olena, A.F., Cha, D.J., Perdigoto, A.L., Marshall, A.F., Carter, B.D., Broadie, K., and Patton, J.G. (2013). "*miR-153* regulates SNAP-25, synaptic transmission, and neuronal development." PloS one *8*, e57080.

[2] CW, EJT and JGP conceived and designed the experiments. CW, EJT, AFO, DJC, ALP and AFM performed the experiments. CW, EJT, AFO, BDC, KB and JGP analyzed the data. CW, EJT and ALP contributed reagents/materials/analysis tools. CW, KB and JGP wrote the paper.

Abstract

SNAP-25 is a core component of the trimeric SNARE complex mediating vesicle exocytosis during membrane addition for neuronal growth, neuropeptide/growth factor secretion, and neurotransmitter release during synaptic transmission. Here, we report a novel microRNA mechanism of SNAP-25 regulation controlling motor neuron development, neurosecretion, synaptic activity, and movement in zebrafish. Loss of *miR-153* causes overexpression of SNAP-25 and consequent hyperactive movement in early zebrafish embryos. Conversely, overexpression of *miR-153* causes SNAP-25 down regulation resulting in near complete paralysis, mimicking the effects of treatment with Botulinum neurotoxin. *miR-153*-dependent changes in synaptic activity at the neuromuscular junction are consistent with the observed movement defects. Underlying the movement defects, perturbation of *miR-153* function causes dramatic developmental changes in motor neuron patterning and branching. Together, our results indicate that precise control of SNAP-25 expression by *miR-153* is critically important for proper neuronal differentiation as well as neurotransmission.

Introduction

Trimeric soluble N-ethylmaleimide-sensitive factor attachment protein receptor (SNARE) complexes form the core machinery mediating vesicular exocytosis (Jahn and Scheller, 2006; Sudhof and Rothman, 2009; Wickner and Schekman, 2008). In the nervous system, SNARE complexes are involved in membrane addition during neuronal growth as well as both dense core vesicle (DCV) release of proteins and synaptic vesicle (SV) release of fast neurotransmitters. At synapses, the core SNARE protein SNAP-25 interacts with accessory proteins that together regulate SV exocytosis by linking Ca^{2+} sensing to membrane fusion and neurotransmitter release (Choi et al., 2010; Matteoli et al., 2009; Schiavo et al., 1997; Vrljic et al., 2010). SNAP-25 is a specific target of Botulinum neurotoxin proteases that block vesicle release, resulting in rapid paralysis and death (Blasi et al., 1993; Schiavo et al., 1993). Misregulation of SNAP-25 is associated with several human diseases and neurodegenerative disorders including Huntington's Disease (Smith et al., 2007), Alzheimer's Disease (Dessi et al., 1997), and diabetes (Ostenson et al., 2006).

SNAP-25 is required for action potential-evoked glutamatergic, cholinergic, and glycinergic transmission in neurons (Keller et al., 2004; Washbourne et al., 2002). Mouse knockouts of SNAP-25 are therefore lethal although neuronal cultures from SNAP-25 null mutants maintain the ability to exhibit stimulus-independent transmitter release (Sorensen et al., 2003; Washbourne et al., 2002). GABAergic inhibitory synapses express lower levels of SNAP-25 and may be more sensitive to calcium regulation, whereas glutamatergic excitatory synapses express higher amounts of SNAP-25 that alters calcium sensitivity (Matteoli et al., 2009). Part of this differential regulation could be due to accessory proteins that control SNAP-25 distribution and levels to modulate

synaptic activity (Augustin et al., 1999; Gitler et al., 2004; Schoch et al., 2002). Transcriptional mechanisms regulating SNAP-25 levels have also been suggested to play key roles in the dynamic control of synaptic function (Atouf et al., 1997; Chong et al., 1995; Qureshi and Mehler, 2009; Vo et al., 2010; Wu and Xie, 2006).

Several miRNAs have been shown to regulate synapse formation or homeostasis, mostly within the post-synaptic dendrite (Cohen et al., 2011; Schratt, 2009; Vo et al., 2010). On the presynaptic side, most forms of regulation center on modulation of calcium channels and calcium-dependent vesicle release (Catterall and Few, 2008; Verhage and Sorensen, 2008). In this study, we show that *miR-153* inhibits SNAP-25 expression in the developing nervous system. Precise control of SNAP-25 by *miR-153* is necessary not only for presynaptic vesicle release, but also for protein secretion, motor neuron differentiation, and outgrowth.

Results

miR-153 regulates embryonic movement

miR-153 has been proposed to be one of a limited number of ancient miRNAs that evolved with the establishment of tissue identity (Christodoulou et al., 2010). It is conserved among bilaterians displaying distinct expression patterns in neurosecretory brain cells of the deuterostome marine worm *Platynereis dumerilii* and the protostome annelid *Capitella* (Christodoulou et al., 2010). In zebrafish, *miR-153* is expressed in distinct regions of the developing nervous system and brain, including neurosecretory cells of the hypothalamus (Kapsimali et al., 2007; Wienholds et al., 2005a). Using deep sequencing and *in situ* localization, we detected robust *miR-153* expression in the developing zebrafish brain and reduced, but detectable levels in the spinal cord as early as

the 18 somite stage, with progressively increasing expression thereafter (Thatcher et al., 2007; Wei et al., 2012; Wienholds et al., 2005a).

To determine the function of *miR-153*, we injected either synthetic *miR-153* or antisense morpholino oligonucleotides (MOs) against *miR-153* into single cell embryos and allowed development to proceed for 1-2 days. Two different morpholinos were used to ensure specificity and we verified overexpression and knockdown of *miR-153* using northern blots (Figure 20). No gross morphological changes were observed in injected embryos and normal expression of neuronal markers was detected at the midbrain-hindbrain boundary, inner ear, and retina at 1-2 dpf (data not shown). Despite the lack of morphological changes, we observed striking behavioral movement defects in injected embryos. To quantify movement, embryos were recorded over time (Supplemental Movie 1) with analyses restricted to embryos within the chorion at 24 hpf. Normal zebrafish embryos move within the chorion with a characteristic frequency of ~1 twitch/minute at 24 hpf (Figure 21). Strikingly, embryos injected with *miR-153* were almost completely motionless, with little or no spontaneous movement, although their hearts were beating normally and minimal movement could be elicited by touch stimulation (Figure 21). In contrast, knockdown of *miR-153* caused a dramatic and significant 7-fold increase in the frequency of spontaneous movement (Figure 21). Interestingly, upon touch stimulation, *miR-153* morphants would initially respond with unusually robust, hyperactive movements after which all motion would cease altogether for a period of time (whether touched or not), followed by a resumption of hyperactive movement upon stimulation. At 52 hpf, *miR-153* overexpressing fish embryos were still mostly motionless, while *miR-153* knockdown embryos were still hyperactive (data not shown).

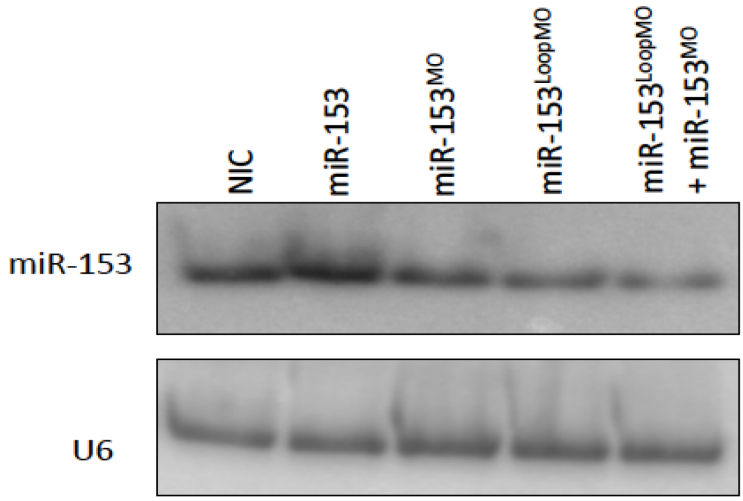

Figure 20. Northern blot of *miR-153* overexpression and knockdown.
Perturbations of *miR-153* expression levels by injection of *miR-153* or MOs against different regions of pre-*miR-153* were verified by northern blot. U6 served as a loading control.

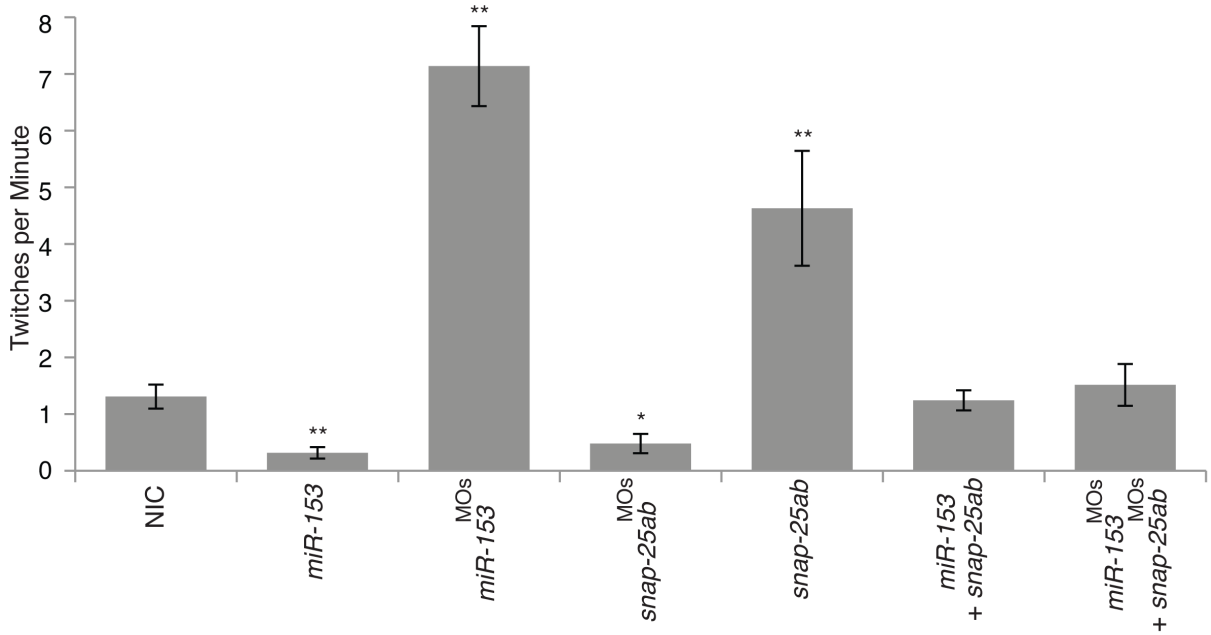

Figure 21. *miR-153* regulates embryonic movement
Embryonic movement was recorded at 1dpf for each of the singly and multiple injected conditions shown (see Movies). The number of twitches per minute was counted and significance determined by comparing the noninjected control (NIC) embryos to all other conditions using ANOVA with Dunnett's post-test. *, $p<0.05$; **, $p<0.01$. Movements were counted for approximately 60 embryos over 2-5 minutes for each condition.

miR-153* targets *snap-25

To identify mRNAs regulated by *miR-153*, we used target prediction algorithms, compared the expression patterns of both potential mRNA targets and *miR-153,* and assayed phenotypes from gain and loss of function experiments. Based on these criteria, *snap-25* proved to be a *bona fide* target for *miR-153* based on the results of reporter silencing experiments and consistent with conservation of miRNA recognition elements (MREs) from fish to humans (Figure 22).

There are two SNAP-25 paralogs in zebrafish (*a* and *b* isoforms) with similar, but not identical, 3' UTRs (Bark et al., 2004; Risinger et al., 1998). For reporter assays, we fused the 3' UTR from both *snap-25* isoforms to the GFP reading frame (*snap-25a* data shown in Figure 23; *snap-25b* shown in Figure 24). Synthetic mRNAs prepared from these reporters were injected into single cell embryos in the presence or absence of exogenous *miR-153* or *miR-153* morpholino oligonucleotides. Based on fluorescence levels in live embryos at 1 dpf, co-injection of *miR-153* resulted in obvious down-regulation of GFP for both isoforms (Figure 23B). To confirm that the loss of GFP was due to pairing with the predicted MREs, we created deletions of individual and combinations of MREs in *snap-25a* and *snap-25b*. Deletion of both MREs from *snap-25a* and all three MREs from *snap-25b* abolished the ability of *miR-153* to silence expression (Figure 23B; Figure 24B). For *snap-25a*, we tested each of the individual MREs and found that deletion of a single MRE resulted in only modest silencing whereas deletion of both MREs caused a loss of silencing. We conclude that *miR-153* targets both isoforms of *snap-25* in an MRE-dependent manner.

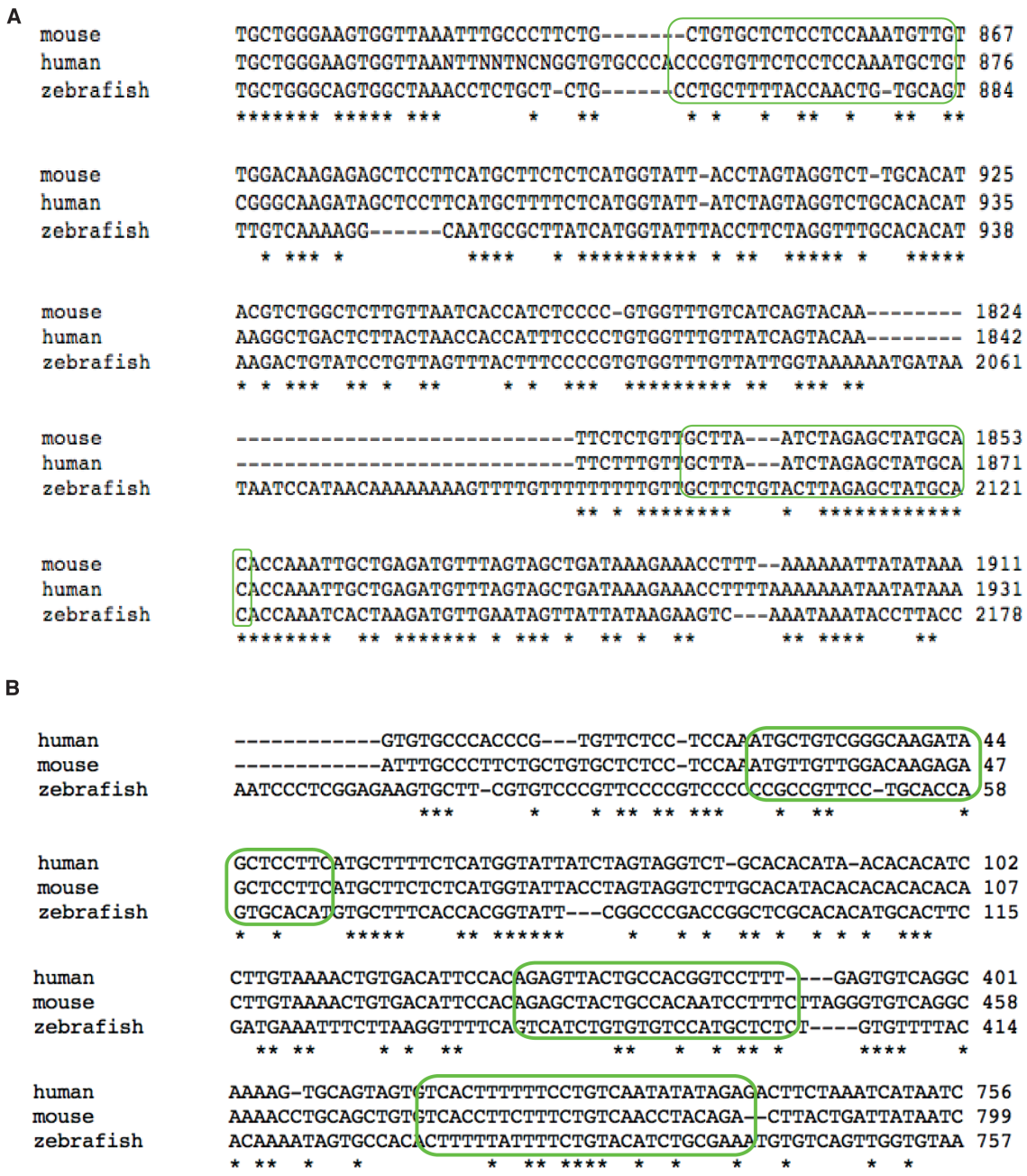

Figure 22. Conservation of *snap-25* 3' UTR sequences.
The 3' UTRs from mouse, human and zebrafish *snap-25a* (A) and *snap-25b* (B) are shown with the MREs that pair with *miR-153* boxed in green. Conserved nucleotides are marked by asterisks. The exact pairings between the MREs and *miR-153* are shown in Figure 2 and Figure S3. Despite different levels of conservation, both MREs in *snap-25a* pair extensively with *miR-153* in the seed region.

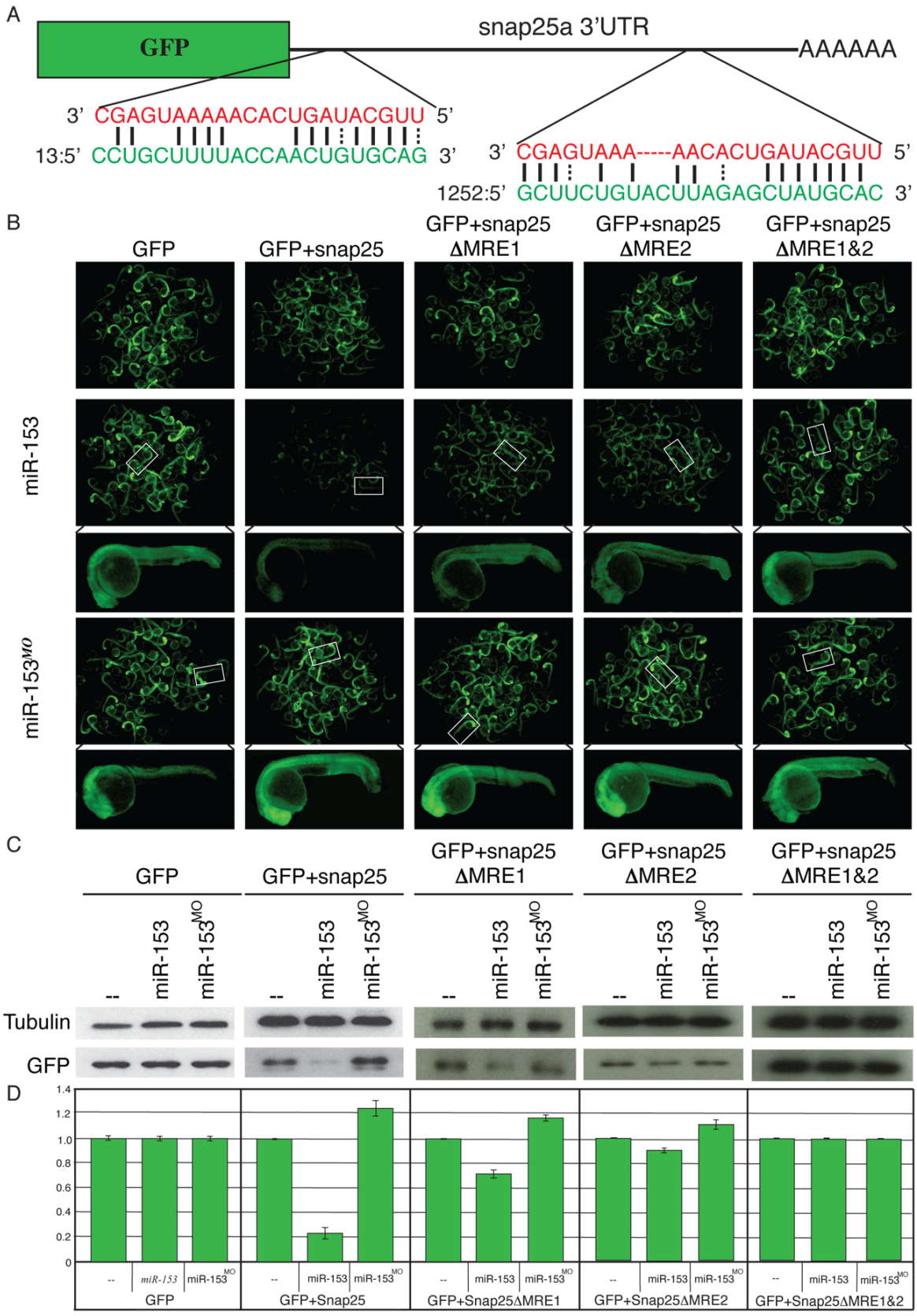
A
GFP
snap25a 3'UTR
AAAAAA
3' CGAGUAAAAACACUGAUACGUU 5'
13:5' CCUGCUUUUACCAACUGUGCAG 3'
3' CGAGUAAA-----AACACUGAUACGUU 5'
1252:5' GCUUCUGUACUUAGAGCUAUGCAC 3'
B
GFP
GFP+snap25
GFP+snap25 ΔMRE1
GFP+snap25 ΔMRE2
GFP+snap25 ΔMRE1&2
miR-153
miR-153MO
C
GFP
GFP+snap25
GFP+snap25 ΔMRE1
GFP+snap25 ΔMRE2
GFP+snap25 ΔMRE1&2
--
miR-153
miR-153MO
Tubulin
GFP
D
1.4
1.2
1.0
0.8
0.6
0.4
0.2
0
GFP
GFP+Snap25
GFP+Snap25ΔMRE1
GFP+Snap25ΔMRE2
GFP+Snap25ΔMRE1&2

Figure 23. *miR-153* targets *snap-25a*
(A) GFP reporter constructs were created by fusing the reading frame of GFP to the *snap-25a* 3'UTR. Two predicted miRNA recognition elements (MREs) were identified in the *snap-25a* 3' UTR. The *miR-153* sequence is indicated in red and the corresponding *snap-25a* UTR sequence is shown in green. (B) Single cell zebrafish embryos were injected with mRNAs derived from GFP reporters lacking a UTR (GFP), fused to the full length *snap-25a* UTR (+*snap-25),* or mutant versions of the *snap-25a* UTR lacking individual MREs (*snap-25a*ΔMRE1 and *snap-25a*ΔMRE2) or both MREs (*snap-25a*ΔMRE1&2). Embryos were injected in the presence or absence of exogenous *miR-153* or morpholinos against *miR-153* (*miR-153*^{MO}). Fluorescence levels were examined at 1dpf. Clusters of embryos (~60) are shown as well as a high magnification image of a single representative embryo. (C) Lysates from ~100 embryos were prepared from embryos treated as in B and GFP protein levels were determined by western blotting using antibodies against GFP or control antibodies against α-tubulin. (D) Quantitation of westerns was performed with a paired Student's t-test (n=5).

Figure 24 *miR-153* targets *snap-25b*.
(A) GFP reporter constructs were created by fusing the reading frame of GFP to the *snap-25b* 3'UTR. Three predicted miRNA recognition elements (MREs) were identified in the *snap-25b* 3' UTR. The *miR-153* sequence is indicated in red and the corresponding *snap-25a* UTR sequence is shown in green. (B) Single cell zebrafish embryos were injected with mRNAs derived from GFP reporters lacking a UTR (GFP), fused to the full length *snap-25b* UTR (GFP+*snap-25b),* or mutant version of the *snap-25b* UTR lacking all MREs (GFP+*snap-25b*ΔMRE1, 2&3). Embryos were injected in the presence or absence of exogenous *miR-153* or morpholinos against *miR-153* (*miR-153*^{MO}). Fluorescence levels were examined at 1dpf. Clusters of embryos (~30) are shown. (C) Lysates from ~100 embryos were prepared from embryos treated as in B and GFP protein levels were determined by western blotting using antibodies against GFP or control antibodies against α-tubulin.

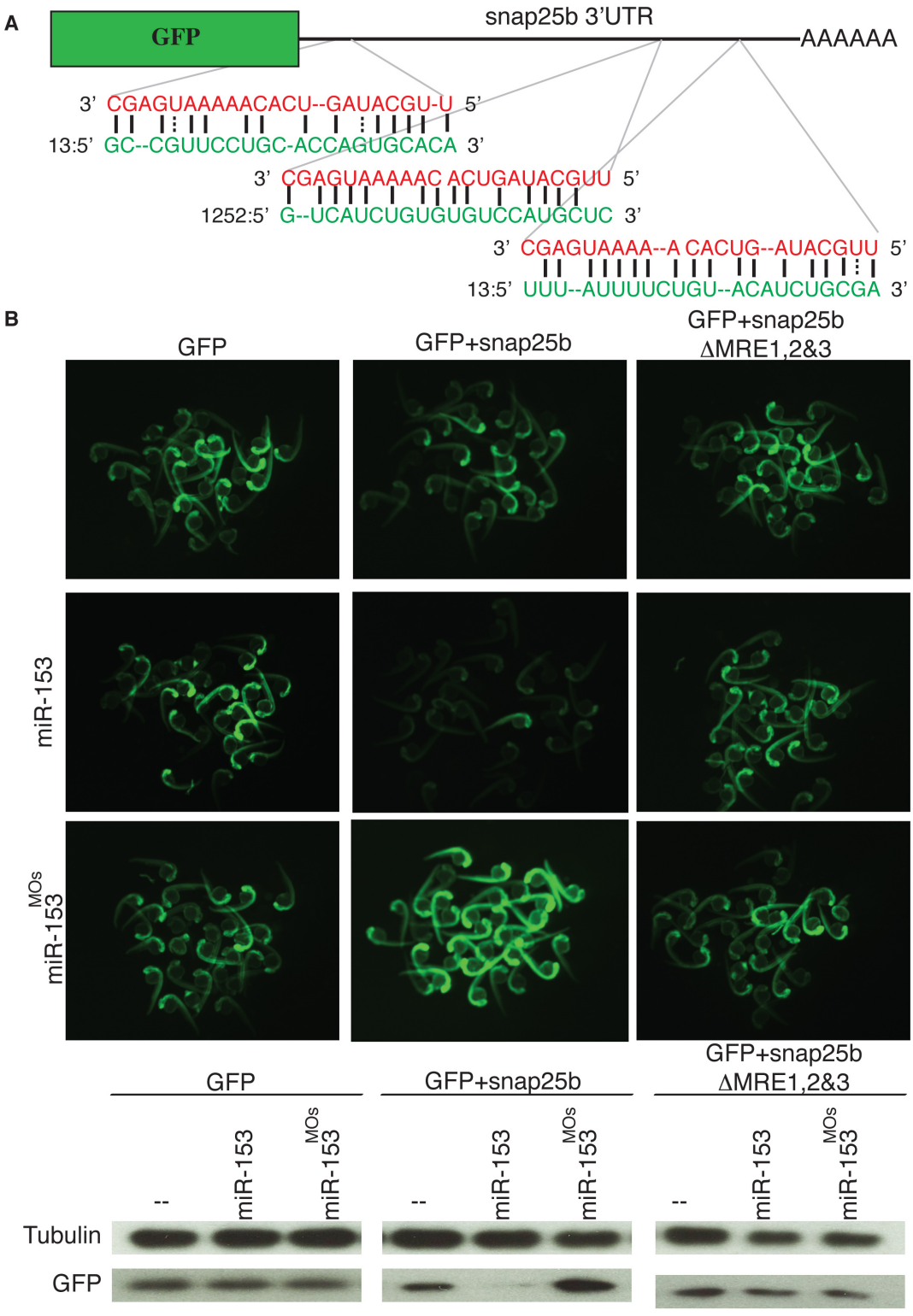
A
GFP
snap25b 3'UTR
AAAAAA
3' CGAGUAAAAACACU--GAUACGU-U 5'
13:5' GC--CGUUCCUGC-ACCAGUGCACA 3'
3' CGAGUAAAAAC ACUGAUACGUU 5'
1252:5' G--UCAUCUGUGUGUCCAUGCUC 3'
3' CGAGUAAAA--A CACUG--AUACGUU 5'
13:5' UUU--AUUUUCUGU--ACAUCUGCGA 3'
B
GFP
GFP+snap25b
GFP+snap25b ΔMRE1,2&3
miR-153
MOs miR-153
GFP
GFP+snap25b
GFP+snap25b ΔMRE1,2&3
--
miR-153
MOs miR-153
Tubulin
GFP

We next tested whether *miR-153* targets endogenous *snap-25*. Single cell embryos were injected with either *miR-153* or antisense morpholinos followed by western blots on pooled 1 dpf embryo lysates using antibodies against SNAP-25. Titration experiments were performed to optimize the levels of injected reagents (Figure 25, 26). After optimization, protein levels were analyzed and fold changes in expression were determined compared to the amounts detected in noninjected controls (NIC) (Figure 27). Under these conditions, excess *miR-153* led to a ~50% decrease in SNAP-25 levels whereas knockdown of endogenous *miR-153* increased SNAP-25 levels ~2-fold. To test for specificity we co-injected embryos with combinations of *miR-153*, *snap-25a,b* mRNAs, or morpholinos against both (Figure 27). Injection of mRNAs encoding *snap-25a,b* resulted in a 2-fold elevation in SNAP-25 levels whereas injection of morpholinos that block the translation start site of *snap-25* led to a ~50% decrease in SNAP-25 levels. Importantly, co-injection of combinations of RNAs and morpholinos could suppress these effects and rescue SNAP-25 levels (Figure 27). For both suppression experiments, the effects were dose dependent. Even though *snap-25a* was more effective than *snap-25b* at rescuing endogenous SNAP-25 levels, combinations of both were most effective (Figure 27). These results indicate specific targeting of *snap-25* by *miR-153*. Although *miR-153* is likely to have additional targets, the ability to specifically rescue the effects of overexpression and knockdown of both *miR-153* and *snap-25* indicates that the effects we observe are specific to targeting of *snap-25* by *miR-153*.

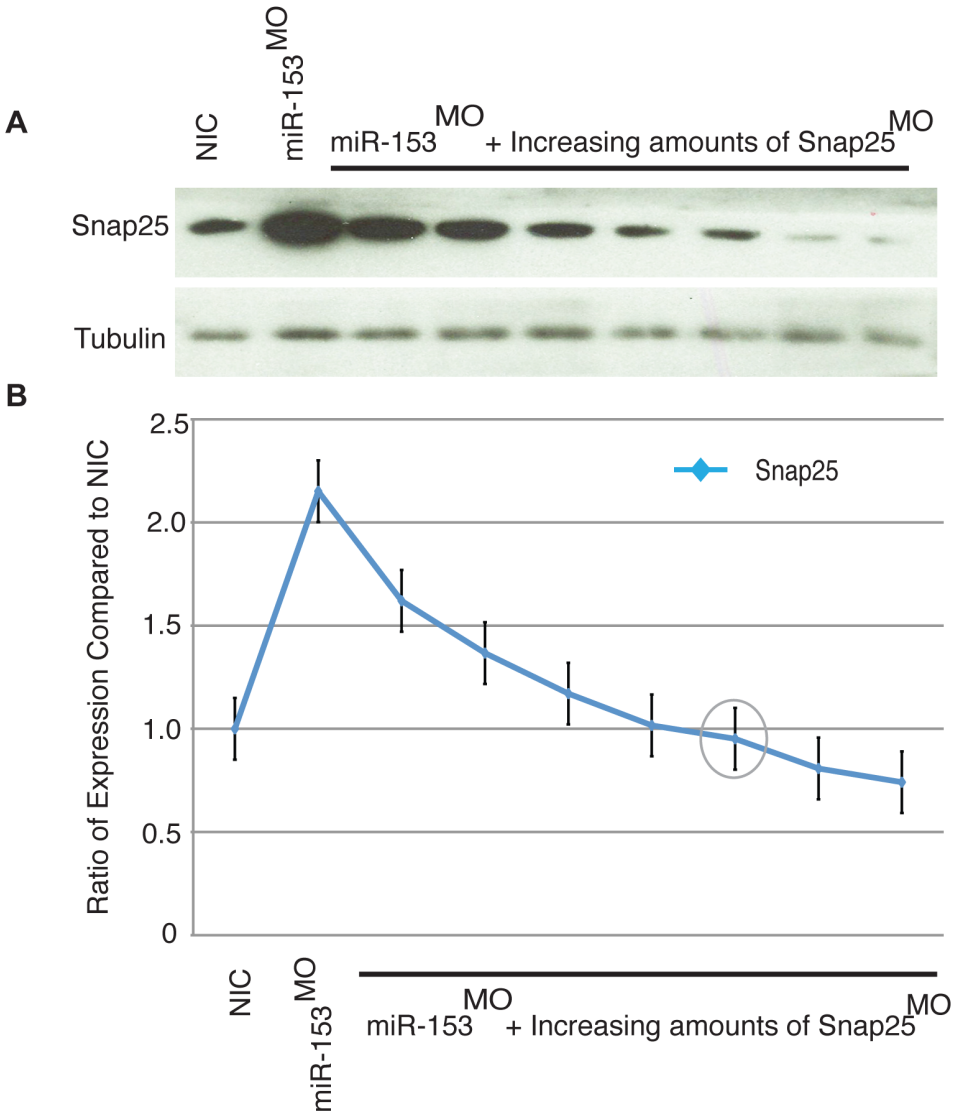

Figure 25. Dose-dependent rescue of *miR-153* knockdown
(A) Single cell embryos were injected with a constant level of *miR-153*^{MO} and increasing amounts (increments of 2ng) of *snap-25*^{MOs}. Embryo lysates from ~60 embryos in each group were prepared and SNAP-25 protein levels determined by western blotting. (B) Quantitation of westerns (n=3) from A. The grey circle represents the amount of *snap-25*^{MO} (10 ng) used in co-injection rescue experiments.

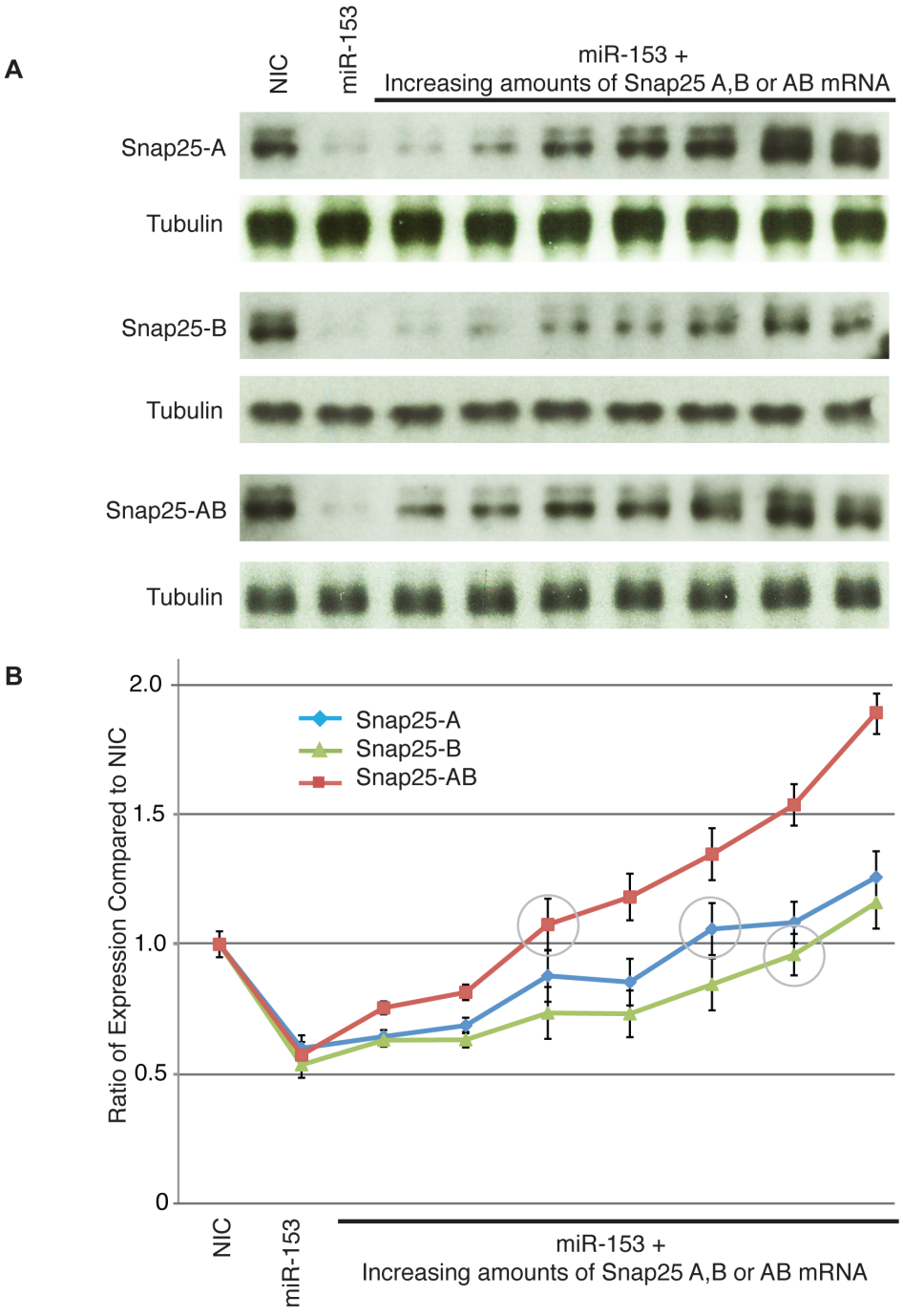

Figure 26. Dose-dependent rescue of *miR-153* over-expression
(A) Single cell embryos were injected with a constant level of *miR-153* and increasing amounts (increments of 50 pg) of *snap-25a*, *snap-25b*, or *snap-25a&b* mRNA. Embryo lysates from ~60 embryos were prepared from embryos in each treatment group and SNAP-25 protein levels were determined by western blotting. (B) Quantitation of westerns (n=3) from A. The grey circles represent the amounts used in co-injection rescue experiments (75 pg each of *snap-25a* and b, 250 pg of *snap-25a*, and 300 pg of *snap-25b*).

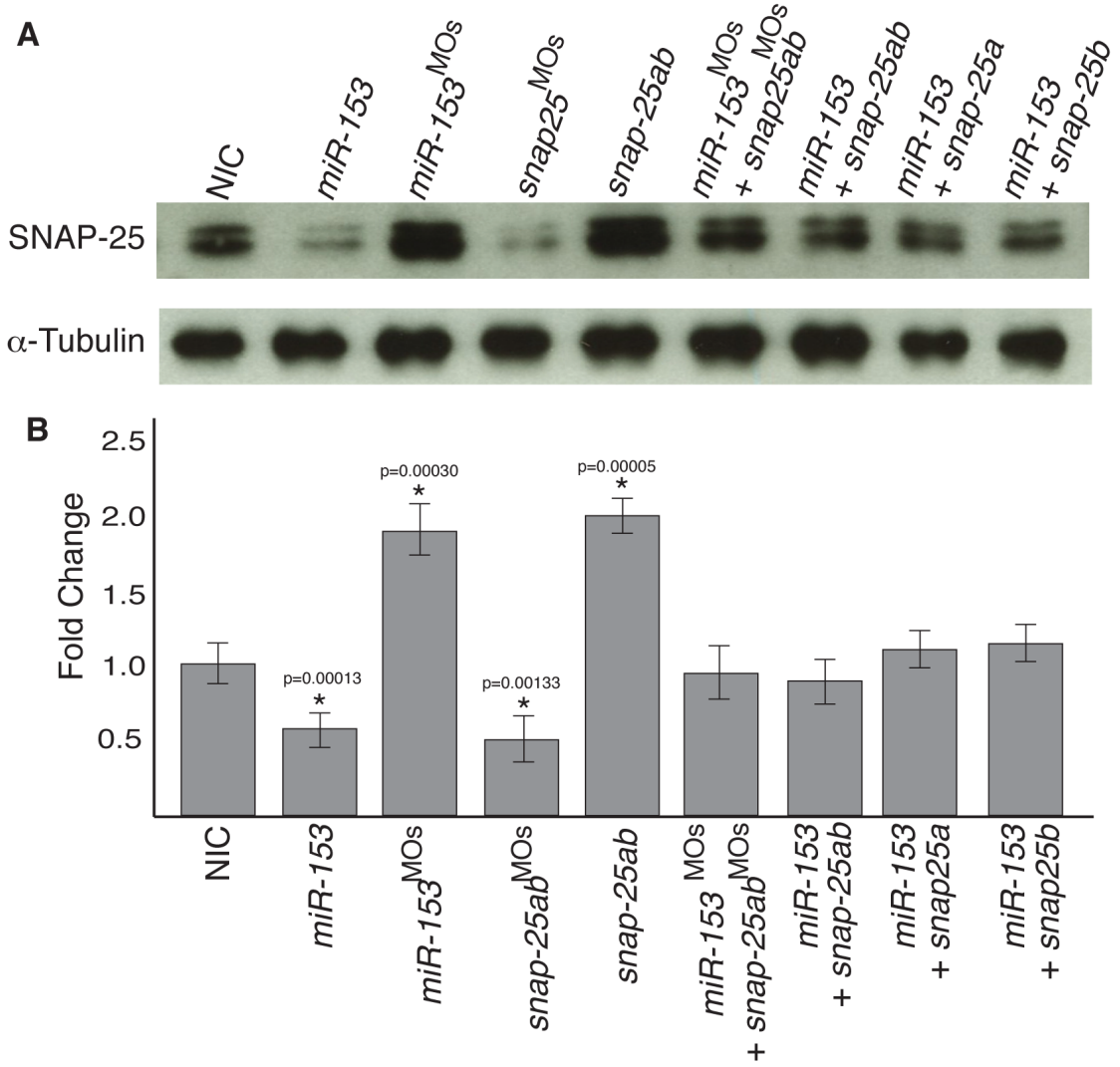

Figure 27. *miR-153* regulates endogenous *snap-25a* expression
(A) Embryo lysates were prepared from either NIC embryos or embryos injected with *miR-153*, *miR-153*^{MO}, mRNAs encoding *snap-25a* and *snap-25b*, morpholinos against *snap-25,* or combinations thereof, as indicated. Western blots were performed using antibodies against SNAP-25 and α-tubulin. (B) Quantification of SNAP-25 levels from the western blots (n=3) shown in A. Significance was determined by a two-tailed Student's t-test. Error bars show s.e.m.

***miR-153* regulates *snap-25* to control movement**

Because we could specifically suppress the effects of overexpression or knockdown of *miR-153* by co-injection of either *snap-25a,b* mRNA or morpholinos against *snap-25a,b*, we next sought to test whether the movement defects caused by altered *miR-153* levels could likewise be rescued in a *snap-25* dependent manner. Embryonic movements were quantitated at 24 hpf after injection of antisense morpholinos against *snap-25* (*snap25*^{MO}) or with *snap-25a,b* mRNAs (Figure 21; Supplemental Movie 1). Knockdown of *snap-25* resulted in dramatically decreased embryonic movements, similar to overexpression of *miR-153* (Figure 21). In contrast, overexpression of *snap-25a,b* increased movement approximately 5-fold over control NIC embryos (Figure 21). For rescue experiments, co-injection of *snap-25a,b* mRNA with *miR-153* restored near normal movement (Figure 21; Supplemental Movie 1). Similarly, co-injection of morpholinos against both *snap-25* and *miR-153* also restored normal movement (Figure 21; Supplemental Movie 1). Thus, not only were SNAP-25 protein levels restored to normal, but also movement defects were suppressed, demonstrating specific targeting of *snap-25* by *miR-153*.

SNAP-25 is a known target of Botulinum neurotoxin (BoNT) proteases A and E (Blasi et al., 1993; Schiavo et al., 1993). If *miR-153* is targeting *snap-25*, the effects of increased *miR-153* should mimic the effects of BoNT A. To test this prediction, injected zebrafish were exposed to BoNT A for 30 minutes at 27 hpf. One hour later, western blots were performed on pooled protein samples to determine whether it was possible to rescue SNAP-25 over-expression phenotypes associated with *miR-153* knockdown or injection of *snap25a,b* mRNAs. Exposure to BoNT A dramatically reduced SNAP-25

levels, recapitulating the effects of *miR-153* knockdown and over-expression (Figure 28A,B). For movement, exposure to BoNT A suppressed the hyperactive phenotypes observed after injection with MOs against *miR-153* or overexpression of *snap-25a&b* mRNAs (Figure 28C; Supplemental Movie 1). Together, these experiments strongly support the conclusion that *miR-153* specifically targets *snap-25* to regulate embryonic movement.

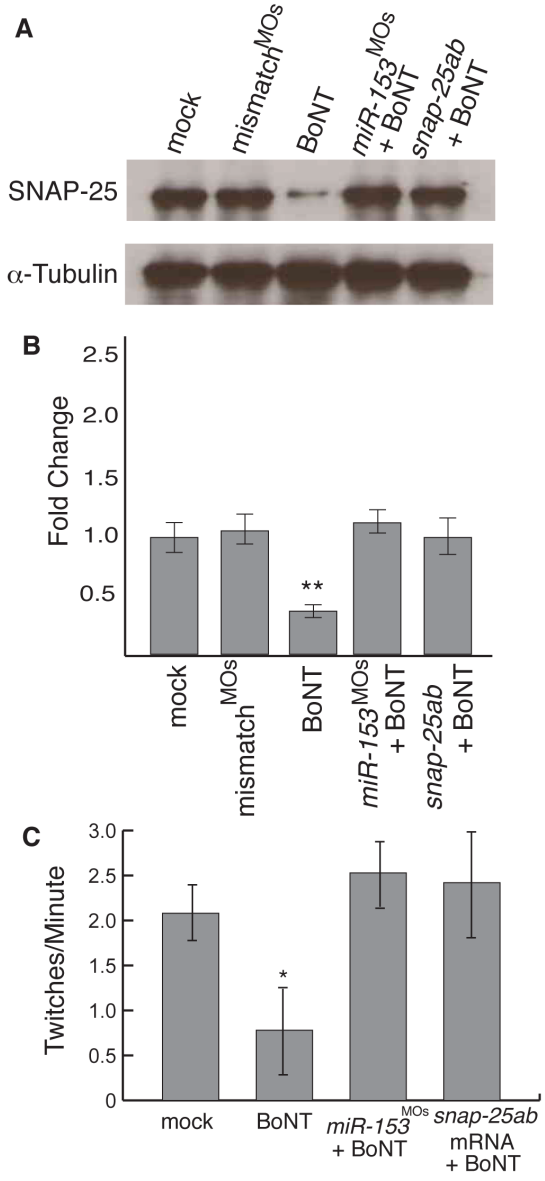

Figure 28. *miR-153* mimics the effects of BoNT A.
(A) Single cell embryos were injected as indicated and then at 27 hpf, exposed to Botulinum neurotoxin A (BoNT) for 30 minutes. After recovery for 1 hour, western blots were performed on embryo lysates using antibodies against SNAP-25 or α-tubulin. (B) Quantitation of SNAP-25 levels from A, n=3. **, $p<0.01$ (C) Embryonic movement in the presence or absence of BoNT A. The number of twitches per minute was counted as in Fig. 1 for embryos treated as indicated. Significance was determined by comparing mock embryos to all other conditions using ANOVA with Dunnett's post-test, n=15. *, $p<0.05$.

miR-153 regulation of motor neuron development

SNAP-25 is a well-characterized t-SNARE protein, with an established function in vesicular exocytosis (Jahn and Scheller, 2006; Sudhof and Rothman, 2009; Wickner and Schekman, 2008). In the developing nervous system, the SNARE complex mediates vesicular membrane addition driving neurite outgrowth and morphological patterning (Hepp and Langley, 2001; Jahn and Scheller, 2006; Sudhof and Rothman, 2009; Wickner and Schekman, 2008). Moreover, DCV-mediated release of signaling proteins and growth factors is important for axon guidance, path finding, and morphological development (Asakura et al., 2010; Cohen-Cory et al., 2010; Lu, 2003; Mai et al., 2009). We therefore sought to determine whether *snap-25* regulation by *miR-153* would alter neuronal morphogenesis. Because zebrafish motor neuron development is well characterized (Appel et al., 1995; Eisen, 1991; Eisen et al., 1986; Lewis and Eisen, 2003; Myers et al., 1986; Westerfield et al., 1986), we decided to focus on the effects of *miR-153* on motor neurons during early zebrafish development.

We first injected *miR-153* or morpholinos against *miR-153* to observe the effects on the development and morphology of motor neurons in a transgenic zebrafish line in which motor neurons are specifically labeled with RFP (*Tg(mnx1:TagRFP-T)* (Arber et al., 1999; Tanabe et al., 1998). Perturbation of *miR-153* levels caused striking changes in motor neuron structure and branching (Figure 29A,B). Compared with NICs, overexpression of *miR-153* dramatically changed the axonal architecture with significant decreases in branch numbers and length (Figure 29C, D). Knockdown of *miR-153* resulted in completely opposite effects with increased motor projection architectural complexity, increased axonal length, and increased branch numbers (Figure 29B-D). To test whether the effects were specific, we conducted rescue experiments, as above.

Injection of *snap-25a,b* mRNA or morpholinos against *snap-25a/b* produced virtually the same phenotypes observed in embryos subjected to *miR-153* knockdown or overexpression, respectively. In contrast, co-injection of *miR-153* and *snap-25a,b* mRNAs or morpholinos against *miR-153* and *snap-25a,b* almost completely restored the normal patterning and branching of motor neurons (Figure 29B-D). These results indicate that *miR-153* regulates motor neuron development via control of *snap-25a,b*.

To further dissect the function of *miR-153* on motor neuron development, immunofluorescence was performed on whole-mount zebrafish embryos (55hpf) with antibodies that label primary (Znp-1 or anti-synaptotagmin 2) or secondary (Zn-8 or Alcama) motor neurons (Trevarrow et al., 1990). Compared to NIC embryos, a striking difference in primary motor neuron axon architecture was observed with both *miR-153* overexpression (*miR-153*) and knockdown (*miR-153*^{MO})(Figure 30). A significant decrease in branching was observed in *miR-153* injected embryos whereas knockdown of *miR-153* caused a dramatic increase in branching. Likewise, injection of *snap-25a,b* mRNA led to increased axonal growth and branching in primary motor neurons whereas knockdown of *snap-25a,b* caused decreased outgrowth and branching (Figure 30). Co-injection experiments showed that *snap-25a,b* mRNA and morpholinos against *snap-25* could partially counteract the effects of the corresponding gain and loss of *miR-153*.

For secondary motor neurons, rostral axon outgrowth was similarly stunted and/or irregularly spaced by *miR-153* overexpression and slightly elongated by *miR-153* knockdown (Figure 31). Differences in the caudal region were minimal compared to earlier developing rostral neurons, possibly reflecting temporal limitations to injection experiments or perhaps increased vulnerability of rostral motor neurons to altered SNAP-25 levels. Focusing on rostral effects, injection of *snap-25a,b* mRNA phenocopied *miR-*

153 knockdown and injection of morpholinos against *snap-25* resulted in patterns that closely resembled *miR-153* overexpression. Co-injection of morpholinos against both *miR-153* and SNAP-25 largely restored normal secondary motor neuron patterning, although the injection of *snap-25a,b* mRNAs was not as effective at rescuing the defects that resulted from *miR-153* overexpression (Figure 31). This may indicate a possible additional function for *miR-153* in regulating axonal growth and patterning during secondary motor neuron development.

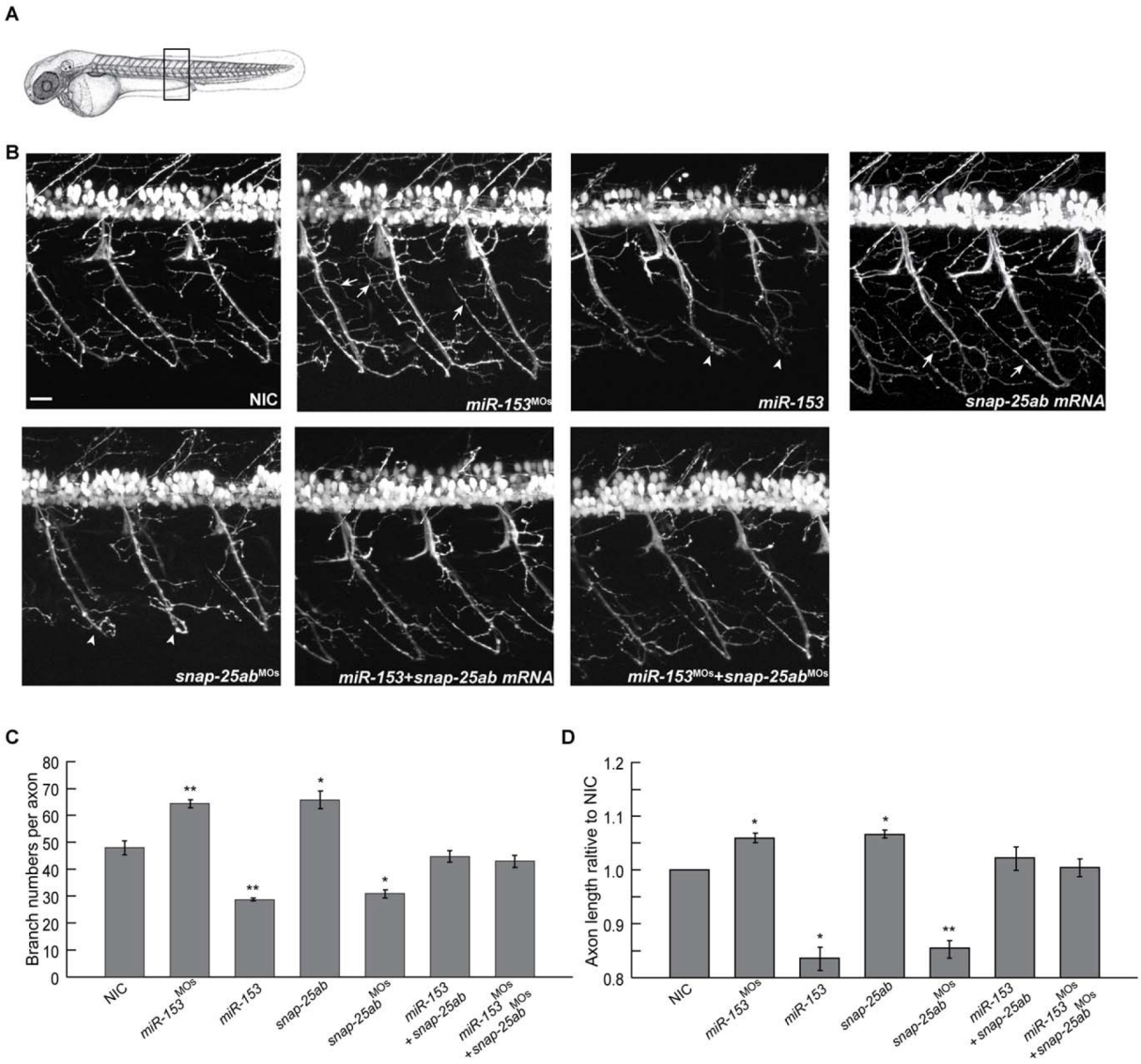

Figure 29. *miR-153* regulates the morphology and structure of motor neurons
(A) A transgenic zebrafish line, *Tg(mnx1:TagRFP-T)*), that expresses RFP in motor neurons was used to monitor the effects of altered levels of *miR-153* and *snap-25* at 55 hpf. For all confocal images, developing motor neurons were examined from the same somites, as indicated. (B) Morphology of developing motor neurons under each of the indicated conditions. Arrows indicate increased branching after knockdown *miR-153* (*miR-153MO*) or overexpression *snap-25a,b* mRNA. Arrowheads indicate the structural defects after *miR-153* overexpression or knockdown of *snap-25a,b* (*snap-25a,b^{MO}*). Scale bar: 20μm. (C) Quantification of motor neuron axonal branch number under the different conditions shown in (B). Error bars show s.e.m. Significance was determined using ANOVA with Dunnett's post-test, n=5. *, p<0.01; **, p<0.005. (D) Quantification of motor neuron axon length relative to uninjected control under the different conditions shown in (B). Error bars show s.e.m. ANOVA with Dunnett's post-test, n=5. *, p<0.05; **, p<0.01.

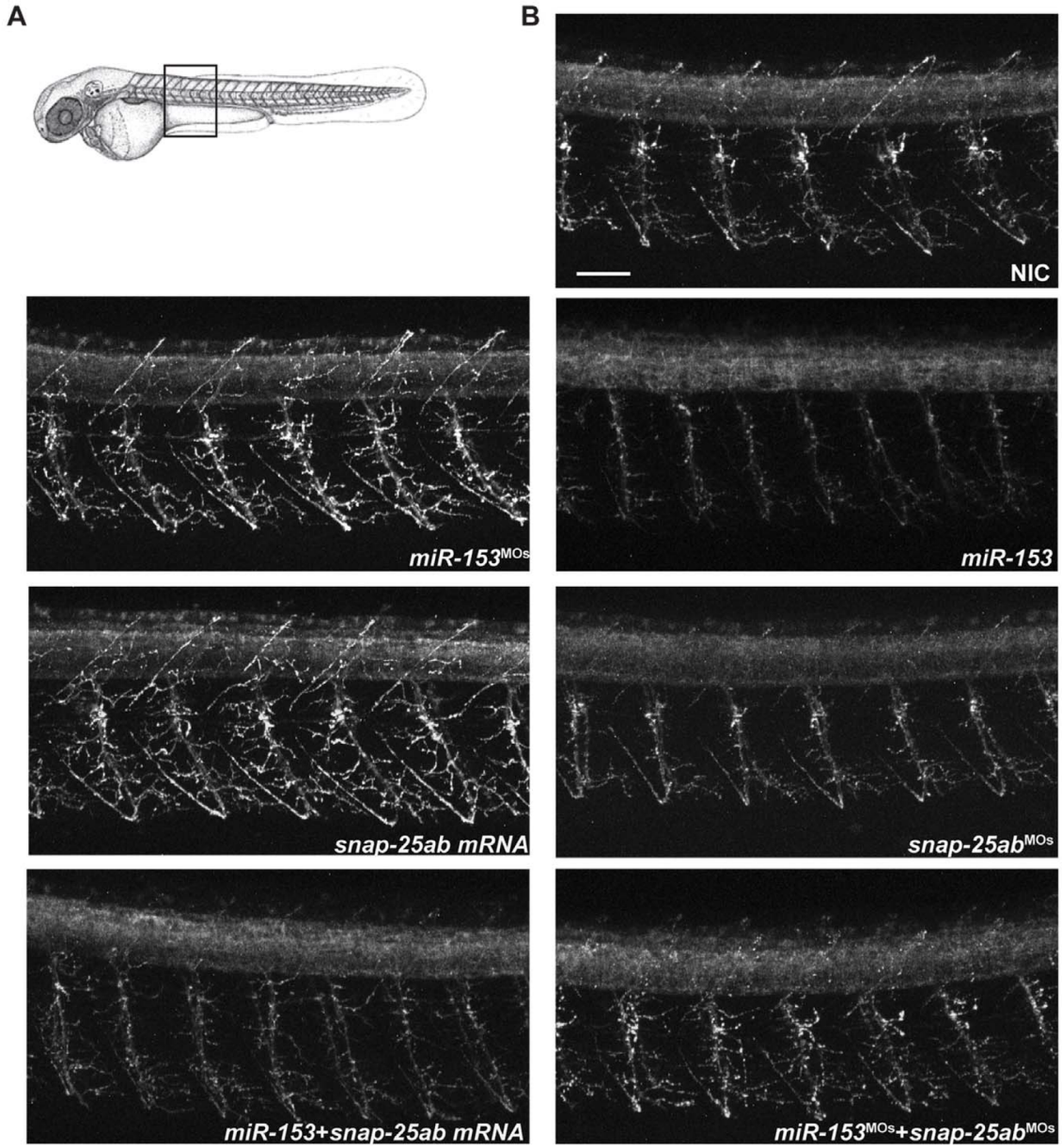

Figure 30. ***miR-153*** **regulates primary motor neuron development**
(A) Immunofluorescence performed on whole mount zebrafish embryos at 55 hpf using Znp-1 antibodies to label primary motor neurons. Confocal images were acquired from the same somites for all embryos, as indicated. (B) Effects on primary motor neuron structure and branching under the indicated conditions. Scale bar: 40μm.

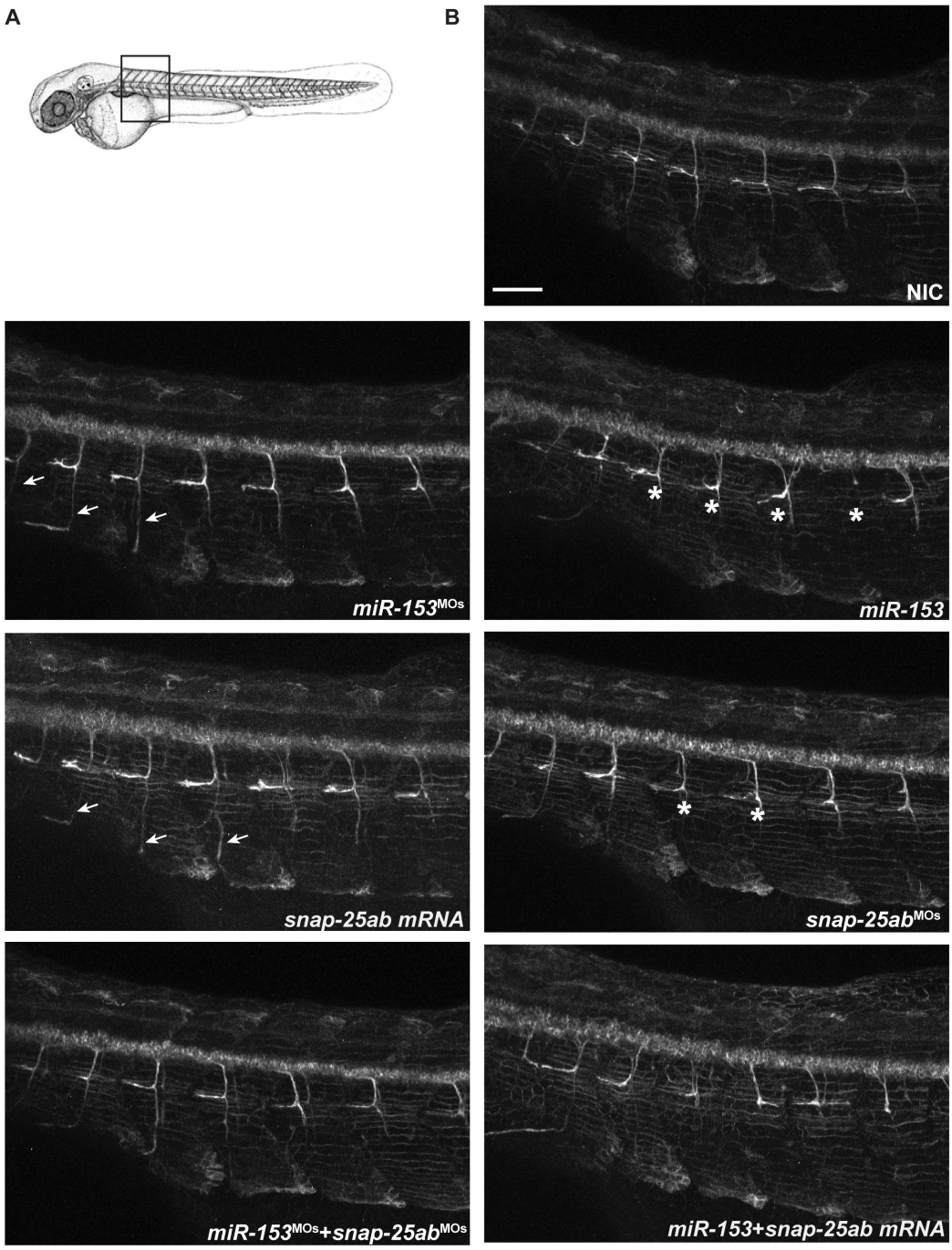

Figure 31. *miR-153* regulates secondary motor neuron development
(A) Immunofluorescence was performed on whole mount zebrafish embryos at 55 hpf using Zn-8 antibodies to label secondary motor neurons. Confocal images were acquired from the same somites for all embryos, as indicated. (B) *miR-153* knockdown (*miR-153MO*) and *snap-25a,b* overexpression significantly increased the growth of secondary motor neuron axons (arrows). Overexpression of *miR-153* or knockdown of *snap-25a,b* (*snap-25a,b^{MO}*) caused severe defects in axon development and architecture (asterisks). Scale bar: 40μm.

Expression of *miR-153* in Motor Neurons

To ensure that the effects of *miR-153* on motor neuron patterning were due to expression of *miR-153* in these cells, we FACS sorted cells from the trunks of 52 hpf (*Tg(mnx1:TagRFP-T)* embryos and conducted RT/qPCR. As shown in Figure 32, there was a greater than 10-fold enrichment for *miR-153* in RFP+ cells compared to RFP- cells. Prior work had shown that *miR-153* is expressed in the brain and spinal cord but these results show that *miR-153* is expressed in developing motor neurons.

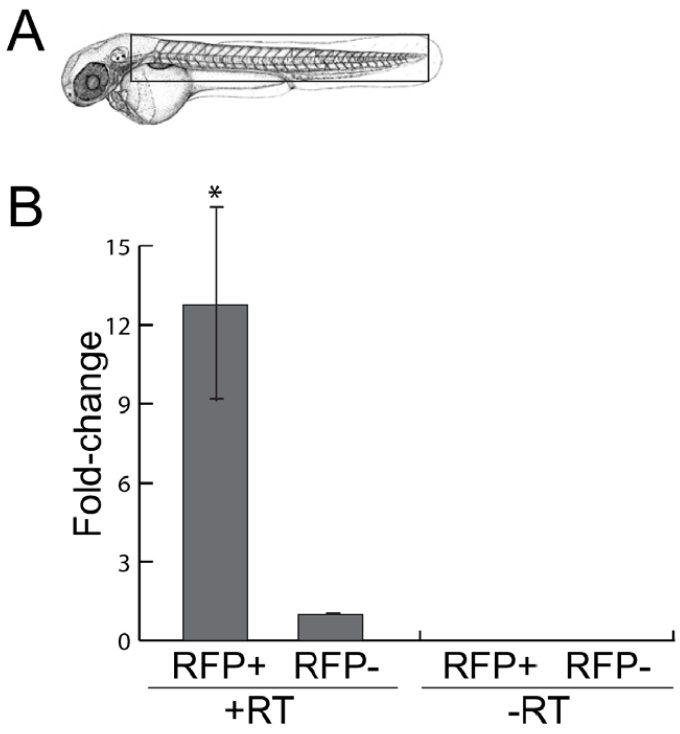

Figure 32. *miR-153* is expressed in motor neurons.
To enrich for motor neurons, heads were removed from 52 hpf embryos just posterior to the otic vesicle and trunks were dissociated to facilitate sorting of RFP+ and RFP- cells. RNA was isolated from these cell fractions and RT/PCR was performed to determine *miR-153* levels relative to U6 snRNA. Significance was determined by a two-tailed Student's t-test with the error bars representing s.e.m.; $p<0.02$.

***miR-153* regulates vesicular exocytosis to control signaling**

Since SNAP-25 has a well-established function in the fusion and release of numerous vesicle types, we next examined the role that *miR-153* plays in modulating exocytosis. Owing to the core role of *miR-153* in movement control, we first focused on synaptic activity at the neuromuscular junction (NMJ) in zebrafish embryos. For this analysis, we measured synaptic vesicle (SV) cycling using the styryl dye, FM1-43 (Gaffield and Betz, 2006; Li et al., 2003). At 55 hpf, embryonic NMJs were imaged with Alexa 594-conjugated α-bungarotoxin (α-Btx) to label postsynaptic acetylcholine receptor (AChR) clusters, while monitoring FM1-43 uptake into NMJ presynaptic boutons (Figure 33). The terminals were acutely depolarized for 5 minutes with high $[K^+]$ saline (45 mM) to drive the SV cycle and load FM1-43, whereas only weak loading was evident in low $[K^+]$ conditions. In non-injected controls, fluorescence was observed along terminal axon branches with intense staining at individual synaptic varicosity boutons (Figure 33A). Compared to NIC labeling, *miR-153* overexpression resulted in a significant decrease in FM1-43 loading in presynaptic terminals, indicating slowing of the SV cycle (Figure 33B). In sharp contrast, knockdown of *miR-153* showed a significant increase in FM1-43 loading, indicating an elevated SV cycling rate (Figure 33C). The significant difference between *miR-153* knockdown and overexpression conditions indicates that *miR-153* plays an important role in controlling the rate of vesicle cycling (Figure 33D). Together, these results reveal a key function for *miR-153* in the control of presynaptic vesicle release at the embryonic NMJ, consistent with a role for *miR-153* in the regulation of embryonic movement. The overall effects on movement are therefore a combination of effects on motor neuron development and patterning as well as overall exocytotic activity.

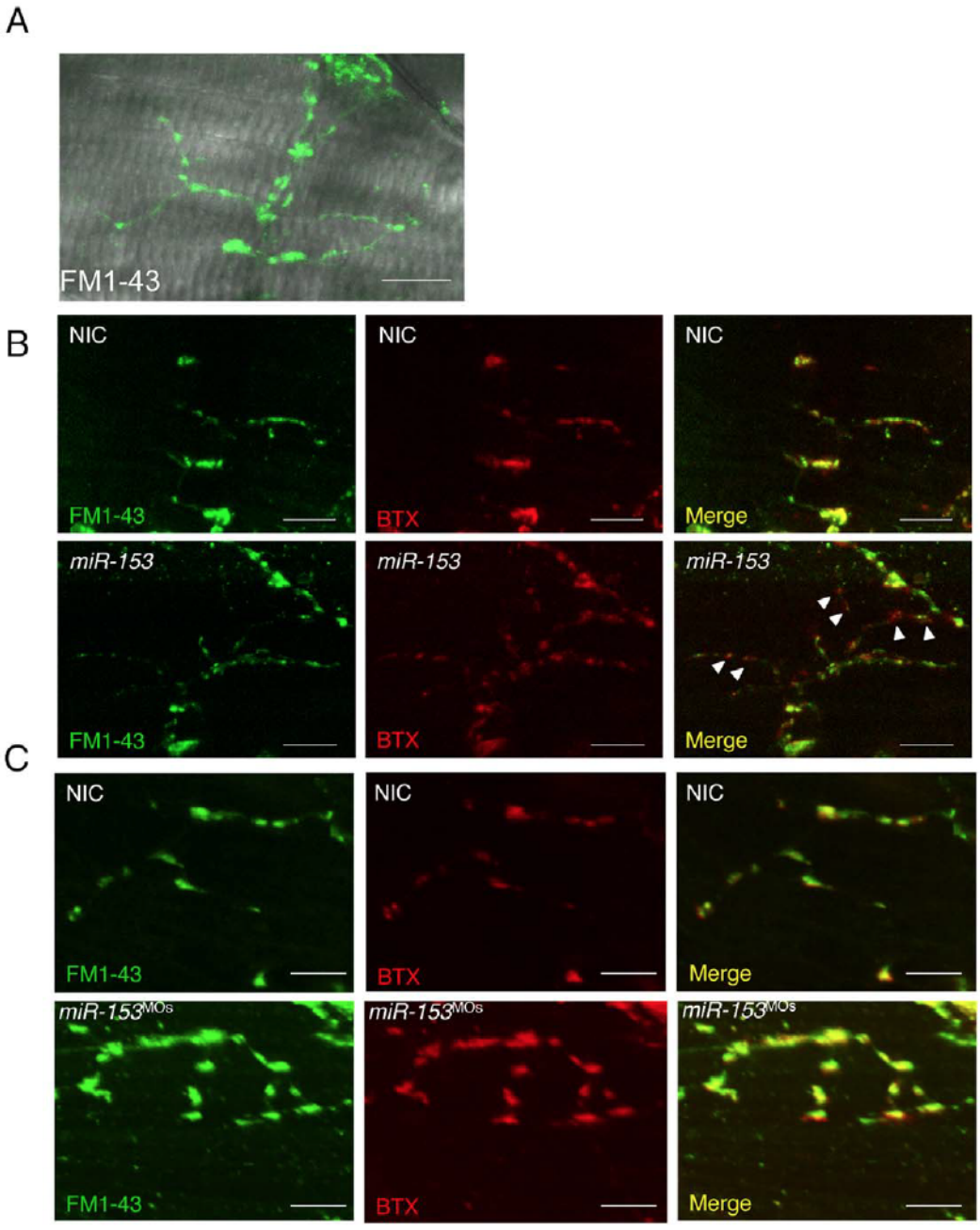
A
FM1-43
B
NIC
FM1-43
NIC
BTX
NIC
Merge
miR-153
FM1-43
miR-153
BTX
miR-153
Merge
C
NIC
FM1-43
NIC
BTX
NIC
Merge
miR-153MOs
FM1-43
miR-153MOs
BTX
miR-153MOs
Merge
D
Fluorescence Intensity
1.6
1.4
1.2
1
0.8
0.6
0.4
0.2
0
*
**
NIC
miR-153 MOs
miR-153

Figure 33. *miR-153* regulates synaptic activity at the neuromuscular junction
(A) FM1-43 loading of neuromuscular junction (NMJ) boutons in 55hpf fish embryos. (B) Postsynaptic clusters of AChRs were labeled with Alexa 594-conjugated α-bungarotoxin. Overexpression of *miR-153* caused decreased FM1-43 loading, indicating down-regulation of the synaptic vesicle cycle within NMJ boutons (arrowheads). (C) Knockdown of *miR-153* (*miR-153*^{MO}) promoted greater uptake of FM1-43 dye, indicating increased synaptic vesicle cycling. Scale bar: 10μm. (D) Quantification of FM1-43 fluorescent intensity with a paired Student's t-test. Error bars show s.e.m. *$p<0.01$; **$p<0.02$.

SNAP-25 has a highly conserved role mediating vesicular fusion in both neurons and other neurosecretory cells where it is critical for DCV release (Burgoyne and Morgan, 2003). To test whether *miR-153* plays a role in this secretory context, we examined exocytosis in a rat neuroendocrine pituitary cell line (GH4C1) expressing human growth hormone (hGH) (Kannenberg et al., 2007). Release of hGH in these cells provided a functional readout of exocytic activity (Figure 34). GH4C1 cells were therefore transfected with *miR-153*, morpholinos against *miR-153*/*snap-25*, or vectors expressing *snap-25a,b,* followed by determination of hGH levels in the media by ELISA. Overexpression of *miR-153* and knockdown of *snap-25a,b* (*snap-25a,b*^{MO}) reduced the levels of hGH to below the amount detected in culture media from mock transfected cells (Figure 34). In sharp contrast, knockdown of *miR-153* and overexpression of *snap-25* both significantly increased the amount of secreted hGH 8-10 fold over the mock transfected control (Figure 34). The differences observed due to perturbation of *miR-153* levels in the GH4C1 cell line compared to embryonic NMJs are most likely due to differences in the efficiency of *miR-153*/*miR-153*^{MO} delivery between the two experiments, as well as developmental differences. Nevertheless, the effects in this case were fully suppressed by co-expression of either *miR-153*/*snap-25a,b* mRNA or MOs against *miR-153*/*snap-25a,b*, demonstrating specific regulation of *snap-25* by *miR-153*. These data strongly support the conclusion that *miR-153* functions to precisely control SNAP-25 levels to regulate vesicle exocytosis.

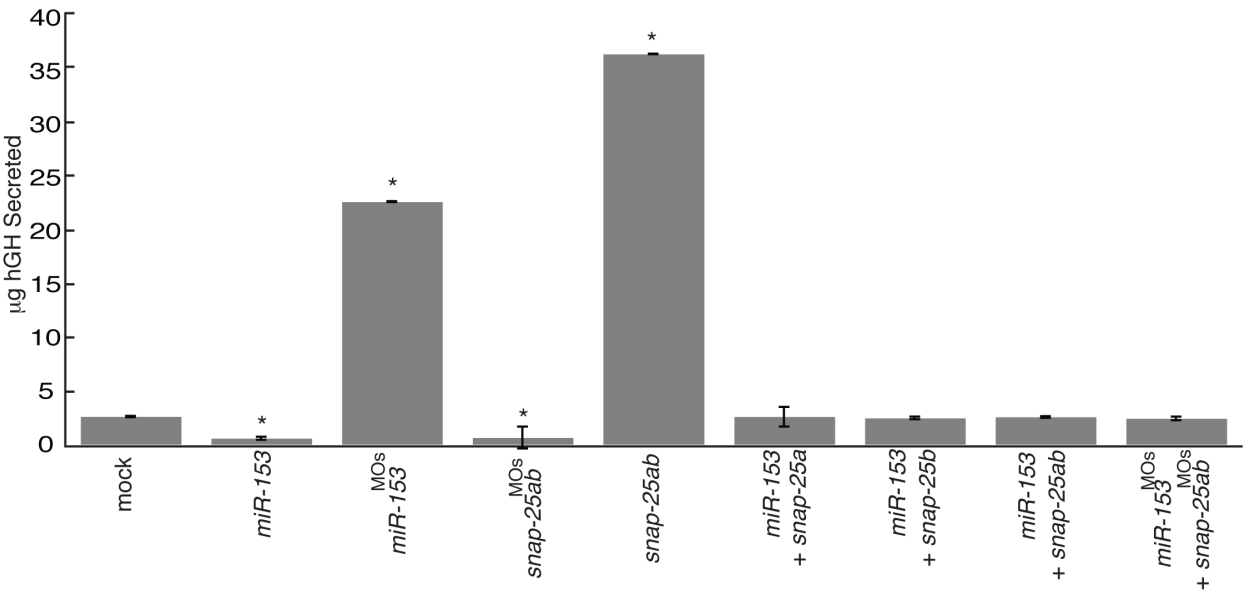

Figure 34. *miR-153*/*snap-25* regulates vesicular exocytosis
GH4C1 cells stably expressing human growth hormone (hGH) were transfected, as indicated. The effects of exogenous expression on hGH levels secreted into the culture media were determined by ELISA using hGH antibodies. Significance was determined by comparing mock transfected to all other treatments using ANOVA with Dunnett's post-test. Error bars show s.e.m. *, $p<0.01$.

Discussion

In this study, we show that *miR-153* regulates the critical core SNARE component, SNAP-25, to modulate exocytosis and neuronal development. Increased *miR-153* levels cause decreased SNAP-25 expression resulting in decreased embryonic movement, decreased neuronal secretion, and decreased neuronal growth/branching. Conversely, *miR-153* knockdown causes elevated SNAP-25 expression resulting in hyperactive movement, increased neuronal secretion, and increased neuronal growth/branching. Accumulating evidence suggests that SNAP-25 misregulation plays a role in numerous human disease states including ADHD, schizophrenia, bipolar I disorder, Huntington's Disease, Alzheimer's Disease, and diabetes (Gray et al., 2010). Regulated expression of *miR-153* provides an attractive model to mechanistically explain tight control of SNAP-25 levels.

SNAP-25 Functions during Development

It is well established that axon outgrowth during neuronal development occurs via SNARE-dependent addition of membrane for growth cone extension (Hepp and Langley, 2001; Kimura et al., 2003). Axonal growth, pathfinding, and target recognition are secondarily modulated by SNARE-dependent release of developmental signals via dense core vesicle (DCV) exocytosis (Igarashi et al., 1996; Igarashi et al., 1997; Martinez-Arca et al., 2001; Osen-Sand et al., 1993; Osen-Sand et al., 1996; Zhou et al., 2000). The outgrowth of both axons and dendrites is blocked by Botulinum neurotoxins A and C1, proteases specific for SNAP-25, demonstrating a direct role of SNAP-25 in neuronal morphogenesis (Grosse et al., 1999; Igarashi et al., 1996; Osen-Sand et al., 1996). Likewise, inhibition of SNAP-25 by antisense oligonucleotides blocks axonal outgrowth

(Osen-Sand et al., 1993). In stark contrast, neuronal outgrowth was surprisingly not inhibited in SNAP-25 null mice (Washbourne et al., 2002). The explanation for this inconsistency is not clear. Our results show a clear requirement for SNAP-25 in motor neuron outgrowth and branching in zebrafish. It is possible that the requirement for SNAP-25 may be species specific but we found that altered levels of *miR-153* caused similar branching defects in rat PC12 cells as observed in zebrafish motor neurons, strongly arguing against this (data not shown). Perhaps the differences are due to cell-specific requirements for SNAP-25. In the retina, for example, SNAP-25 is expressed in a dynamic spatiotemporal pattern and such differential expression may underlie specific development of cholinergic amacrine cells and photoreceptors (Greenlee et al., 2002). An intriguing possibility based on the results presented here is that developmental, stage-specific and/or cell-specific expression of *miR-153* may similarly regulate SNAP-25 levels, which then drives developmental and cell-specific effects.

SNAP-25 in Synaptic Vesicle Exocytosis

SNAP-25 is one of three SNARE proteins that contribute α-helices that mediate fusion between synaptic vesicles and presynaptic membranes (Jahn and Scheller, 2006; Sudhof and Rothman, 2009). Blockage of synaptic transmission by Clostridium and Botulinum neurotoxins first established that SNARE proteins are critical for neurotransmitter release (Schiavo et al., 2000). Cleavage of SNAP-25 by Botulinum neurotoxin A causes a paralytic phenotype that resembles the loss of movement we observe in zebrafish embryos expressing excess *miR-153*. SNAP-25 haploinsufficient mice show no observable phenotypic defects but complete loss of SNAP-25 blocks evoked synaptic transmission (Washbourne et al., 2002). Moreover, overexpression of

SNAP-25 inhibits normal calcium responsiveness and can impair memory-associated synaptic plasticity (McKee et al., 2010). These findings suggest that modulation of SNAP-25 levels are important for overall SNARE function, especially in generating differences in calcium dependence between neuronal and non-neuronal secretory vesicular fusion events. Matteoli and colleagues (2009) have shown that SNAP-25 is differentially expressed between excitatory glutamatergic and inhibitory GABAergic neurons in a developmental-specific manner (Matteoli et al., 2009). These results remain controversial, as earlier studies did not observe this difference, but the data are consistent with an important role for SNAP-25 as a required component for both glutamatergic and GABAergic transmission (Delgado-Martinez et al., 2007; Tafoya et al., 2008). Mechanisms for how SNAP-25 levels might be regulated in a development- and/or cell-specific manner are uncertain, but our data strongly support miRNA regulation as a likely candidate and a critical mechanism controlling SNAP-25 levels. A recent report describing the effects of chronic overexpression of SNAP-25 in the rat dorsal hippocampus demonstrated the critical importance of controlling SNAP-25 levels (McKee et al., 2010). Elevated expression of SNAP-25 produced increased levels of secreted glutamate with cognitive deficits similar to those observed in ADHD and schizophrenia. We propose that *miR-153* control of SNAP-25 levels allows for precise regulation of SNAP-25 during development and exocytosis.

miRNAs Regulation of Neuronal morphogenesis and Synaptic Activity

Localized translation control in synaptic dendrites is common, requiring repression of mRNA translation during transport. miRNA mediated inhibition of translation is an attractive mechanism that can precisely control gene expression in

neurons. Consistent with this hypothesis, many miRNAs are neuron or brain specific (Bicker and Schratt, 2008). Moreover, the effector complexes that carry out repression of translation (RNA Induced Silencing Complexes; RISCs) are composed of several subunits that have been implicated in both neuronal function and disease (Ashraf et al., 2006; Schratt, 2009; Vo et al., 2010). For example, nervous system specific miRNAs have been shown to regulate the maturation of dopamine neurons in the midbrain as well as control serotonin transport by regulating the serotonin transporter (Baudry et al., 2010; Kim et al., 2007). Likewise, *miR-1, miR-124, miR-125b, miR-132*, *bantam*, *miR-34* and the *miR-310* cluster have all been implicated in the modulation of synaptic homeostasis (Agostini et al., 2011; Impey et al., 2010; Parrish et al., 2009; Rajasethupathy et al., 2009; Simon et al., 2008; Tsurudome et al., 2010; Wayman et al., 2008). Similarly, synaptic plasticity is reportedly regulated by *miR-134* through targeting of SIRT1 or Limk1, which control dendritic spine morphogenesis (Gao et al., 2010; Schratt et al., 2006). In addition, *miR-124* in retinal ganglion cell growth cone was shown to act through CoREST to regulate the intrinsic temporal sensitivity to Sema3A, a guide cue during axonal pathfinding and morphogenesis (Baudet et al., 2012). Our work demonstrates that *miR-153* is a member of this subset of miRNAs implicated in neuronal function but by a distinctly different mechanism through targeting of *snap-25*. *miR-153* also likely targets other mRNAs (Doxakis, 2010), but SNAP-25 regulation alone is required and sufficient to explain the role of *miR-153* regulation of movement, motor neuron morphogenesis, and SNARE-mediated secretion.

Materials and Methods

Ethics Statement

The Animal Care and Use Committee monitors all animal care and research at Vanderbilt. Vanderbilt University has on file with the Office for Protection from Research Risks of the NIH an Assurance of Compliance with Public Health Service regulations and requirements and provisions of the Animal Welfare Act. All zebrafish experiments in this paper were approved by the Vanderbilt University Institutional Animal Care and Use Committee (IACUC) under protocol M-09-398. In accordance with that protocol, all necessary means were taken to avoid pain. For any manipulations that might induce pain, animals were anesthetized with a 0.15% solution of Tricaine (3-amino-benzoic acidethylester). The approved method for euthanizing zebrafish is incubation in ice water.

Microinjections

Single cell zebrafish male and female embryos were injected with 200pg of *miR-153*, 5ng each of *miR-153*^{MO} and *miR-153*^{loopMO} and/or 100pg of *in vitro*-transcribed, capped GFP reporter with or without the *snap-25a* or *b* 3'UTR. Zebrafish *snap-25a,b* 3' UTR sequences were amplified by PCR and subcloned downstream of the GFP ORF in pCS2+ (Rupp et al., 1994). Rescue experiments used injection of 3ng of *snap-25*^{StartMO} and *snap-25*$^{5'UTRMO}$, 150pg of *snap-25a,b* mRNA, 250pg of *snap-25a* mRNA, or 300pg of *snap-25b* mRNA without 3'UTRs.

Two different morpholinos against *miR-153* were utilized. One was perfectly complementary to the mature sequence; the second was complementary to a portion of the mature sequence and then extending into the precursor loop. Targeting of *snap-25a,b* mRNAs was performed using morpholinos against the region including the start codon.

Botulinum Toxin Analysis

Embryos injected at the 1-cell stage were treated with purified Botulinum neurotoxin A (Metabiologics, Inc., Madison, WI). Initial titration experiments were performed testing a range of BoNT A concentrations with final selection of 1ng per 10 ml of water for 30 minutes at either 24-hpf or 48-hpf. Embryos were washed 10 times in fresh water and the allowed to recover for 1 hour prior to protein extraction or video capture to monitor movement.

qRT-PCR and Northern Blots

Total RNA extracted from both RFP+ and RFP- cells were reverse transcribed (Taqman RT kit, Life Technologies, NY). qPCR reactions were carried out using Taqman miRNA assays (Life Technologies, NY) using the CFX96 Real-time PCR system (Bio-Rad), as previously described (Wei et al., 2012). Northern blots were also performed as described (Flynt et al., 2007; Sempere et al., 2003).

Western Blots

Embryos were dechorionated, deyolked, and sonicated in lysis buffer as described (Flynt et al., 2007). Approximately 100 embryos were pooled and one-tenth of the resulting samples were loaded into each lane. Membranes were probed with antibodies against α-tubulin (Abcam, ab15246), GFP (Torrey Pines, TP401) or SNAP-25 (Alomone Labs). For detection, anti-rabbit or anti-mouse HRP-conjugated secondary antibodies were used followed by visualization with ECL.

GFP Reporter Analyses

Reporter analyses and western blots were as described (Flynt et al., 2007). To generate

the *snap-25a,b* GFP reporters, the GFP ORF was fused to the 3' UTR sequence of zebrafish *snap-25a* or *b*. *snap-25a,b* UTRs were cloned from zebrafish whole embryo RNA preparations using oligo d(T) primed reverse transcription followed by PCR amplification with gene specific primers. Images were acquired with a Leica MZFIII dissecting scope equipped with a fluorescent laser using a Qimaging camera with Qimaging software and imported into Adobe Photoshop for orientation and cropping.

Immunofluorescence

Embryos were fixed in 4% PFA overnight at 4°C and then permeabilized in 0.5% TritonX-100 for 60 minutes followed by treatment with protease K (20μg/ul) for 10 minutes at room temperature. Samples were washed in PBT-DMSO before blocking overnight at 4ºC (PBT-DMSO, 2% BSA, 5% goat serum). Primary antibodies (SNAP-25, 1:1000; SV-2, 1:300; ZNP-1, 1:2000; ZN-8, 1:25) were incubated overnight at 4ºC, washed with PBT-DMSO, and then embryos were incubated with Cy5 or Cy3-conjugated donkey anti-mouse or rabbit antibodies (Jackson Immuno) for 4 hrs at room temperature. Before mounting and visualization, embryos were washed with PBT-DMSO. PC12 cells were fixed in 4% PFA for 15 mins, washed in PBS before incubating with primary antibodies for 1hr, washed, incubated with secondary antibodies for 1 hr, Hoechst dye for 5 mins, washed, and visualized.

Tissue Dissociation and Motor Neuron Isolation

Tg(mnx1:TagRFP-T) zebrafish embryos of 52hpf were dechorionated, deyolked and then dissected just posterior to the otic vesicle to collect the trunks (excluding the hearts). Tissues were kept in buffer (1xPBS, pH 6.4, 1%BSA) and then dissociated using 16U/ml

papain and 0.2U/ml Dispase (Worthington, NJ) for 30 mins at 28°C on a rotator. After complete dissociation of the tissue by careful pipetting up and down, cells were pelleted at 8000× g for 2mins. Resuspended cells were then treated with 1mg/ml Leupeptin (Worthington, NJ) and 100U/ml DNaseI (Sigma-Aldrich) in PBS at pH 7.4 containing 2mg/ml $MgCl_2$ for 10 mins at room temperature and then kept on ice for RFP+ and RFP- cell isolation. Gating was based on cell size and fluorescence intensity, determined by the control sample of dissociated cells from WT fish at the same developmental stage.

FM1-43 Dye Labeling

Embryos at 55 dpf were incubated in HBSS (137mM NaCl, 5.4mM KCl, 1mM $MgSO_4$, 0.44 mM KH_2PO_4, 0.25mM Na2HPO4, 4.2mM NaHCO3, 1.3mMCaCl2, 5mM Na-HEPES) containing 0.2% Tricaine and glued onto sylgard coated glass chambers before removing the skin using a glass needle. FM1-43 and α-bungarotoxin (α-Btx) labeling procedures were as previously published (Li et al., 2003), except the preloading incubation of FM1-43 dye was omitted and the Advasep incubation period was elongated to 15 mins. For data analysis, axons with puncta labeled with α-Btx were considered as synaptic boutons. FM1-43 puncta with sizes of 0.5-2mm were collected for analysis using Image J.

Cell Culture and ELISA

PC12 cells (ATCC CRL-1721) were maintained using Ham's F12K media with 15% horse serum and 5% FBS, and transfected individually or in combination with miRNAs, mRNAs, and morpholinos. Transfections were performed with 300 nM *miR-153*,

biotinylated *snap-25* MOs and *miR-153* MOs and 1.5 μg of *snap-25a,b* using Lipofectamine 2000 (Tsuji et al., 2001). Co-transfection of a GFP plasmid was used to determine transfection efficiencies. Efficiencies less than 50% were discarded. One day after transfection, 50ng/ml nerve growth factor was added to media to induce differentiation. Neurite outgrowth was assayed at day 5 by immunostaining with antibodies against acetylated α-tubulin. Stably transfected GH4C1 cells were a gift from Dr. K. Kannenberg (Kannenberg et al., 2007). ELISAs were performed after 5 days of transfection and human growth hormone was assayed following the Diagnostic Systems ELISA kit.

Acknowledgments

We thank Drs. Sarah Kucenas, Bruce Appel, and Victor Ambros for critical comments and suggestions and Dr. Jeff Rohrbough and Dr. Ricardo Pineda for help with the FM1-43 experiments. We also thank Drs. Li-En Jao and Susan Wente for providing the *mnx1*:*TagRFP-T* fish.

CHAPTER 4:

Regulation of zebrafish pharyngeal arch morphogenesis by *miR-27*

Chunyao Wei, Nergis Kara and James G. Patton[1]

Department of Biological Sciences, Vanderbilt University, Nashville, TN 37235 USA

[1] CW and JGP conceived and designed the experiments. CW and NK performed the experiments. CW, NK and JGP analyzed the data.

Introduction

Correct formation of craniofacial cartilage is a crucial aspect of vertebrate development. Human birth defects in this process include DiGeorge and Pfeiffer syndromes (Lindsay, 2001; Wilkie, 1997). In zebrafish, the program of skeletogenesis is essentially conserved with that of higher vertebrates, but with simpler spatial patterns involving a smaller number of cells (Yelick and Schilling, 2002). Fate-mapping and lineage tracing studies in the embryos of fish, amphibians, birds, and mammals have all shown that the pharyngeal skeleton or "viscerocranium" is derived from cranial neural crest (CNC) cells originating from the hindbrain (Couly et al., 1993; Lumsden et al., 1991; Osumi-Yamashita et al., 1994; Schilling and Kimmel, 1994). CNC cells migrate from the dorsal neural tube in three distinct streams into a series of pharyngeal arches that eventually give rise to pharyngeal cartilage and bone including the mandible (stream 1), hyoid (stream 2), and five branchial arches (stream 3). In each arch, a mesoderm-derived core is surrounded by CNC cells to generate a cylinder-like structure, which is in turn covered by endodermal- and ectodermal-derived epithelia (Knight and Schilling, 2006).

The fate of CNC cells in the arches is regulated by intrinsic and extrinsic cues. These include the origin of CNC cells in the neural tube prior to migration, the position in the arch post-migration, and local interactions with signaling centers such as surface ectoderm and the pharyngeal endoderm. Nested expression patterns of Homeobox (Hox) genes in CNC cells along the anterior-posterior axis are necessary to confer positional identity (Santagati and Rijli, 2003). Along the dorsal-ventral (D-V) axis, Endothelin 1 (Edn1), arising from either the pharyngeal ectoderm or endoderm, functions as a morphogen to specify D-V identity of CNC cells in each arch (Clouthier and Schilling,

2004). In addition, epithelial-mesenchymal interactions between CNC cells and the pharyngeal endoderm or ectoderm are also very important for CNC-derived cartilage development and patterning (David et al., 2002; Hall, 1980, 1981; Trumpp et al., 1999).

Studies with specific miRNA and conditional Dicer deletions have revealed that miRNAs are required for the proper development of a number of tissues including lung, muscle, skin and limbs (Flynt et al., 2007; Harfe et al., 2005; Harris et al., 2006; Yi et al., 2009). During vertebrate craniofacial development, deletion of Dicer in NC cells in the mouse disrupts proper CNC cell and cartilage development (Kobayashi et al., 2008; Zehir et al., 2010). Several individual miRNAs from different species were reported to modulate specific signaling pathways in various developmental stages, such as PDGF, BMP, and Wnt signaling (Eberhart et al., 2008; Ning et al., 2013; Sheehy et al., 2010). Here, we show that the zebrafish *miR-27* family is necessary for pectoral appendage outgrowth and pharyngeal arch morphogenesis during early development. By regulating the proper activities of CNC cells during mesenchymal condensation and chondrogenesis, we show that *miR-27* is required for extracellular matrix (ECM) secretion and subsequent cartilage formation.

Results and Discussion

miR-27 regulates pectoral fin bud outgrowth and craniofacial morphogenesis.

As one of the best-known miRNA families, the *miR-27* family is highly conserved among vertebrates and displays tissue-specific expression patterns (Wienholds et al., 2005a). In zebrafish, *miR-27* expression is restricted to the tail bud of embryos before 24 hours-post-fertilization (hpf), as indicated by high-throughput sequencing and in situ

hybridization (Wienholds et al., 2005a). Starting from 48 hpf, expression of *miR-27* decreases in the tail but becomes detectable in the pharyngeal arches, progressively increasing in expression thereafter. By 72hpf, *miR-27* is readily detectable in the pharyngeal arches and pectoral fins (Figure 35A,B).

To determine the function of *miR-27* during early zebrafish development, we designed antisense morpholinos (MOs) against *miR-27a/b* and their corresponding Drosha cleavage sites for loss-of-function experiments. Morpholinos were injected into single cell embryos after which development was allowed to proceed for 3 days to examine possible morphological phenotypes (Figure 35). As shown in Figure 35C, injection of morpholinos resulted in an approximate 70% loss of *miR-27a,b*. Despite some developmental defects observed in the caudal fin and ventral blood vessels, possibly due to the repression of multiple targets, the major defects we discovered was a lack of pectoral fins with an associated swimming impairment (Figure 35D-J). Injection of control MOs did not cause any noticeable morphological defects. However, upon closer inspection, the pectoral fins of *miR-27* morphants were, in fact, initiated, but developed much smaller in size and seem to lack all endoskeleton elements compared to wild-type embryos of the same stage (Figure 31F-J). Consistent with this, *in situ* hybridization showed the expected expression of multiple transcription factors and FGF ligands that are required for pectoral fin bud initiation. In almost all cases, the patterns of expression were indistinguishable between wild-type control fish and the *miR-27* morphants, suggesting that *miR-27* does not block pectoral fin bud initiation but rather its outgrowth (Figure 36).

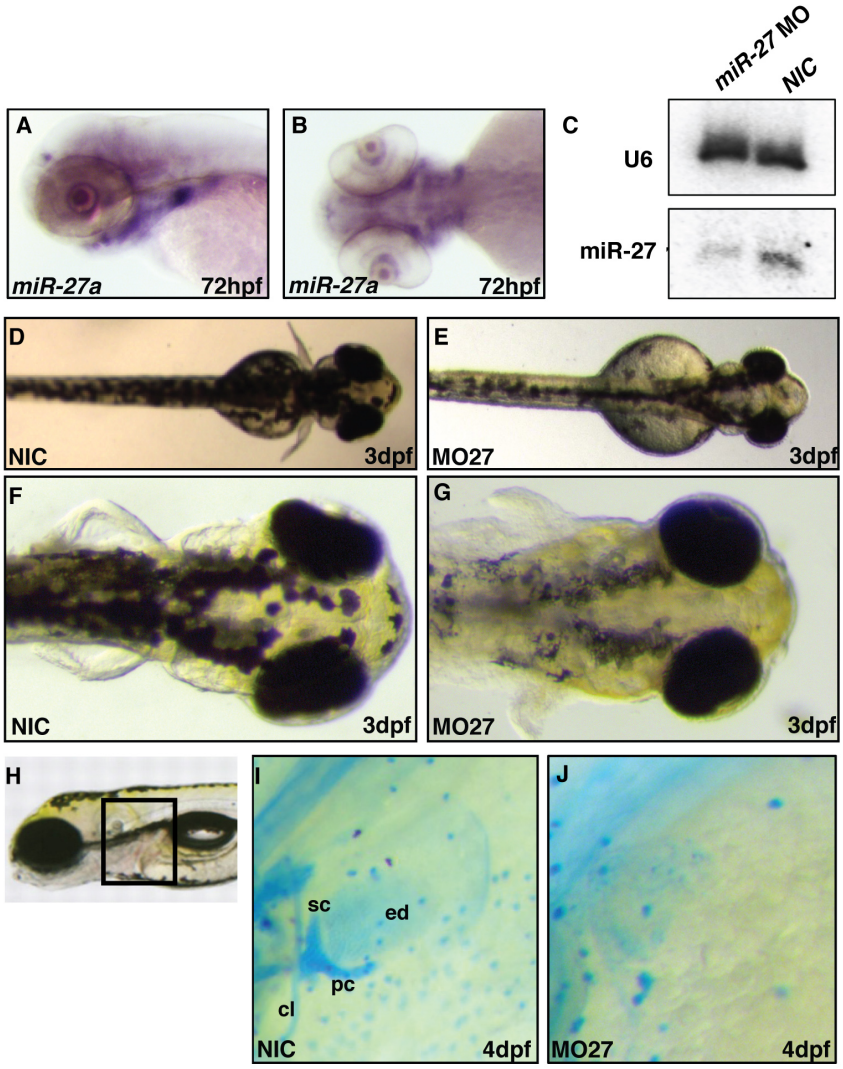

Figure 35. *miR-27* knockdown results in defects of pectoral fin development. (A-B) *miR-27a* is expressed in the pharyngeal arches at 72 hpf. (C) Injection of *miR-27* MOs (MO27) leads to efficient knockdown of endogenous *miR-27*. (D-G) The phenotypes of *miR-27* knockdown fish at 3 dpf. (F-G) High magnification images of fish indicated in (D and E) after removal of the yolk. (H-J) Whole mount embryos at 4 dpf were stained with alcian blue with the pectoral fins indicated in (H) enlarged in (I and J). ed, endodermal disc; sc, scapulocoracoid; pc, postcoracoid; cl, cleithrum.

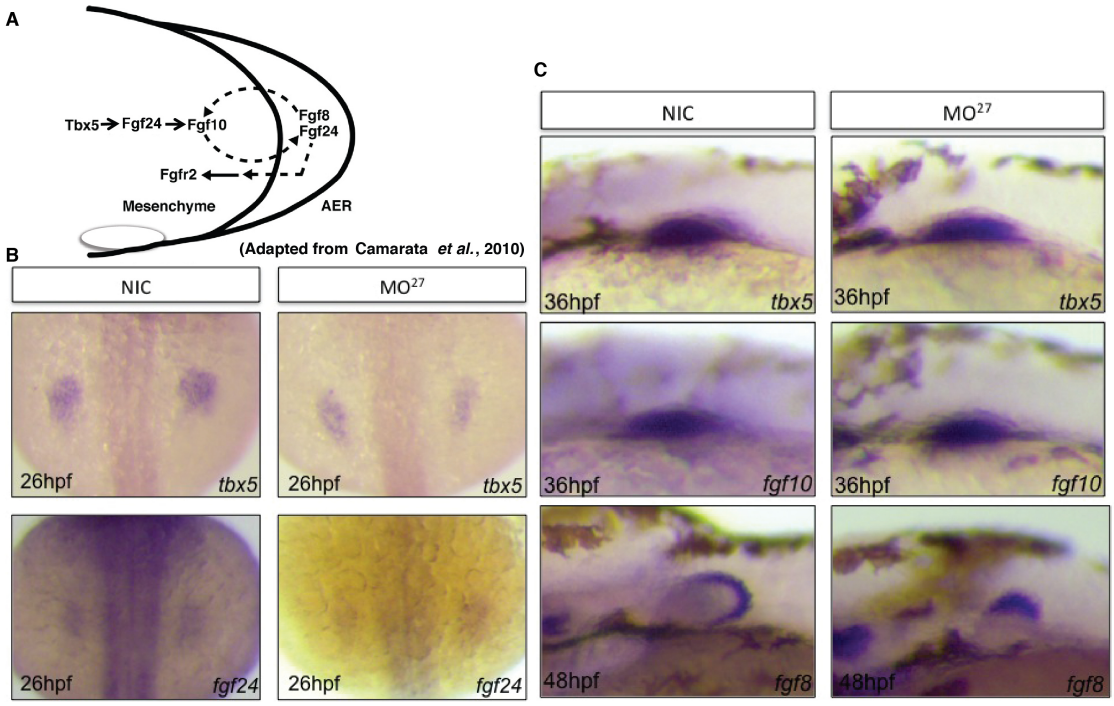

Figure 36. Loss of *miR-27* does not affect *tbx5* and *fgf* ligand expression.
(A) *tbx5* and fgf signaling pathways are essential for pectoral fin bud initiation. (B) Expressions of *tbx5* and *fgf24* between wild-type fish and *miR-27* knockdown fish are indistinguishable at 26 hpf. (C) Expression of *tbx5*, *fgf10* and *fgf8* are not changed between wild-type and *miR-27* knockdown fish.

Besides defects in pectoral fin outgrowth, we also noted defects in jaw formation. Compared to wild-type control fish at 4dpf, *miR-27* morphant fish at the same age lacked a lower jaw (Figure 37A,B). To gain insight into overall craniofacioal defects, we stained *miR-27* morphants with Alcian blue at 4 dpf which showed a total loss of cartilage in the pharyngeal arches as well as the pectoral fins (Figure 37C-F). In addition, knockdown of *miR-27* resulted in an abridged palate in the upper jaw, where the bilateral trabeculae were joined in the midline but the ethmoid plate did not extend properly (Figure 37D,F). Consistent with the loss of cartilage, the expression of *col2a1a*, a major component of ECM in cartilage, was abolished in *miR-27* knockdown fish (Figure 37G-J). At 5 dpf, the cartilaginous elements of each arch were still defective in *miR-27* knockdown fish. In contrast, over-expression of *miR-27* did not disrupt embryogenesis although we detected severe edema at higher concentrations (data not shown). The loss of function defects in both the pectoral fins and craniofacial development suggest that *miR-27* plays a major role in controlling cartilage formation.

Overexpression of *miR-27*

The expression of *miR-27* is precisely regulated during development. Prior to 24 hpf, the expression of *miR-27* is restricted to undefined areas of the tail bud. Starting at 36 hpf, expression of *miR-27* can be detected in the future jaw (Figure 38A,B). However, overexpression of *miR-27* by injection into single-cell embryos did not cause any dramatic morphological defects in the jaw and the major cartilage elements are intact and appropriately positioned (data not shown). In addition, injection-mediated overexpression could easily cause off-target effects in many tissues where *miR-27* is not supposed to be expressed during development. This is similar to the effect of *wnt9a*,

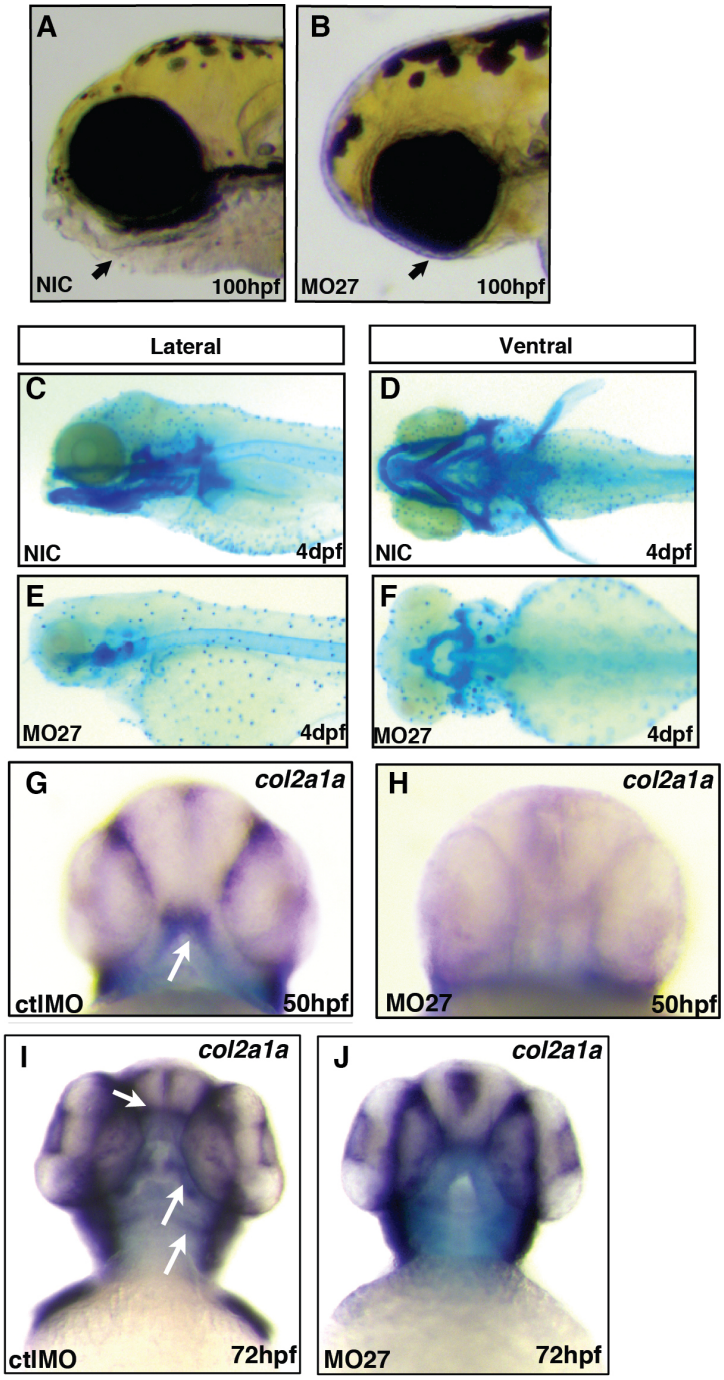

Figure 37. Knockdown of *miR-27* leads to the loss of pharyngeal arch extracellular matrix.
(A, B) *miR-27* morphants lack a lower jaw, as indicated with the black arrows. (C-F) Zebrafish embryos at 4 dpf were treated with alcian blue to stain the ECM. (E-H) Expression of *col2a1a*, the major component of ECM, is lost in the pharyngeal arches (white arrows) upon knockdown of *miR-27* at 50 hpf (G, H) and 72 hpf (I, J) using whole-mount *in situ* hybridization.

which is also required for zebrafish craniofacial development (Curtin et al., 2011). To overexpress *miR-27* endogenously in a time- and tissue-specific manner, we created transgenic fish expressing *miR-27* driven by either the *sox10* or the hsp70 heat shock promoter. We have been able to demonstrate successful overexpression of *miR-27* upon heat shock by using *in situ* hybridization at 72 hpf (Figure 38C-F), but *miR-27* overexpression with *sox10* promoter remains to be validated. We plan to use these fish to examine the effects of *miR-27* on the expression of transcriptional factors and molecular markers related to CNC in different stages of CNC cell condensation and chondrogenesis. By comparison to *miR-27* knockdown fish, we expect to identify the exact stages at which *miR-27* is required and the specific genes that are regulated by *miR-27*.

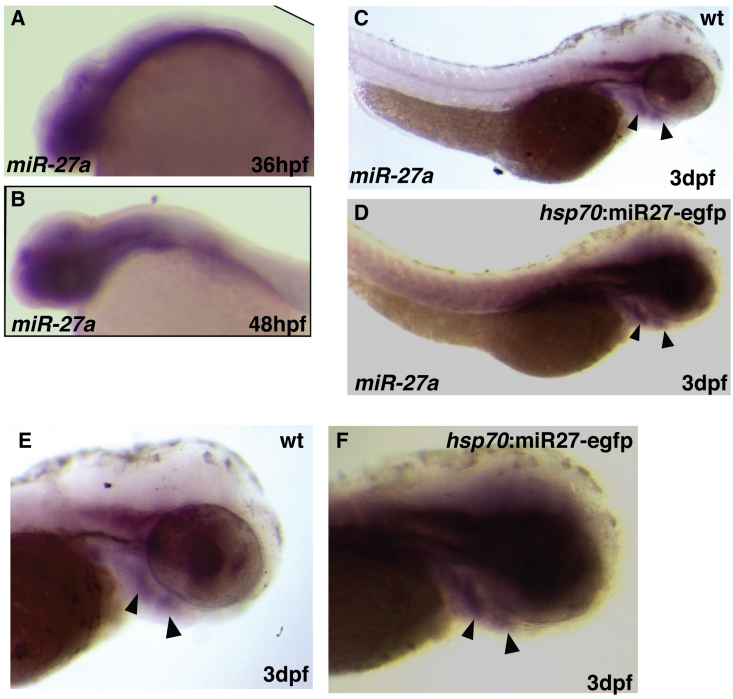

Figure 38. *In situ* hybridization for *miR-27*.
(A-B) Expression of endogenous *miR-27* in zebrafish embryos at 36 hpf and 48 hpf. (C-D) Overexpression of *miR-27* in *Tg(hsp70: miR27-egfp)* and wild-type fish. (E-F) High magnification images focusing on the heads of wild-type and *Tg(hsp70: miR27-egfp)* fish. Black arrowheads indicate expression of *miR-27* in the pharyngeal arches.

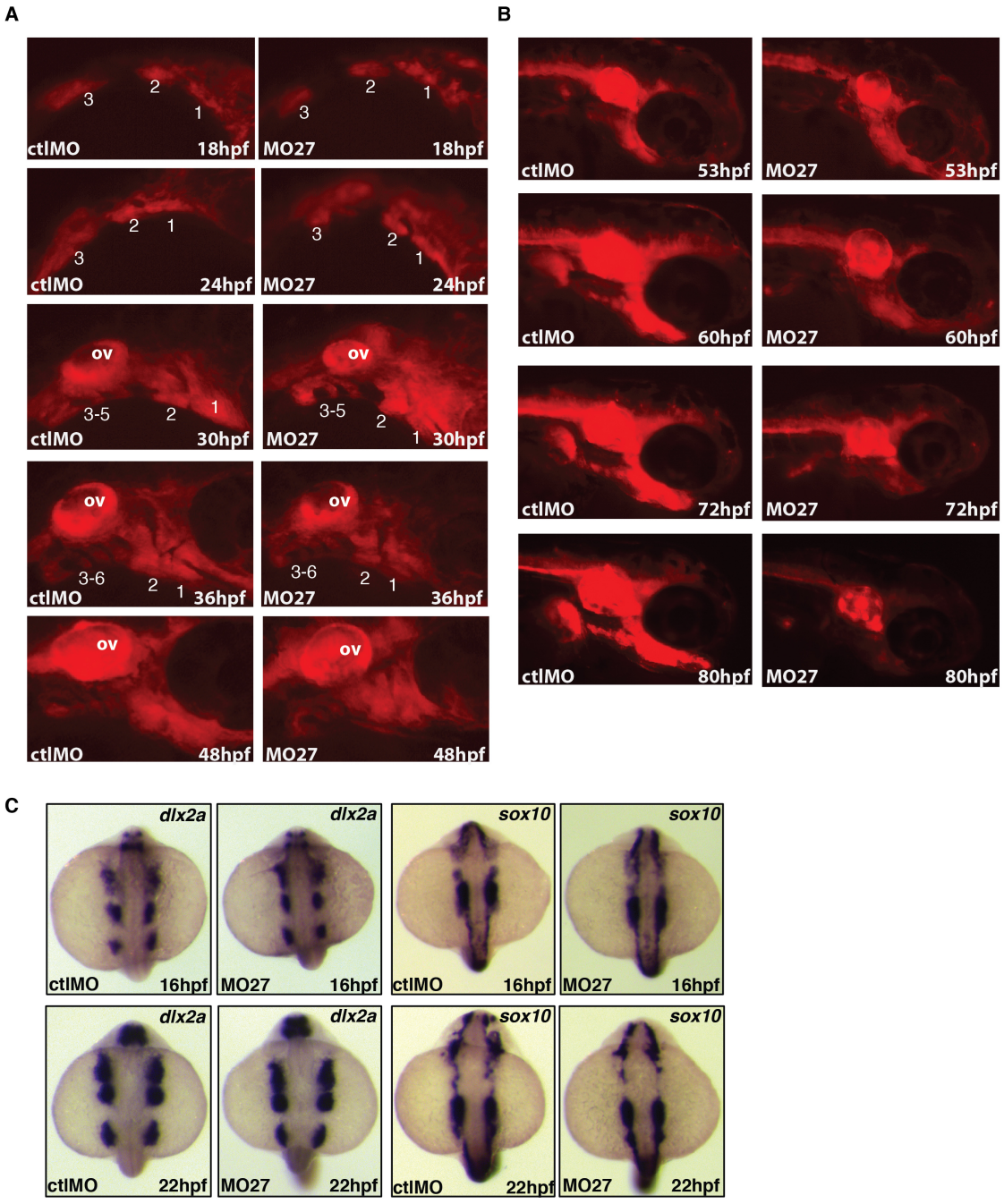

Figure 39. *miR-27* is required in post-migratory CNC cells.
(A-B) *Tg*(*sox10:mRFP)* transgenic embryos were injected with either control or *miR-27* MOs and monitored from 18 hpf to 48 hpf (A) and 53hpf to 80 hpf (B). Numbers indicate positions of CNC cell populations or the developing arches. Images show the lateral side of the fish, with the head on the right side. ov, otic vesicle. (C) *In situ* hybridization of *dlx2a* and *sox10* in control embryos and *miR-27* knockdown embryos at 16 hpf and 22hpf.

miR-27 is required in post-migratory CNC cells

Craniofacial development depends on proper migration and development of cranial neural crest cells. In order to examine the role of *miR-27* during CNC migration, we monitored morphology of growing arches over time using *Tg*(*sox10:mRFP)* transgenic embryos following *miR-27* MO and control MO injections (Kucenas et al., 2008). During early embryogenesis, CNC cells before and during migration were not affected by the reduction of *miR-27*. The earliest time point where *miR-27* morphants start to show different phenotypes from the control MO is 48-53 hpf, when CNC cell migration into the developing arches is largely accomplished (Figure 39A,B). This indicates that perturbation of *miR-27* levels does not appear to alter CNC migration, suggesting that *miR-27* functions post-migration. Consistent with this, the expression pattern of *dlx2a*, a specific marker of CNC cells, is also indistinguishable from wild-type embryos during cell migration, as indicated by *in situ* hybridization (Figure 39C).

Cell proliferation and apoptosis

Histological sections of pharyngeal arches from zebrafish at 72 hpf indicated that not only was the ECM not secreted, but very few chondrocytes were appropriately stacked and differentiated (Figure 40A-C). *Sox9a*, a marker for chondrogenic differentiation, is expressed in chondrocytes as expected, but its levels are dramatically altered (Figure 42), suggesting that the differentiation of progenitors or the proliferation of chondrocytes is potentially inhibited. TUNEL staining of sectioned arches at 60 hpf did not show increased apoptosis in *miR-27* knockdown fish, although overall apoptosis was slightly increased in the head (Figure 40D-G). This is possibly because cell death

and cell removal occur before 60 hpf. Thus, earlier stages (e.g. 48 hpf and 55 hpf) need to be focused on in the future to verify cell apoptosis in pharyngeal arches.

Another possibility is that chondrocyte proliferation could be inhibited. To provide insight into this possibility, we labeled DNA replication by incorporation of BrdU. Although more experimental repeats are needed, our preliminary results show that compared with control MO-injected fish, chondrocyte proliferation is decreased upon *miR-27* knockdown (Data not shown).

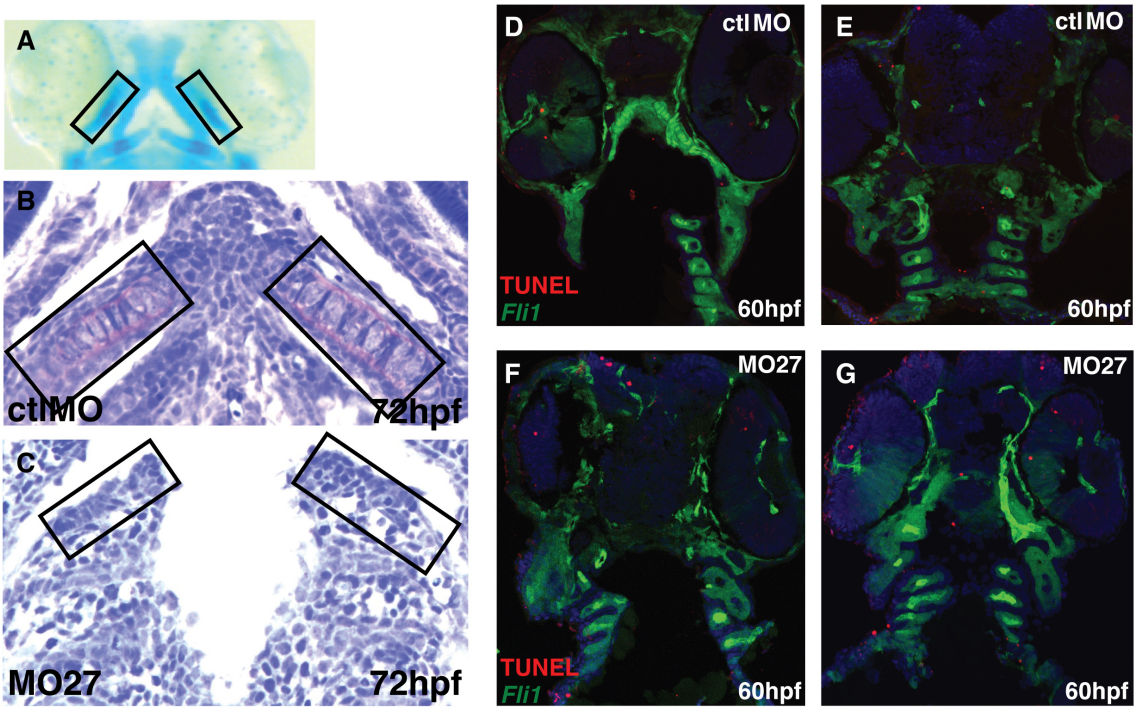

Figure 40. Knockdown of *miR-27* results in the loss of chondrocytes.
(A-C) Toluidine blue staining of chondrocytes from the first arch as indicated by the rectangles in (A), in control fish (B) and *miR-27* knockdown fish (C) at 72 hpf. (D-G) TUNEL assay on zebrafish embryo sections in at 60 hpf. Pharyngeal arches are labeled by the expression of GFP driven by the Fli1 promoter. Two representative images for each condition are shown.

ptk2.2 is a target of *miR-27*

In order to identify endogenous targets of *miR-27* in zebrafish, we performed high-throughput mRNA sequencing using mRNA samples isolated from the transcriptome of zebrafish heads at 48 and 72hpf, following the injection of either *miR-27* MO or control MOs. Since miRNAs are negative regulators of gene expression, we expected that *miR-27* target genes would be up-regulated, with increased RPKMs in *miR-27* knockdown fish compared to control MOs. Thus, we selected potential *miR-27* targets from sequencing lists of up-regulated transcripts in combination with miRNA target prediction algorithms. In addition, co-localization of both potential mRNA targets and *miR-27* was also taken into consideration. Based on these criteria, we predicted *ptk2.2*, a protein tyrosine kinase, as a *miR-27* target.

To test whether *ptk2.2* is indeed a target of *miR-27*, we first analyzed the expression of *ptk2.2* mRNAs using our mRNA-seq data and found a slight increase in mRNAs levels upon the loss of *miR-27* at 48 hpf, consistent with the previous reports that *miR-27* regulates targets without dramatically decreasing mRNA levels (Urbich et al., 2012). To test whether *miR-27* could target the 3'UTR of *ptk2.2*, we used a GFP reporter assay. The 3'UTR of *ptk2.2* was fused to the GFP open reading frame (Figure 41A). Synthetic mRNAs from this fusion construct were prepared and injected into single cell embryos in the presence or absence of *miR-27*. After 1 day development, fluorescence imaging of embryos showed that co-injection of *miR-27* resulted in obvious down-regulation of GFP (Figure 41B). This suggests that *miR-27* could physically interact with *ptk2.2* mRNAs and potentially regulate expression level of endogenous *ptk2.2*.

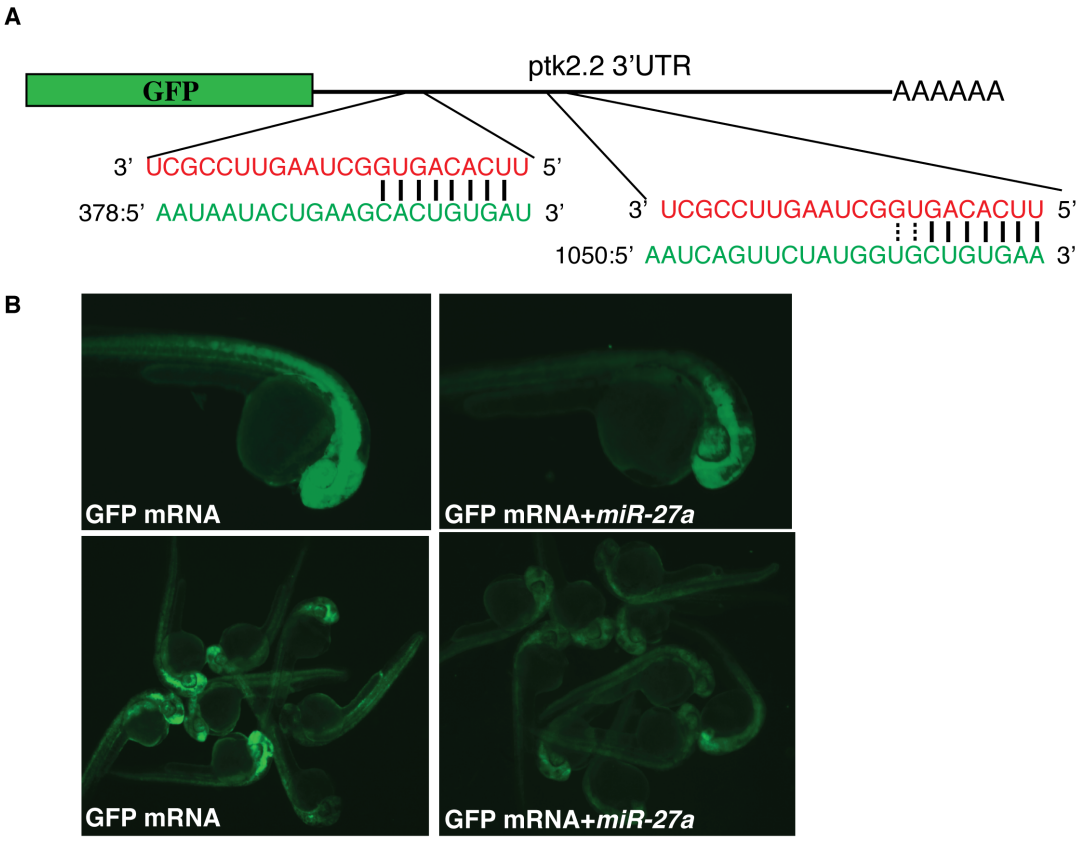

Figure 41. *miR-27* targets *ptk2.2*.
(A) GFP reporter constructs were created by fusing the reading frame of GFP to the *ptk2.2* 3'UTR. The *miR-27* sequence is indicated in red and the corresponding *ptk2.2* UTR sequence is shown in green. Seed pairings between *miR-27* and *ptk2.2* 3'UTR are indicated with black lines. (B) Single cell zebrafish embryos were injected with mRNAs derived from the GFP reporters fused to the full length *ptk2.2* UTR. Embryos were either uninjected or injected with exogenous *miR-27*. Fluorescence levels were examined at 1 dpf. Clusters of embryos are shown as well as a high magnification image of a single representative embryo.

Identify targets involved into pharyngeal arch development

Although we identified *ptk2.2* as a potential endogenous target of *miR-27*, the current known roles of protein tyrosine kinase in affecting ECM formation cannot completely explain all the existing morphological defects observed in the pharyngeal arches of *miR-27* knockdown fish, especially the abnormal proliferation of chondrocytes. Therefore, it is likely that there are other *miR-27* target genes that are involved in pharyngeal arch development. Previously published literature indicated that loss of *wnt9a* in zebrafish resulted in developmental defects in pharyngeal arches that mimic the phenotypes of *miR-27* knockdown fish (Curtin et al., 2011). It is possible that *miR-27* targets inhibitors of Wnt signaling pathway to regulate development.

In addition, we are testing whether *miR-27* targets MMPs (matrix metalloproteinases) that mediate the cleavage and degradation of many ECM proteins (Williams et al., 2012). It has been reported that increased tyrosine kinase activity (such as Ptk2.2) can suppress MMP14 endocytosis and enhanced the activity of MMP14 (Washbourne et al., 2002). Therefore, the loss of ECM may be accompanied by increased activity of MMPs. Paradoxically, knockdown of MMP14a, but not MMP14b, led to a complete loss of pharyngeal arches that is almost identical to that of our *miR-27* knockdown fish. In addition, it has been shown that MMP9 and MMP13a are also involved into the degradation of different types of collagen components during cartilage formation (Gioia et al., 2009; Lausch et al., 2009). Currently, we are trying to determine whether or not they are indeed targets of *miR-27*.

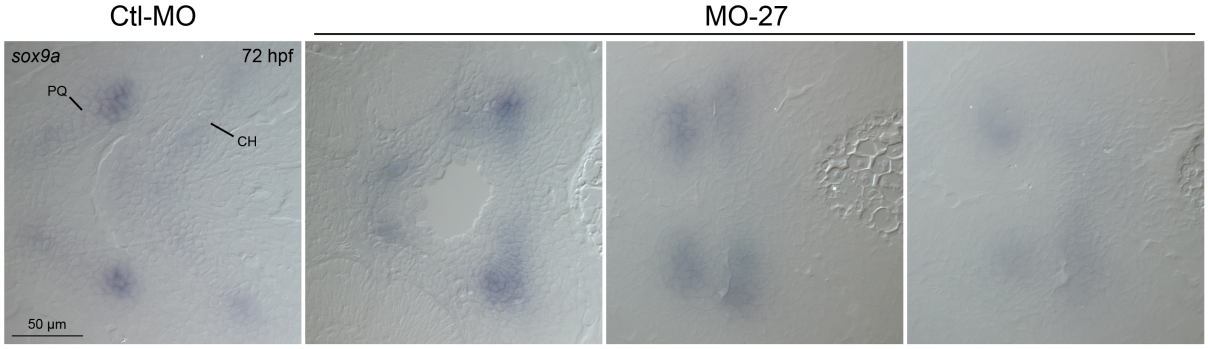

Figure 42. *sox9a* expression in control (ctl-MO) and *miR-27* knockdown (MO-27) fish. Whole-mount embryos at 72hpf after *in situ* hybridization of *sox9a* were embedded and sectioned. 3 images on the right side indicate 3 morphants corresponding to a mild, moderate and severe phenotypes in *miR-27* knockdown fish.

CHAPTER 5:

Discussion

Significance

Since the discovery of *lin-4* and *let-7*, miRNAs have been extensively studied for more than 10 years. Extensive progress has been made including identification of numerous miRNAs from multiple species, mapping of the genomic loci encoding these miRNAs, and identification of many of the components of the biogenesis pathway. miRNAs have been identified in organisms as diverse as viruses, unicellular algae, plants, worms, flies, fish, mammals, and humans (Bartel, 2004; Skalsky and Cullen, 2010; Zhao et al., 2007). Studies in lower organisms such as plants and worms imply that small RNAs might have evolved to combat viral infections and protect the genome from transposon insertion (Baulcombe, 1999; Ketting et al., 1999; Ratcliff et al., 1999; Tabara et al., 1999). Compared with other surveillance players, such as proteins, production of small RNAs bypasses translation, saving energy and providing a quicker response without compromising specificity. From potential initial selection as antivirals or as a form of genome immunity, higher organisms appear to have expanded roles for miRNAs into processes such as homeostasis, responses to environment stress, neuronal circuitry, pathogenesis, and cancer.

Given the probable binding of each miRNA to multiple targets, complete understanding of the function of a single miRNA is still very challenging. This requires studies in specific cell types and specific timing during embryogenesis and pathogenesis to elucidate all targets for each miRNAs. A single mRNA is likely regulated by multiple

miRNAs. Also, given the limited pairing, it remains to be determined exactly how binding affinities are determined. It has been reported that the secondary structure of the 3'UTR of mRNAs can affect the accessibility of a miRNA to its target (Kedde et al., 2010; Long et al., 2007). Thus, it is very likely that the flanking sequence of a miRNA targeting site might also be relevant toward recruitment of miRNAs. In support of this idea, limited analysis suggested that many miRNA targeting sites are within repeat-rich regions of mammalian mRNAs (Schnall-Levin et al., 2011). Another interesting finding is that miRNA-mRNA interactions are very likely cellular context dependent, meaning a single miRNA-mRNA interaction could be enhanced or diminished by other co-expressed regulators. Recently published examples of ceRNAs or circular RNAs belong to this category (Memczak et al., 2013; Salmena et al., 2011). Therefore, experimental validation of the mechanism of binding of each miRNA and its targets should be reported and analyzed continuously to accumulate strong evidence from which major discoveries can be made.

miRNA expression patterns during the Maternal-Zygotic Transition

The maternal-zygotic transition is a stage during early embryonic development when maternal mRNA transcripts are removed while the zygotic genome becomes active for transcription (Schier, 2007). In zebrafish, the MZT appears during the midblastula stage, around 3 hpf. Studies in the Schier group found that the *miR-430* family is required for the clearance of maternal mRNAs but whether or not other miRNAs are expressed or involved during the MZT is still unknown (Giraldez et al., 2006a). Previous studies using microarrays suggested that few miRNAs are expressed in embryos until 1 dpf. This is possibly due to the difficulty of detecting miRNAs at low expression levels

in array-based analyses. However, given the fact that miRNAs can instruct the specification of single neurons (Chang et al., 2004), it is possible that many rare miRNAs accumulate in some individual cells with likely biological significance but with limited ability to detect such transcripts. Using high-throughput sequencing, we identified 198 miRNAs that are expressed during the MZT. Their expression patterns are subject to dedicated regulation, suggesting that they are not derived from transcriptional background or noise. At the 256-cell stage, which is about 2.5 hpf (before the MZT), we discovered numerous miRNAs at relatively high levels which are then rapidly down-regulated during the MZT. It is likely that many of these miRNAs are maternally deposited (e.g. *miR-34*) (Soni et al., 2013) and their subsequent removal is by a novel mechanism coincident with the clearance of maternal mRNAs during MZT. Another possibility is that these miRNAs are transcribed from the zygotic genome (as we observed with the *miR-430* family) (Cohen and Brennecke, 2006; Giraldez et al., 2006a). If true, this would suggest that initiation of zygotic transcription may occur before the MZT.

miRNA 3' termini heterogeneity

The deep coverage of miRNA high throughput sequencing shed light on the heterogeneous composition of reads for many expressed miRNAs, with individual miRNAs having extra uridine or adenine additions at the 3' termini. In my sequencing of zebrafish embryos, I identified a substantial fraction of miRNA reads exhibiting 3' end nucleotide additions. The addition of uridine is reported to largely decrease the expression levels of mature miRNAs, and despite the controversial underlying mechanism, the findings remain largely correlative. I speculate that the down-regulation

of many miRNAs from the 256-cell stage to the sphere and shield stages is due to targeted degradation mediated by uridine addition to the 3' end. When analyzing miRNAs expressed at the 256-cell and the sphere stages, I found that ~70% of miRNAs had an increased percentage of uridine additions. Importantly, the levels of *miR-430* quickly decrease after the sphere stage, coinciding with the detection of increasing uridine addition at the 3' end. Interestingly, prior to this time, I detected an increased percentage of *miR-430* reads with adenine addition at the 3' end, coinciding when *miR-430* functions to remove maternal mRNAs. These data indicate that uridylation and adenylation of *miR-430* serve to regulate the levels of *miR-430* family during the MZT and post-MZT stages. My data support the hypothesis that miRNA 3' terminal addition of adenine stabilizes half-life whereas uridine addition promotes degradation.

miR-153 and SNAP-25 in motor neuron development

SNAP-25 is a key component of soluble N-ethylmaleimide-sensitive factor attached protein (SNAP) receptor (SNARE) machinery. It associates with Syntaxin to form t-SNARE complexes on the target membrane and interacts with Synaptobrevin, the v-SNARE on the vesicle membrane, to mediate docking and fusion of the vesicles to the plasma membrane (Jahn and Scheller, 2006; Sudhof and Rothman, 2009). During development of the nervous system, neurite outgrowth is dependent on membrane expansion at the growth cone, located at the tips of axons where vesicles transported from the cell body are added to the plasma membrane in an exocytic manner. Inhibition or cleavage of SNAP-25 in rat cortical neurons and PC12 cells *in vitro* prevents neurite elongation and axon growth, consistent with the morphological phenotypes of zebrafish motor neurons that we observed in our experiments (Hepp and Langley, 2001; Kimura et

al., 2003). Currently there are contradictory reports concerning the opposite effects of syntaxin inhibition on neurite outgrowth (Igarashi et al., 1996; Yamaguchi et al., 1996), raising questions as to the involvement of SNAREs during neurite outgrowth. However, our data strongly support the hypothesis that SNAP-25 is required for axonal outgrowth and branching, acting either through SNARE complexes or by other novel mechanisms. Besides effects on axonal outgrowth, the loss of SNAP-25 also caused defects in axonal trajectory projections over the surface of axial muscles implying that SNAP-25 is also involved in regulating growth cone responses to attractive and repulsive cues. This result, together with the effects on neurite outgrowth, suggests that SNAP-25 regulates motor neuron development by means of multiple novel mechanisms.

Surprisingly, neuronal outgrowth was not inhibited in hippocampal E17.5-18.5 neuron cultures from SNAP-25 null mice (Washbourne et al., 2002). The explanation for this inconsistency is not clear. It is possible that the requirement for SNAP-25 may be species or cell type specific but my work argues against this because we detected outgrowth defects in both zebrafish embryos and mammalian cultured cell lines. The neurons from the SNAP-25 null mice showed subsequent loss of VAMP-2 positive processes that were followed by further degeneration, suggesting that the differences may be due to timing rather than species or cell specific differences.

We have shown that *miR-153* regulate SNAP-25 in motor neurons to control development and synaptic activity. The majority of *miR-153* is expressed in the brain suggesting that precise regulation of SNAP-25 is also required for appropriate neuronal function and development in the zebrafish brain. In fact, our preliminary data indicate that *miR-153* is also required during synaptic vesicle formation in the brain.

Furthermore, our data from rat neuroendocrine pituitary cells (GH4C1) clearly indicate *miR-153* can also regulate growth factor secretion in neurosceretory cells. Thus, *miR-153* may control SNAP-25 levels in multiple settings, perhaps including other neuroendocrine glands including the pituitary, the pineal gland and the adrenal glands (Hepp and Langley, 2001). Future work needs to focus on the *in vivo* role of *miR-153* in brains, especially neurite outgrowth of specific neurons and regulation of homeostasis and secretion activities in neuroendocrine glands.

miR-27 in pharyngeal arch development

The knockdown of *miR-27* using morpholinos resulted in the total loss of pharyngeal arches and deformed trabeculae. However, overexpression of *miR-27* seemed not cause any dramatic morphological phenotypes in the jaw. Alcian blue staining of ECM indicates that the fish overexpressing *miR-27* have all the necessary cartilage elements in the appropriate positions. This could be due to sufficient silencing of targets by endogenous levels of *miR-27* or possibly due to short half-life of injected *miR-27* before chondrogenesis begins. To overcome these problems, I created transgenic fish that overexpress *miR-27* driven by either the hsp 70 heat-shock promoter or the *sox10* promoter to enable temporal and tissue specific control of *miR-27* expression. The construct I created contains pri-*miR-27* sequences in an artificial intron of GFP such that splicing results in expression of GFP and therefore an indicator or *miR-27* expression (Nicoli et al., 2010). Using *in situ* hybridization, I have shown that *miR-27* can be successfully overexpressed in fish at 72 hpf upon heat shock. Future work is needed to characterize the morphological phenotypes in these fish and identify dysregulated genes

upon overexpression of *miR-27*. By comparison to *miR-27* knockdown fish, the goal is identify differentially expressed genes subject to *miR-27* control.

miR-27 has been reported to be a cancer-related miRNA due to its function in mediating degradation of extracellular matrix. We obtained preliminary evidence indicating that *miR-27* can target *Ptk2.2*, a tyrosine kinase that is concentrated in focal adhesions that form among cells attaching to extracellular matrix constituents. Increased tyrosine kinase activity suppresses MMP14 endocytosis and enhances the activity of MMP14 (Washbourne et al., 2002). Given the fact that MMP14 is a matrix metalloproteinase that mediates cleavage and degradation of many ECM proteins (Williams et al., 2012), it is possible that up-regulation of *Ptk2.2* upon the loss of *miR-27* is responsible for the phenotypes we observed in *miR-27* knockdown fish. A second zebrafish tyrosine kinase, Ptk2.1 is also predicted to be a target of *miR-27*, raising the possibility that these two kinases function coordinately to regulate ECM formation and cartilage development. Future work is needed is provide insight into the mechanism by which *Ptk2.2* and possibly *Ptk2.1* regulate pharyngeal arch development.

APPENDIX

A. Details of small RNA sequencing data.

The following tables are available at http://rnajournal.cshlp.org/content/18/5/915/suppl/DC1

Supplemental Table 1. Expression of miRNAs.

Reads whose cloning frequency is less than 2 are eliminated and miRNA profiles of different stages are deposited into 4 different spread sheets. miRNA star sequences and loop sequences are highlighted in green and yellow, respectively. Reads derived from 2 neighboring cleavages sites on both sides at the 5' end are labeled in red. Some RNA reads that are inside of the mature miRNAs are also underlined. For *miR-430*, only mature miRNA sequences with more than 5 copies are retained.

Supplemental Table 2. miRNA 3' termini heterogeneity.

miRNA reads whose abundance is less than 3 were discarded. miRNA star sequences and loop sequences are highlighted in green and yellow, respectively. Small RNA reads mapping to different miRNA families are separated with a blank line. RNA reads derived from different stages are separated into different sheets.

Supplemental Table 3. piRNA clusters

piRNA clusters were analyzed using all piRNAs reads as listed below. In each cluster, the total number of reads may be smaller than the number of unique RNA sequences because the total number of reads in each position is weighted by dividing by the number of mapped positions in genome.

Supplemental Table 4. The sequences and expression of tRNA-derived small RNAs.

Small RNA reads derived from tRNAs were collected and deposited into different spread sheets based on the stages when they were discovered. Only those whose copy number is larger than 100 are shown. The start position indicates the position where a read mapped to one of the known tRNAs. Each read might map to more than one tRNA. Some random tRNA degradation reads might also be included in this list based on abundance.

Supplemental Table 5. The numbers of sequencing reads from the 4 developmental stages

Supplemental Table 6. The log2 value of all single miRNAs and miRNA families throughout development

Tab1: Normalized expression levels of miRNA families are indicated as log2 value of the read number of miRNA families across 4 development stages. miRNA family reads include reads exactly matching the genomic loci and reads having sequence variations at the 3' end. "-" means no expression.

Tab 2: Expression levels of each miRNA are indicated as log2 value of the number of miRNA reads across 4 development stages, including "3p" and "5p" miRNAs. Star strands are not included. Normalization was performed using expression ratios of *miR-9* across development. miRNA reads include those exactly matching the genomic loci and reads having sequence variations at the 3' end. "-" means no expression.

B. Movies of zebrafish movement.

The supplemental movie is available at
http://www.plosone.org/article/info%3Adoi%2F10.1371%2Fjournal.pone.0057080

Supplemental Movie 1. Embryo Movements in different conditions.

0:00-0:11. NIC Embryo Movements at 24 hpf

Noninjected control (NIC) zebrafish embryos at 24 hpf were filmed for one minute. Twitching was counted from individual embryos over multiple movies, as quantitated in Figure 17.

0:11-0:21. Effects of miR-153 Overexpression on Movement at 24 hpf

Single cell zebrafish embryos were injected with *miR-153* and filmed for one minute at 24 hpf. Twitching was counted from individual embryos over multiple movies, as quantitated in Figure 17.

0:22-0:32. Effects of Knockdown of *miR-153* on Movement at 24 hpf

Single cell zebrafish embryos were injected with *miR-153*^{MOs} and filmed for one minute at 24 hpf. Twitching was counted from individual embryos over multiple movies, as

quantitated in Figure 17.

0:33-0:42. Effects of Decreased SNAP-25 Expression on Movement at 24 hpf

Single cell zebrafish embryos were injected with *snap-25a,b*^{MO} and filmed for one minute at 24 hpf. Twitching was counted from individual embryos over multiple movies, as quantitated in Figure 17.

0:42-0:52. Effects of Increased SNAP-25 Expression on Movement at 24 hpf

Single cell zebrafish embryos were injected with snap-25a,b mRNA and filmed for one minute at 24 hpf. Twitching was counted from individual embryos over multiple movies, as quantitated in Figure 17.

0:52-1:02. Effects of co-Injection of *miR-153* and *snap-25a,b* on Movement at 24 hpf

Single cell zebrafish embryos were co-injected with *miR-153* and *snap-25a,b* mRNA and filmed for one minute at 24 hpf. Twitching was counted from individual embryos over multiple movies, as quantitated in Figure 17.

1:02-1:12. Effects of co-Injection of *miR-153*^{MO} and *snap-25a,b*^{MO} on Movement at 24 hpf

Single cell zebrafish embryos were co-injected with *miR-153*^{MO} and *snap-25a,b*^{MO} and filmed for one minute at 24 hpf. Twitching was counted from individual embryos over multiple movies, as quantitated in Figure 17.

1:12-1:22. NIC Embryo Movements at 28 hpf

Noninjected control (NIC) zebrafish embryos at 28 hpf were filmed for one minute at the same time that the following Movies were created. Twitching was counted from individual embryos, as quantitated in Figure 24C.

1:22-1:32. Effects of Botulinum Toxin Treatment on Movement at 28 hpf

Single cell zebrafish embryos were injected with injection dye and treated with Botulinum toxin A at 27 hpf. After a 30 min treatment, embryos were washed and allowed to recuperate for 1 hour before being filmed. Twitching was counted from individual embryos, as quantitated in Figure 24C.

1:33-1:42. Effects of Botulinum Exposure and co-Injection of *miR-153*^{MO} on Movement at 28 hpf

Single cell zebrafish embryos were injected with *miR-153*^{MOs} and treated with Botulinum toxin A at 27 hpf. After a 30 min treatment, embryos were washed and allowed to

recuperate for 1 hour before being filmed. Twitching was counted from individual embryos, as quantitated in Figure 24C.

1:42-1:52. Effects of Botulinum Exposure and co-Injection of *snap-25a,b* mRNA on Movement at 28 hpf

Single cell zebrafish embryos were injected with *snap-25a,b* mRNA and treated with Botulinum toxin A at 27 hpf. After a 30 min treatment, embryos were washed and allowed to recuperate for 1 hour before being filmed. Twitching was counted from individual embryos, as quantitated in Figure 24C.

C. Novel Zebrafish miRNA sequences.

The precursor sequence of each novel miRNA candidate is list below in red with its predicted secondary structure. The corresponding reads and their alignment are also indicated with their abundance on the right side. For Novel_6-Novel_8, which were derived from the alignment with known miRNAs of other species, the homologous miRNA sequences are also indicated on the top of the novel miRNAs.

The novel miRNAs and sequence alignments are available in the next page.

Novel_1:

```
UUGGGACCUUGUUUUCCAUUUUGAAAACUGUUAUCAGUAAGUAUAGUAUUCAACACAAACUAAAUAAUCAAUAAUACAUACAUAAAUACAUACAUAAACAACAAUGGAAGCCAAUGGUUACCAG
((((((((((.((((((((((...((((....))))..((((.(((((.......................))))))))).................))).))))))))).))).)))).))))
....................................................................................................ACAAUGGAAGCCAAUGGUUA......2
....................................................................................................ACAAUGGAAGCCAAUGGUUAC....33
....................................................................................................ACAAUGGAAGCCAAUGGUUACC...15
....................................................................................................ACAAUGGAAGCCAAUGGUUACCA...1
....................................................................................................CAAUGGAAGCCAAUGGUUA......2
....................................................................................................CAAUGGAAGCCAAUGGUUAC....19
....................................................................................................CAAUGGAAGCCAAUGGUUACC..152
....................................................................................................CAAUGGAAGCCAAUGGUUACCA...5
....................................................................................................CAAUGGAAGCCAAUGGUUA......2
```

Novel_2:

```
GACAGAAAAAGAGAUAUUUUGAAAAAUGUUGUAAGCCGGUAACCAUUGACCUCCAUAGUAUUUGUUUUCCCUGUUAUGAAGGUCAAUGGUUACCAGUUUUCAGCUUUCUUCUGAACAUCAUCUUUUUUGUU
(((((((((.(((((.(((.(((.((.((((.((((.(((((((((((((((.(((((.............)))))..)))))))))))))))).))))..))))..)).)))..)))..)))..)))))))))))
.....................................GUAACCAUUGACCUCCAUAGU.....................................................................1
.....................................UAACCAUUGACCUCCAUAGUA.....................................................................1
.....................................................................AUGAAGGUCAAUGGUUACCAGU.....................................1
.....................................................................UGAAGGUCAAUGGUUACCAG.......................................1
.....................................................................UGAAGGUCAAUGGUUACCAGU......................................15
.....................................................................UGAAGGUCAAUGGUUACCAGUU.....................................79
.....................................................................UGAAGGUCAAUGGUUACCAGUUU....................................3
.....................................................................GAAGGUCAAUGGUUACCAGUUU.....................................3
```

Novel_3:

```
GAGUGCCCAGUGCUGUACCAUGCUGGUAGCCAGUAUGAAAUAGGGCUUGCUGGUAACCAGCGUUGUGCCCCACUGGUUGCUC
((((..((((((..((((.(((((((((.(((((((.............)))))))..)))))))).))))..))))))..))))
............UGUACCAUGCUGGUAGCCAGU.....................................................................13
............UGUACCAUGCUGGUAGCCAGUA....................................................................13
```

Novel_4:

```
GCUAAUACUAGUAAUGGAAAUACUCGCUGAUACUGCAAGAAUUGUGGCAUCGGUAUAAGCCAGUAUUUCCGAUACUAGUAUUGGU
((((((((((((.((((((((((.(((.((((((.............))))))..))).))))))))))..))))))))))))
............AAUGGAAAUACUCGCUGAUACU.....................................................................23
............AAUGGAAAUACUCGCUGAUACUG....................................................................5
............AAUGGAAAUACUCGCUGAUACUGCA..................................................................1
............AUGGAAAUACUCGCUGAUACU.....................................................................1
............AUGGAAAUACUCGCUGAUACUG....................................................................48
............AUGGAAAUACUCGCUGAUACUGCA..................................................................1
............UGGAAAUACUCGCUGAUACUGC....................................................................1
.....................................................UAUAAGCCAGUAUUUCCGAU.....................................1
```

Novel_5:
AGAAACUGUGAAUCCUACACUGGAAGGUUGAUGUUUUACAGUUCUCUUCCAAGUGUUAUGAGUCAAAGUUUCU
((((((.(((.((..((((((((((....((.....))....))))))).))))))...)).))).)))))))
......UGUGAAUCCUACACUGGAAGG.....40
......UGUGAAUCCUACACUGGAAGGU.....1
.....UUCCAAGUGUUAUGAGUCA.....1
.....UUCCAAGUGUUAUGAGUCAAAG.....1
.....UUCCAAGUGUUAUGAGUCAAAGU.....16

Novel_6:
GCUGAUCAGUAGUGGGAUCGCGCCUGUGAAUAGCCACUGUACUCCAGCCUGGGCAACAUAGCGAGACCCCGUCUCUUUUG..... ssc-mir-1285
GCUGAUCAGUAGUGGGAUCGCGCCUGUGAAUAGACACUGCAGUGCAGCCUGAGCAACACAGAGAGACGCAGACUUUUCUU
.......((.((((.(..((.((((.((((....(...(((.....)))......)..)))))).).))..).).)))).
.....GUAGUGGGAUCGCGCCUG.....9
.....GUGGGAUCGCGCCUGUGAAU.....7
.....GUGGGAUCGCGCCUGUGA.....6
.....GUGGGAUCGCGCCUGUGAAUA.....4
.....GUGGGAUCGCGCCUGUGA.....6
...GAUCAGUAGUGGGAUCGCGC.....7

Novel_7:
CCACCUCCCCUGCAAACGUCCAGUGAUGCAGAGGUAAUGGACGUUGGCUCUGGUGGUG.....bta-miR-1306
UCCACCACCUCCCCUGCAAACGUCCAGUGACGCAGAGGAAAUGGACGUUAGCUCUGGUGGUGAUGGACA
((((.((((.((...((.(((((((((.............)))))))).))...)).)))).)))))..
....CCACCUCCCCUGCAAACGUCCA.....7

Novel_8:
CGGGUGGAGCCGCCGCGGGUGCAGAUCUUGGUGGUAGUAGCAAAUAUUCAAACGAGAACUUUGAAGGCCGAAGUGGAGAAGGGUUCCAUGUG.....mdo-mir-739
CGGGUGGAGCCGCCGCGGGUGCAGAUCUUGGUGGUAGUAGCAAAUAUUCAAACGAGAGCUUUGAAGGCCGAAGUGGAGAAGGGUUCCAUGUG
((.(((((((.((((.(((.(((((((((.....(((.....)))).....))))))..))))).....)))...))))..)))))))).))
.....GAAGUGGAGAAGGGUUCC.....113
.....GGCCGAAGUGGAGAAGGG.....99
.....GCCGAAGUGGAGAAGGGU.....98
.....AGCCGCCGCGGGUGCAGAU.....7
.....GAAGUGGAGAAGGGUUCCAU.....69
.....GAAGUGGAGAAGGGUUCCAUG.....69
.....UGCAGAUCUUGGUGGUAGU.....22
.....GUGCAGAUCUUGGUGGUAGU.....17

REFERENCES

Agostini, M., Tucci, P., Steinert, J.R., Shalom-Feuerstein, R., Rouleau, M., Aberdam, D., Forsythe, I.D., Young, K.W., Ventura, A., Concepcion, C.P., *et al*. (2011). microRNA-34a regulates neurite outgrowth, spinal morphology, and function. Proceedings of the National Academy of Sciences of the United States of America *108*, 21099-21104.

Ajay, S.S., Parker, S.C., Abaan, H.O., Fajardo, K.V., and Margulies, E.H. (2011). Accurate and comprehensive sequencing of personal genomes. Genome research *21*, 1498-1505.

Akerblom, M., Sachdeva, R., Barde, I., Verp, S., Gentner, B., Trono, D., and Jakobsson, J. (2012). MicroRNA-124 is a subventricular zone neuronal fate determinant. The Journal of neuroscience : the official journal of the Society for Neuroscience *32*, 8879-8889.

Amack, J.D., Wang, X., and Yost, H.J. (2007). Two T-box genes play independent and cooperative roles to regulate morphogenesis of ciliated Kupffer's vesicle in zebrafish. Developmental biology *310*, 196-210.

Amack, J.D., and Yost, H.J. (2004). The T box transcription factor no tail in ciliated cells controls zebrafish left-right asymmetry. Current biology : CB *14*, 685-690.

Ameres, S.L., Horwich, M.D., Hung, J.H., Xu, J., Ghildiyal, M., Weng, Z., and Zamore, P.D. (2010). Target RNA-directed trimming and tailing of small silencing RNAs. Science *328*, 1534-1539.

Anokye-Danso, F., Trivedi, C.M., Juhr, D., Gupta, M., Cui, Z., Tian, Y., Zhang, Y., Yang, W., Gruber, P.J., Epstein, J.A., *et al*. (2011). Highly efficient miRNA-mediated reprogramming of mouse and human somatic cells to pluripotency. Cell stem cell *8*, 376-388.

Appel, B., Korzh, V., Glasgow, E., Thor, S., Edlund, T., Dawid, I.B., and Eisen, J.S. (1995). Motoneuron fate specification revealed by patterned LIM homeobox gene expression in embryonic zebrafish. Development *121*, 4117-4125.

Aravin, A., Gaidatzis, D., Pfeffer, S., Lagos-Quintana, M., Landgraf, P., Iovino, N., Morris, P., Brownstein, M.J., Kuramochi-Miyagawa, S., Nakano, T., *et al*. (2006). A novel class of small RNAs bind to MILI protein in mouse testes. Nature *442*, 203-207.

Aravin, A.A., Sachidanandam, R., Girard, A., Fejes-Toth, K., and Hannon, G.J. (2007). Developmentally regulated piRNA clusters implicate MILI in transposon control. Science *316*, 744-747.

Arber, S., Han, B., Mendelsohn, M., Smith, M., Jessell, T.M., and Sockanathan, S. (1999). Requirement for the homeobox gene Hb9 in the consolidation of motor neuron identity. Neuron *23*, 659-674.

Arvanitis, D.N., Jungas, T., Behar, A., and Davy, A. (2010). Ephrin-B1 reverse signaling controls a posttranscriptional feedback mechanism via miR-124. Molecular and cellular biology *30*, 2508-2517.

Asakura, T., Waga, N., Ogura, K., and Goshima, Y. (2010). Genes required for cellular UNC-6/netrin localization in Caenorhabditis elegans. Genetics *185*, 573-585.

Ashraf, S.I., McLoon, A.L., Sclarsic, S.M., and Kunes, S. (2006). Synaptic protein synthesis associated with memory is regulated by the RISC pathway in Drosophila. Cell *124*, 191-205.

Atouf, F., Czernichow, P., and Scharfmann, R. (1997). Expression of neuronal traits in pancreatic beta cells. Implication of neuron-restrictive silencing factor/repressor element silencing transcription factor, a neuron-restrictive silencer. The Journal of biological chemistry *272*, 1929-1934.

Augustin, I., Rosenmund, C., Sudhof, T.C., and Brose, N. (1999). Munc13-1 is essential for fusion competence of glutamatergic synaptic vesicles. Nature *400*, 457-461.

Babiarz, J.E., Ruby, J.G., Wang, Y., Bartel, D.P., and Blelloch, R. (2008). Mouse ES cells express endogenous shRNAs, siRNAs, and other Microprocessor-independent, Dicer-dependent small RNAs. Genes & development *22*, 2773-2785.

Baek, D., Villen, J., Shin, C., Camargo, F.D., Gygi, S.P., and Bartel, D.P. (2008). The impact of microRNAs on protein output. Nature *455*, 64-71.

Bar, M., Wyman, S.K., Fritz, B.R., Qi, J., Garg, K.S., Parkin, R.K., Kroh, E.M., Bendoraite, A., Mitchell, P.S., Nelson, A.M., *et al*. (2008). MicroRNA discovery and profiling in human embryonic stem cells by deep sequencing of small RNA libraries. Stem Cells *26*, 2496-2505.

Bark, C., Bellinger, F.P., Kaushal, A., Mathews, J.R., Partridge, L.D., and Wilson, M.C. (2004). Developmentally regulated switch in alternatively spliced SNAP-25 isoforms alters facilitation of synaptic transmission. The Journal of neuroscience : the official journal of the Society for Neuroscience *24*, 8796-8805.

Bartel, D. (2004). MicroRNAs: genomics, biogenesis, mechanism, and function. Cell *116*, 281-297.

Bartel, D.P. (2009). MicroRNAs: target recognition and regulatory functions. Cell *136*, 215-233.

Bartel, D.P., and Chen, C.Z. (2004). Micromanagers of gene expression: the potentially widespread influence of metazoan microRNAs. Nature reviews Genetics *5*, 396-400.

Baudet, M.L., Zivraj, K.H., Abreu-Goodger, C., Muldal, A., Armisen, J., Blenkiron, C., Goldstein, L.D., Miska, E.A., and Holt, C.E. (2012). miR-124 acts through CoREST to control onset of Sema3A sensitivity in navigating retinal growth cones. Nature neuroscience *15*, 29-38.

Baudry, A., Mouillet-Richard, S., Schneider, B., Launay, J.M., and Kellermann, O. (2010). miR-16 targets the serotonin transporter: a new facet for adaptive responses to antidepressants. Science *329*, 1537-1541.

Baulcombe, D.C. (1999). Fast forward genetics based on virus-induced gene silencing. Current opinion in plant biology *2*, 109-113.

Benetti, R., Gonzalo, S., Jaco, I., Munoz, P., Gonzalez, S., Schoeftner, S., Murchison, E., Andl, T., Chen, T., Klatt, P., *et al*. (2008). A mammalian microRNA cluster controls DNA methylation and telomere recombination via Rbl2-dependent regulation of DNA methyltransferases. Nature structural & molecular biology *15*, 998.

Bentley, D.R., Balasubramanian, S., Swerdlow, H.P., Smith, G.P., Milton, J., Brown, C.G., Hall, K.P., Evers, D.J., Barnes, C.L., Bignell, H.R., *et al*. (2008). Accurate whole human genome sequencing using reversible terminator chemistry. Nature *456*, 53-59.

Berbari, N.F., O'Connor, A.K., Haycraft, C.J., and Yoder, B.K. (2009). The primary cilium as a complex signaling center. Current biology : CB *19*, R526-535.

Berezikov, E., Robine, N., Samsonova, A., Westholm, J.O., Naqvi, A., Hung, J.H., Okamura, K., Dai, Q., Bortolamiol-Becet, D., Martin, R., *et al*. (2011). Deep annotation of Drosophila melanogaster microRNAs yields insights into their processing, modification, and emergence. Genome research *21*, 203-215.

Bernstein, E., Caudy, A.A., Hammond, S.M., and Hannon, G.J. (2001). Role for a bidentate ribonuclease in the initiation step of RNA interference. Nature *409*, 363-366.

Bernstein, E., Kim, S.Y., Carmell, M.A., Murchison, E.P., Alcorn, H., Li, M.Z., Mills, A.M., Elledge, S.J., Anderson, K.V., Hannon G.J. (2003). Dicer is essential for mouse development. Nature Genetcs *35*, 215-217.

Bicker, S., and Schratt, G. (2008). microRNAs: tiny regulators of synapse function in development and disease. Journal of cellular and molecular medicine *12*, 1466-1476.

Blaser, H., Eisenbeiss, S., Neumann, M., Reichman-Fried, M., Thisse, B., Thisse, C., and Raz, E. (2005). Transition from non-motile behaviour to directed migration during early PGC development in zebrafish. Journal of cell science *118*, 4027-4038.

Blasi, J., Chapman, E.R., Link, E., Binz, T., Yamasaki, S., De Camilli, P., Sudhof, T.C., Niemann, H., and Jahn, R. (1993). Botulinum neurotoxin A selectively cleaves the synaptic protein SNAP-25. Nature *365*, 160-163.

Braun, J.E., Huntzinger, E., Fauser, M., and Izaurralde, E. (2011). GW182 proteins directly recruit cytoplasmic deadenylase complexes to miRNA targets. Molecular cell *44*, 120-133.

Brennecke, J., Aravin, A.A., Stark, A., Dus, M., Kellis, M., Sachidanandam, R., and Hannon, G.J. (2007). Discrete small RNA-generating loci as master regulators of transposon activity in Drosophila. Cell *128*, 1089-1103.

Burgoyne, R.D., and Morgan, A. (2003). Secretory granule exocytosis. Physiological reviews *83*, 581-632.

Burns, D.M., D'Ambrogio, A., Nottrott, S., and Richter, J.D. (2011). CPEB and two poly(A) polymerases control miR-122 stability and p53 mRNA translation. Nature *473*, 105-108.

Burroughs, A.M., Ando, Y., de Hoon, M.J., Tomaru, Y., Nishibu, T., Ukekawa, R., Funakoshi, T., Kurokawa, T., Suzuki, H., Hayashizaki, Y., *et al*. (2010). A comprehensive survey of 3' animal miRNA modification events and a possible role for 3' adenylation in modulating miRNA targeting effectiveness. Genome research *20*, 1398-1410.

Cai, X., Hagedorn, C.H., and Cullen, B.R. (2004). Human microRNAs are processed from capped, polyadenylated transcripts that can also function as mRNAs. Rna *10*, 1957-1966.

Cao, J., Shen, Y., Zhu, L., Xu, Y., Zhou, Y., Wu, Z., Li, Y., Yan, X., and Zhu, X. (2012). miR-129-3p controls cilia assembly by regulating CP110 and actin dynamics. Nature cell biology *14*, 697-706.

Castel, S.E., and Martienssen, R.A. (2013). RNA interference in the nucleus: roles for small RNAs in transcription, epigenetics and beyond. Nature reviews Genetics *14*, 100-112.

Catterall, W.A., and Few, A.P. (2008). Calcium channel regulation and presynaptic plasticity. Neuron *59*, 882-901.

Chang, S., Johnston, R.J., Jr., Frokjaer-Jensen, C., Lockery, S., and Hobert, O. (2004). MicroRNAs act sequentially and asymmetrically to control chemosensory laterality in the nematode. Nature *430*, 785-789.

Chekulaeva, M., Mathys, H., Zipprich, J.T., Attig, J., Colic, M., Parker, R., and Filipowicz, W. (2011). miRNA repression involves GW182-mediated recruitment of CCR4-NOT through conserved W-containing motifs. Nature structural & molecular biology *18*, 1218-1226.

Chen, P.Y., Manninga, H., Slanchev, K., Chien, M., Russo, J.J., Ju, J., Sheridan, R., John, B., Marks, D.S., Gaidatzis, D., *et al*. (2005). The developmental miRNA profiles of zebrafish as determined by small RNA cloning. Genes Dev *19*, 1288-1293.

Chen, X., Xu, H., Yuan, P., Fang, F., Huss, M., Vega, V.B., Wong, E., Orlov, Y.L., Zhang, W., Jiang, J., *et al*. (2008). Integration of external signaling pathways with the core transcriptional network in embryonic stem cells. Cell *133*, 1106-1117.

Cheng, L.C., Pastrana, E., Tavazoie, M., and Doetsch, F. (2009). miR-124 regulates adult neurogenesis in the subventricular zone stem cell niche. Nature neuroscience *12*, 399-408.

Chiang, H.R., Schoenfeld, L.W., Ruby, J.G., Auyeung, V.C., Spies, N., Baek, D., Johnston, W.K., Russ, C., Luo, S., Babiarz, J.E., *et al*. (2010). Mammalian microRNAs: experimental evaluation of novel and previously annotated genes. Genes & development *24*, 992-1009.

Choi, U.B., Strop, P., Vrljic, M., Chu, S., Brunger, A.T., and Weninger, K.R. (2010). Single-molecule FRET-derived model of the synaptotagmin 1-SNARE fusion complex. Nature structural & molecular biology *17*, 318-324.

Chong, J.A., Tapia-Ramirez, J., Kim, S., Toledo-Aral, J.J., Zheng, Y., Boutros, M.C., Altshuller, Y.M., Frohman, M.A., Kraner, S.D., and Mandel, G. (1995). REST: a mammalian silencer protein that restricts sodium channel gene expression to neurons. Cell *80*, 949-957.

Christodoulou, F., Raible, F., Tomer, R., Simakov, O., Trachana, K., Klaus, S., Snyman, H., Hannon, G.J., Bork, P., and Arendt, D. (2010). Ancient animal microRNAs and the evolution of tissue identity. Nature *463*, 1084-1088.

Clouthier, D.E., and Schilling, T.F. (2004). Understanding endothelin-1 function during craniofacial development in the mouse and zebrafish. Birth defects research Part C, Embryo today : reviews *72*, 190-199.

Cohen, J.E., Lee, P.R., Chen, S., Li, W., and Fields, R.D. (2011). MicroRNA regulation of homeostatic synaptic plasticity. Proceedings of the National Academy of Sciences of the United States of America *108*, 11650-11655.

Cohen, S.M., and Brennecke, J. (2006). Developmental biology. Mixed messages in early development. Science *312*, 65-66.

Cohen-Cory, S., Kidane, A.H., Shirkey, N.J., and Marshak, S. (2010). Brain-derived neurotrophic factor and the development of structural neuronal connectivity. Developmental neurobiology *70*, 271-288.

Cole, C., Sobala, A., Lu, C., Thatcher, S.R., Bowman, A., Brown, J.W., Green, P.J., Barton, G.J., and Hutvagner, G. (2009). Filtering of deep sequencing data reveals the existence of abundant Dicer-dependent small RNAs derived from tRNAs. RNA *15*, 2147-2160.

Conaco, C., Otto, S., Han, J.J., and Mandel, G. (2006). Reciprocal actions of REST and a microRNA promote neuronal identity. Proceedings of the National Academy of Sciences of the United States of America *103*, 2422-2427.

Corcoran, D.L., Pandit, K.V., Gordon, B., Bhattacharjee, A., Kaminski, N., and Benos, P.V. (2009). Features of mammalian microRNA promoters emerge from polymerase II chromatin immunoprecipitation data. PloS one *4*, e5279.

Couly, G.F., Coltey, P.M., and Le Douarin, N.M. (1993). The triple origin of skull in higher vertebrates: a study in quail-chick chimeras. Development *117*, 409-429.

Crooks, G.E., Hon, G., Chandonia, J.M., and Brenner, S.E. (2004). WebLogo: a sequence logo generator. Genome research *14*, 1188-1190.

Curtin, E., Hickey, G., Kamel, G., Davidson, A.J., and Liao, E.C. (2011). Zebrafish wnt9a is expressed in pharyngeal ectoderm and is required for palate and lower jaw development. Mechanisms of development *128*, 104-115.

Czech, B., Malone, C.D., Zhou, R., Stark, A., Schlingeheyde, C., Dus, M., Perrimon, N., Kellis, M., Wohlschlegel, J.A., Sachidanandam, R., *et al*. (2008). An endogenous small interfering RNA pathway in Drosophila. Nature *453*, 798-802.

Dajas-Bailador, F., Bonev, B., Garcez, P., Stanley, P., Guillemot, F., and Papalopulu, N. (2012). microRNA-9 regulates axon extension and branching by targeting Map1b in mouse cortical neurons. Nature neuroscience.

David, N.B., Saint-Etienne, L., Tsang, M., Schilling, T.F., and Rosa, F.M. (2002). Requirement for endoderm and FGF3 in ventral head skeleton formation. Development *129*, 4457-4468.

Delgado-Martinez, I., Nehring, R.B., and Sorensen, J.B. (2007). Differential abilities of SNAP-25 homologs to support neuronal function. The Journal of neuroscience : the official journal of the Society for Neuroscience *27*, 9380-9391.

Denli, A.M., Tops, B.B., Plasterk, R.H., Ketting, R.F., and Hannon, G.J. (2004). Processing of primary microRNAs by the Microprocessor complex. Nature *432*, 231-235.

Deo, M., Yu, J.Y., Chung, K.H., Tippens, M., and Turner, D.L. (2006). Detection of mammalian microRNA expression by in situ hybridization with RNA oligonucleotides. Developmental dynamics : an official publication of the American Association of Anatomists *235*, 2538-2548.

Dessi, F., Colle, M.A., Hauw, J.J., and Duyckaerts, C. (1997). Accumulation of SNAP-25 immunoreactive material in axons of Alzheimer's disease. Neuroreport *8*, 3685-3689.

Dill, H., Linder, B., Fehr, A., and Fischer, U. (2012). Intronic miR-26b controls neuronal differentiation by repressing its host transcript, ctdsp2. Genes & development *26*, 25-30.

Doxakis, E. (2010). Post-transcriptional regulation of alpha-synuclein expression by mir-7 and mir-153. The Journal of biological chemistry *285*, 12726-12734.

Eberhart, J.K., He, X., Swartz, M.E., Yan, Y.L., Song, H., Boling, T.C., Kunerth, A.K., Walker, M.B., Kimmel, C.B., and Postlethwait, J.H. (2008). MicroRNA Mirn140 modulates Pdgf signaling during palatogenesis. Nature genetics *40*, 290-298.

Eisen, J.S. (1991). Developmental neurobiology of the zebrafish. The Journal of neuroscience : the official journal of the Society for Neuroscience *11*, 311-317.

Eisen, J.S., Myers, P.Z., and Westerfield, M. (1986). Pathway selection by growth cones of identified motoneurones in live zebra fish embryos. Nature *320*, 269-271.

Emara, M.M., Ivanov, P., Hickman, T., Dawra, N., Tisdale, S., Kedersha, N., Hu, G.F., and Anderson, P. (2010). Angiogenin-induced tRNA-derived stress-induced RNAs promote stress-induced stress granule assembly. The Journal of biological chemistry *285*, 10959-10968.

Fabian, M.R., Cieplak, M.K., Frank, F., Morita, M., Green, J., Srikumar, T., Nagar, B., Yamamoto, T., Raught, B., Duchaine, T.F.*, et al*. (2011). miRNA-mediated deadenylation is orchestrated by GW182 through two conserved motifs that interact with CCR4-NOT. Nature structural & molecular biology *18*, 1211-1217.

Fernandez-Valverde, S.L., Taft, R.J., and Mattick, J.S. (2010). Dynamic isomiR regulation in Drosophila development. RNA *16*, 1881-1888.

Fire, A., SiQun Xu, Mary K. Montgomery, Steven A Kostas, Samuel E. Driver, Craig C. Mello (1998). Potent and specific genetic interference by double-stranded RNA in *Caenorahbditis elegans*. Nature *391*, 806-811.

Fliegauf, M., Benzing, T., and Omran, H. (2007). When cilia go bad: cilia defects and ciliopathies. Nature reviews Molecular cell biology *8*, 880-893.

Flynt, A.S., and Lai, E.C. (2008). Biological principles of microRNA-mediated regulation: shared themes amid diversity. Nature reviews Genetics *9*, 831-842.

Flynt, A.S., Li, N., Thatcher, E.J., Solnica-Krezel, L., and Patton, J.G. (2007). Zebrafish miR-214 modulates Hedgehog signaling to specify muscle cell fate. Nature genetics *39*, 259-263.

Friedlander, M.R., Adamidi, C., Han, T., Lebedeva, S., Isenbarger, T.A., Hirst, M., Marra, M., Nusbaum, C., Lee, W.L., Jenkin, J.C., *et al*. (2009). High-resolution profiling and discovery of planarian small RNAs. Proceedings of the National Academy of Sciences of the United States of America *106*, 11546-11551.

Friedlander, M.R., Chen, W., Adamidi, C., Maaskola, J., Einspanier, R., Knespel, S., and Rajewsky, N. (2008). Discovering microRNAs from deep sequencing data using miRDeep. Nat Biotechnol *26*, 407-415.

Gaffield, M.A., and Betz, W.J. (2006). Imaging synaptic vesicle exocytosis and endocytosis with FM dyes. Nature protocols *1*, 2916-2921.

Gao, J., Wang, W.Y., Mao, Y.W., Graff, J., Guan, J.S., Pan, L., Mak, G., Kim, D., Su, S.C., and Tsai, L.H. (2010). A novel pathway regulates memory and plasticity via SIRT1 and miR-134. Nature *466*, 1105-1109.

Ghildiyal, M., Seitz, H., Horwich, M.D., Li, C., Du, T., Lee, S., Xu, J., Kittler, E.L., Zapp, M.L., Weng, Z., *et al*. (2008). Endogenous siRNAs derived from transposons and mRNAs in Drosophila somatic cells. Science *320*, 1077-1081.

Gioia, M., Monaco, S., Van Den Steen, P.E., Sbardella, D., Grasso, G., Marini, S., Overall, C.M., Opdenakker, G., and Coletta, M. (2009). The collagen binding domain of gelatinase A modulates degradation of collagen IV by gelatinase B. Journal of molecular biology *386*, 419-434.

Giraldez, A.J. (2010). microRNAs, the cell's Nepenthe: clearing the past during the maternal-to-zygotic transition and cellular reprogramming. Curr Opin Genet Dev *20*, 369-375.

Giraldez, A.J., Cinalli, R.M., Glasner, M.E., Enright, A.J., Thomson, J.M., Baskerville, S., Hammond, S.M., Bartel, D.P., and Schier, A.F. (2005a). MicroRNAs Regulate Brain Morphogenesis in Zebrafish. Science *308*, 833-838.

Giraldez, A.J., Cinalli, R.M., Glasner, M.E., Enright, A.J., Thomson, J.M., Baskerville, S., Hammond, S.M., Bartel, D.P., and Schier, A.F. (2005b). MicroRNAs regulate brain morphogenesis in zebrafish. Science *308*, 833-838.

Giraldez, A.J., Mishima, Y., Rihel, J., Grocock, R.J., Van Dongen, S., Inoue, K., Enright, A.J., and Schier, A.F. (2006a). Zebrafish MiR-430 Promotes Deadenylation and Clearance of Maternal mRNAs. Science *312*, 75-79.

Giraldez, A.J., Mishima, Y., Rihel, J., Grocock, R.J., Van Dongen, S., Inoue, K., Enright, A.J., and Schier, A.F. (2006b). Zebrafish MiR-430 promotes deadenylation and clearance of maternal mRNAs. Science *312*, 75-79.

Girard, A., Sachidanandam, R., Hannon, G.J., and Carmell, M.A. (2006). A germline-specific class of small RNAs binds mammalian Piwi proteins. Nature *442*, 199-202.

Gitler, D., Takagishi, Y., Feng, J., Ren, Y., Rodriguiz, R.M., Wetsel, W.C., Greengard, P., and Augustine, G.J. (2004). Different presynaptic roles of synapsins at excitatory and inhibitory synapses. The Journal of neuroscience : the official journal of the Society for Neuroscience *24*, 11368-11380.

Goetz, S.C., and Anderson, K.V. (2010). The primary cilium: a signalling centre during vertebrate development. Nature reviews Genetics *11*, 331-344.

Gray, L.J., Dean, B., Kronsbein, H.C., Robinson, P.J., and Scarr, E. (2010). Region and diagnosis-specific changes in synaptic proteins in schizophrenia and bipolar I disorder. Psychiatry research *178*, 374-380.

Greenlee, M.H., Wilson, M.C., and Sakaguchi, D.S. (2002). Expression of SNAP-25 during mammalian retinal development: thinking outside the synapse. Seminars in cell & developmental biology *13*, 99-106.

Gregory, R.I., Yan, K.P., Amuthan, G., Chendrimada, T., Doratotaj, B., Cooch, N., and Shiekhattar, R. (2004). The Microprocessor complex mediates the genesis of microRNAs. Nature *432*, 235-240.

Griffiths-Jones, S. (2004). The microRNA Registry. Nucleic acids research *32 Database issue*, D109-111.

Griffiths-Jones, S., Grocock, R.J., van Dongen, S., Bateman, A., and Enright, A.J. (2006). miRBase: microRNA sequences, targets and gene nomenclature. Nucleic acids research *34*, D140-144.

Griffiths-Jones, S., Saini, H.K., van Dongen, S., and Enright, A.J. (2008). miRBase: tools for microRNA genomics. Nucleic acids research *36*, D154-158.

Grivna, S.T., Pyhtila, B., and Lin, H. (2006). MIWI associates with translational machinery and PIWI-interacting RNAs (piRNAs) in regulating spermatogenesis. Proceedings of the National Academy of Sciences of the United States of America *103*, 13415-13420.

Grosse, G., Grosse, J., Tapp, R., Kuchinke, J., Gorsleben, M., Fetter, I., Hohne-Zell, B., Gratzl, M., and Bergmann, M. (1999). SNAP-25 requirement for dendritic growth of hippocampal neurons. Journal of neuroscience research *56*, 539-546.

Gullerova, M., Moazed, D., and Proudfoot, N.J. (2011). Autoregulation of convergent RNAi genes in fission yeast. Genes & development *25*, 556-568.

Gullerova, M., and Proudfoot, N.J. (2012). Convergent transcription induces transcriptional gene silencing in fission yeast and mammalian cells. Nature structural & molecular biology *19*, 1193-1201.

Guo, H., Ingolia, N.T., Weissman, J.S., and Bartel, D.P. (2010). Mammalian microRNAs predominantly act to decrease target mRNA levels. Nature *466*, 835-840.

Guo, S., and Kemphues, K.J. (1995). par-1, a gene required for establishing polarity in C. elegans embryos, encodes a putative Ser/Thr kinase that is asymmetrically distributed. Cell *81*, 611-620.

Haase, A.D., Fenoglio, S., Muerdter, F., Guzzardo, P.M., Czech, B., Pappin, D.J., Chen, C., Gordon, A., and Hannon, G.J. (2010). Probing the initiation and effector phases of the somatic piRNA pathway in Drosophila. Genes & development *24*, 2499-2504.

Hafner, M., Landgraf, P., Ludwig, J., Rice, A., Ojo, T., Lin, C., Holoch, D., Lim, C., and Tuschl, T. (2008). Identification of microRNAs and other small regulatory RNAs using cDNA library sequencing. Methods *44*, 3-12.

Halic, M., and Moazed, D. (2009). Transposon silencing by piRNAs. Cell *138*, 1058-1060.

Hall, B.K. (1980). Tissue interactions and the initiation of osteogenesis and chondrogenesis in the neural crest-derived mandibular skeleton of the embryonic mouse as seen in isolated murine tissues and in recombinations of murine and avian tissues. Journal of embryology and experimental morphology *58*, 251-264.

Hall, B.K. (1981). The induction of neural crest-derived cartilage and bone by embryonic epithelia: an analysis of the mode of action of an epithelial-mesenchymal interaction. Journal of embryology and experimental morphology *64*, 305-320.

Hammond, S.M., Bernstein, E., Beach, D., and Hannon, G.J. (2000). An RNA-directed nuclease mediates post-transcriptional gene silencing in *Drosophila* cells. Nature *404*, 293-296.

Han, J., Lee, Y., Yeom, K.H., Kim, Y.K., Jin, H., and Kim, V.N. (2004). The Drosha-DGCR8 complex in primary microRNA processing. Genes & development *18*, 3016-3027.

Han, J., Lee, Y., Yeom, K.H., Nam, J.W., Heo, I., Rhee, J.K., Sohn, S.Y., Cho, Y., Zhang, B.T., and Kim, V.N. (2006). Molecular basis for the recognition of primary microRNAs by the Drosha-DGCR8 complex. Cell *125*, 887-901.

Harbers, M., and Carninci, P. (2005). Tag-based approaches for transcriptome research and genome annotation. Nature methods *2*, 495-502.

Harfe, B.D., McManus, M.T., Mansfield, J.H., Hornstein, E., and Tabin, C.J. (2005). The RNaseIII enzyme Dicer is required for morphogenesis but not patterning of the vertebrate limb. Proceedings of the National Academy of Sciences of the United States of America *102*, 10898-10903.

Harris, K.S., Zhang, Z., McManus, M.T., Harfe, B.D., and Sun, X. (2006). Dicer function is essential for lung epithelium morphogenesis. Proceedings of the National Academy of Sciences of the United States of America *103*, 2208-2213.

Haussecker, D., Huang, Y., Lau, A., Parameswaran, P., Fire, A.Z., and Kay, M.A. (2010). Human tRNA-derived small RNAs in the global regulation of RNA silencing. RNA *16*, 673-695.

He, X., Yan, Y.L., DeLaurier, A., and Postlethwait, J.H. (2011a). Observation of miRNA gene expression in zebrafish embryos by in situ hybridization to microRNA primary transcripts. Zebrafish *8*, 1-8.

He, X., Yan, Y.L., Eberhart, J.K., Herpin, A., Wagner, T.U., Schartl, M., and Postlethwait, J.H. (2011b). miR-196 regulates axial patterning and pectoral appendage initiation. Developmental biology *357*, 463-477.

Heo, I., Joo, C., Kim, Y.K., Ha, M., Yoon, M.J., Cho, J., Yeom, K.H., Han, J., and Kim, V.N. (2009). TUT4 in concert with Lin28 suppresses microRNA biogenesis through pre-microRNA uridylation. Cell *138*, 696-708.

Hepp, R., and Langley, K. (2001). SNAREs during development. Cell and tissue research *305*, 247-253.

Hofacker, I.L. (2003). Vienna RNA secondary structure server. Nucleic acids research *31*, 3429-3431.

Houwing, S., Berezikov, E., and Ketting, R.F. (2008). Zili is required for germ cell differentiation and meiosis in zebrafish. The EMBO journal *27*, 2702-2711.

Houwing, S., Kamminga, L.M., Berezikov, E., Cronembold, D., Girard, A., van den Elst, H., Filippov, D.V., Blaser, H., Raz, E., Moens, C.B., *et al*. (2007). A role for Piwi and piRNAs in germ cell maintenance and transposon silencing in Zebrafish. Cell *129*, 69-82.

Hutvagner, G., McLachlan, J., Pasquinelli, A.E., Balint, E., Tuschl, T., and Zamore, P.D. (2001). A cellular function for the RNA-interference enzyme Dicer in the maturation of the let-7 small temporal RNA. Science *293*, 834-838.

Hutvagner, G., and Simard, M.J. (2008). Argonaute proteins: key players in RNA silencing. Nature reviews Molecular cell biology *9*, 22-32.

Igarashi, M., Kozaki, S., Terakawa, S., Kawano, S., Ide, C., and Komiya, Y. (1996). Growth cone collapse and inhibition of neurite growth by Botulinum neurotoxin C1: a t-SNARE is involved in axonal growth. The Journal of cell biology *134*, 205-215.

Igarashi, M., Tagaya, M., and Komiya, Y. (1997). The soluble N-ethylmaleimide-sensitive factor attached protein receptor complex in growth cones: molecular aspects of the axon terminal development. The Journal of neuroscience : the official journal of the Society for Neuroscience *17*, 1460-1470.

Impey, S., Davare, M., Lesiak, A., Fortin, D., Ando, H., Varlamova, O., Obrietan, K., Soderling, T.R., Goodman, R.H., and Wayman, G.A. (2010). An activity-induced microRNA controls dendritic spine formation by regulating Rac1-PAK signaling. Molecular and cellular neurosciences *43*, 146-156.

Irizarry, R.A., Warren, D., Spencer, F., Kim, I.F., Biswal, S., Frank, B.C., Gabrielson, E., Garcia, J.G., Geoghegan, J., Germino, G., *et al*. (2005). Multiple-laboratory comparison of microarray platforms. Nature methods *2*, 345-350.

Jahn, R., and Scheller, R.H. (2006). SNAREs--engines for membrane fusion. Nature reviews Molecular cell biology *7*, 631-643.

Ji, L., and Chen, X. (2012). Regulation of small RNA stability: methylation and beyond. Cell research *22*, 624-636.

Johnson, C.D., Esquela-Kerscher, A., Stefani, G., Byrom, M., Kelnar, K., Ovcharenko, D., Wilson, M., Wang, X., Shelton, J., Shingara, J., *et al*. (2007). The let-7 microRNA represses cell proliferation pathways in human cells. Cancer research *67*, 7713-7722.

Jones, M.R., Quinton, L.J., Blahna, M.T., Neilson, J.R., Fu, S., Ivanov, A.R., Wolf, D.A., and Mizgerd, J.P. (2009). Zcchc11-dependent uridylation of microRNA directs cytokine expression. Nature cell biology *11*, 1157-1163.

Kamminga, L.M., Luteijn, M.J., den Broeder, M.J., Redl, S., Kaaij, L.J., Roovers, E.F., Ladurner, P., Berezikov, E., and Ketting, R.F. (2010). Hen1 is required for oocyte development and piRNA stability in zebrafish. The EMBO journal *29*, 3688-3700.

Kane, D.A., and Kimmel, C.B. (1993). The zebrafish midblastula transition. Development *119*, 447-456.

Kannenberg, K., Wittekindt, N.E., Tippmann, S., Wolburg, H., Ranke, M.B., and Binder, G. (2007). Mutant and Misfolded Human Growth Hormone is Rapidly Degraded Through the Proteasomal Degradation Pathway in a Cellular Model for Isolated Growth Hormone Deficiency Type II. Journal of neuroendocrinology *19*, 882-890.

Kapsimali, M., Kloosterman, W.P., de Bruijn, E., Rosa, F., Plasterk, R.H., and Wilson, S.W. (2007). MicroRNAs show a wide diversity of expression profiles in the developing and mature central nervous system. Genome biology *8*, R173.

Katoh, T., Sakaguchi, Y., Miyauchi, K., Suzuki, T., Kashiwabara, S., and Baba, T. (2009). Selective stabilization of mammalian microRNAs by 3' adenylation mediated by the cytoplasmic poly(A) polymerase GLD-2. Genes & development *23*, 433-438.

Kedde, M., van Kouwenhove, M., Zwart, W., Oude Vrielink, J.A., Elkon, R., and Agami, R. (2010). A Pumilio-induced RNA structure switch in p27-3' UTR controls miR-221 and miR-222 accessibility. Nature cell biology *12*, 1014-1020.

Keller, J.E., Cai, F., and Neale, E.A. (2004). Uptake of botulinum neurotoxin into cultured neurons. Biochemistry *43*, 526-532.

Ketting, R.F., Fischer, S.E., Bernstein, E., Sijen, T., Hannon, G.J., and Plasterk, R.H. (2001). Dicer functions in RNA interference and in synthesis of small RNA involved in developmental timing in C. elegans. Genes & development *15*, 2654-2659.

Ketting, R.F., Fischer, S., Bernstein, E., Sijen, T., Hannon, G.J., and Plasterk, R. (2001). Dicer functions in RNA interfence and in synthesis of small RNA involved in developmental timing in *C. elegans*. Genes & Dev *15*, 2654-2659.

Ketting, R.F., Haverkamp, T.H., van Luenen, H.G., and Plasterk, R.H. (1999). Mut-7 of C. elegans, required for transposon silencing and RNA interference, is a homolog of Werner syndrome helicase and RNaseD. Cell *99*, 133-141.

Khvorova, A., Reynolds, A., and Jayasena, S.D. (2003). Functional siRNAs and miRNAs exhibit strand bias. Cell *115*, 209-216.

Kim, J., Inoue, K., Ishii, J., Vanti, W.B., Voronov, S.V., Murchison, E., Hannon, G., and Abeliovich, A. (2007). A MicroRNA feedback circuit in midbrain dopamine neurons. Science *317*, 1220-1224.

Kim, V.N. (2005). MicroRNA biogenesis: coordinated cropping and dicing. Nature reviews Molecular cell biology *6*, 376-385.

Kim, V.N., Han, J., and Siomi, M.C. (2009). Biogenesis of small RNAs in animals. Nature reviews Molecular cell biology *10*, 126-139.

Kim, V.N., and Nam, J.W. (2006). Genomics of microRNA. Trends Genet *22*, 165-173.

Kimmel, C.B., Ballard, W.W., Kimmel, S.R., Ullmann, B., and Schilling, T.F. (1995). Stages of embryonic development of the zebrafish. Developmental dynamics : an official publication of the American Association of Anatomists *203*, 253-310.

Kimura, K., Mizoguchi, A., and Ide, C. (2003). Regulation of growth cone extension by SNARE proteins. The journal of histochemistry and cytochemistry : official journal of the Histochemistry Society *51*, 429-433.

Kloosterman, W.P., Wienholds, E., Ketting, R.F., and Plasterk, R.H. (2004). Substrate requirements for let-7 function in the developing zebrafish embryo. Nucleic acids research *32*, 6284-6291.

Knaut, H., Pelegri, F., Bohmann, K., Schwarz, H., and Nusslein-Volhard, C. (2000). Zebrafish vasa RNA but not its protein is a component of the germ plasm and segregates asymmetrically before germline specification. The Journal of cell biology *149*, 875-888.

Knight, R.D., and Schilling, T.F. (2006). Cranial neural crest and development of the head skeleton. Advances in experimental medicine and biology *589*, 120-133.

Knight, S.W., Bass, B.L. (2001). A role for the RNase III enzyme DCR-1 in RNA interference and germ line development in *Caenorhabditis elegans*. Science *293*, 2269-2271.

Kobayashi, T., Lu, J., Cobb, B.S., Rodda, S.J., McMahon, A.P., Schipani, E., Merkenschlager, M., and Kronenberg, H.M. (2008). Dicer-dependent pathways regulate chondrocyte proliferation and differentiation. Proceedings of the National Academy of Sciences of the United States of America *105*, 1949-1954.

Kohany, O., Gentles, A.J., Hankus, L., and Jurka, J. (2006). Annotation, submission and screening of repetitive elements in Repbase: RepbaseSubmitter and Censor. BMC Bioinformatics *7*, 474.

Kontges, G., and Lumsden, A. (1996). Rhombencephalic neural crest segmentation is preserved throughout craniofacial ontogeny. Development *122*, 3229-3242.

Kozomara, A., and Griffiths-Jones, S. (2011). miRBase: integrating microRNA annotation and deep-sequencing data. Nucleic acids research *39*, D152-157.

Kreiling, J.A., Balantac, Z.L., Crawford, A.R., Ren, Y., Toure, J., Zchut, S., Kochilas, L., and Creton, R. (2008). Suppression of the endoplasmic reticulum calcium pump during zebrafish gastrulation affects left-right asymmetry of the heart and brain. Mechanisms of development *125*, 396-410.

Kucenas, S., Takada, N., Park, H.C., Woodruff, E., Broadie, K., and Appel, B. (2008). CNS-derived glia ensheath peripheral nerves and mediate motor root development. Nature neuroscience *11*, 143-151.

Ladewig, E., Okamura, K., Flynt, A.S., Westholm, J.O., and Lai, E.C. (2012). Discovery of hundreds of mirtrons in mouse and human small RNA data. Genome research *22*, 1634-1645.

Lagos-Quintana, M., Rauhut, R., Meyer, J., Borkhardt, A., and Tuschl, T. (2003). New microRNAs from mouse and human. Rna *9*, 175-179.

Landgraf, P., Rusu, M., Sheridan, R., Sewer, A., Iovino, N., Aravin, A., Pfeffer, S., Rice, A., Kamphorst, A.O., Landthaler, M., *et al*. (2007). A mammalian microRNA expression atlas based on small RNA library sequencing. Cell *129*, 1401-1414.

Landthaler, M., Yalcin, A., and Tuschl, T. (2004). The human DiGeorge syndrome critical region gene 8 and Its D. melanogaster homolog are required for miRNA biogenesis. Current biology : CB *14*, 2162-2167.

Laneve, P., Gioia, U., Andriotto, A., Moretti, F., Bozzoni, I., and Caffarelli, E. (2010). A minicircuitry involving REST and CREB controls miR-9-2 expression during human neuronal differentiation. Nucleic acids research *38*, 6895-6905.

Langmead, B., Trapnell, C., Pop, M., and Salzberg, S.L. (2009). Ultrafast and memory-efficient alignment of short DNA sequences to the human genome. Genome biology *10*, R25.

Lau, N.C., Robine, N., Martin, R., Chung, W.J., Niki, Y., Berezikov, E., and Lai, E.C. (2009). Abundant primary piRNAs, endo-siRNAs, and microRNAs in a Drosophila ovary cell line. Genome research *19*, 1776-1785.

Lau, N.C., Seto, A.G., Kim, J., Kuramochi-Miyagawa, S., Nakano, T., Bartel, D.P., and Kingston, R.E. (2006). Characterization of the piRNA Complex from Rat Testes. Science *313*, 363-367.

Lausch, E., Keppler, R., Hilbert, K., Cormier-Daire, V., Nikkel, S., Nishimura, G., Unger, S., Spranger, J., Superti-Furga, A., and Zabel, B. (2009). Mutations in MMP9 and MMP13 determine the mode of inheritance and the clinical spectrum of metaphyseal anadysplasia. American journal of human genetics *85*, 168-178.

Lee, R.C., Feinbaum, R.L., and Ambros, V. (1993). The C. elegans heterochronic gene lin-4 encodes small RNAs with antisense complementarity to lin-14. Cell *75*, 843-854.

Lee, Y., Ahn, C., Han, J., Choi, H., Kim, J., Yim, J., Lee, J., Provost, P., Radmark, O., Kim, S.*, et al*. (2003). The nuclear RNase III Drosha initiates microRNA processing. Nature *425*, 415-419.

Lee, Y., Jeon, K., Lee, J.T., Kim, S., and Kim, V.N. (2002). MicroRNA maturation: stepwise processing and subcellular localization. The EMBO journal *21*, 4663-4670.

Lee, Y., Kim, M., Han, J., Yeom, K.H., Lee, S., Baek, S.H., and Kim, V.N. (2004). MicroRNA genes are transcribed by RNA polymerase II. The EMBO journal *23*, 4051-4060.

Lee, Y.S., Shibata, Y., Malhotra, A., and Dutta, A. (2009). A novel class of small RNAs: tRNA-derived RNA fragments (tRFs). Genes & development *23*, 2639-2649.

Lehrbach, N.J., Armisen, J., Lightfoot, H.L., Murfitt, K.J., Bugaut, A., Balasubramanian, S., and Miska, E.A. (2009). LIN-28 and the poly(U) polymerase PUP-2 regulate let-7 microRNA processing in Caenorhabditis elegans. Nature structural & molecular biology *16*, 1016-1020.

Lessard, J., Wu, J.I., Ranish, J.A., Wan, M., Winslow, M.M., Staahl, B.T., Wu, H., Aebersold, R., Graef, I.A., and Crabtree, G.R. (2007). An essential switch in subunit composition of a chromatin remodeling complex during neural development. Neuron *55*, 201-215.

Lewis, B.P., Burge, C.B., and Bartel, D.P. (2005). Conserved seed pairing, often flanked by adenosines, indicates that thousands of human genes are microRNA targets. Cell *120*, 15-20.

Lewis, B.P., Shih, I.H., Jones-Rhoades, M.W., Bartel, D.P., and Burge, C.B. (2003). Prediction of mammalian microRNA targets. Cell *115*, 787-798.

Lewis, K.E., and Eisen, J.S. (2003). From cells to circuits: development of the zebrafish spinal cord. Progress in neurobiology *69*, 419-449.

Li, C., Vagin, V.V., Lee, S., Xu, J., Ma, S., Xi, H., Seitz, H., Horwich, M.D., Syrzycka, M., Honda, B.M., *et al*. (2009). Collapse of germline piRNAs in the absence of Argonaute3 reveals somatic piRNAs in flies. Cell *137*, 509-521.

Li, N., Wei, C., Olena, A.F., and Patton, J.G. (2011). Regulation of endoderm formation and left-right asymmetry by miR-92 during early zebrafish development. Development *138*, 1817-1826.

Li, W., Ono, F., and Brehm, P. (2003). Optical measurements of presynaptic release in mutant zebrafish lacking postsynaptic receptors. The Journal of neuroscience : the official journal of the Society for Neuroscience *23*, 10467-10474.

Lian, S.L., Li, S., Abadal, G.X., Pauley, B.A., Fritzler, M.J., and Chan, E.K. (2009). The C-terminal half of human Ago2 binds to multiple GW-rich regions of GW182 and requires GW182 to mediate silencing. RNA *15*, 804-813.

Lim, L.P., Lau, N.C., Garrett-Engele, P., Grimson, A., Schelter, J.M., Castle, J., Bartel, D.P., Linsley, P.S., and Johnson, J.M. (2005). Microarray analysis shows that some microRNAs downregulate large numbers of target mRNAs. Nature *433*, 769-773.

Lin, C.H., Jackson, A.L., Guo, J., Linsley, P.S., and Eisenman, R.N. (2009). Myc-regulated microRNAs attenuate embryonic stem cell differentiation. The EMBO journal *28*, 3157-3170.

Lindsay, E.A. (2001). Chromosomal microdeletions: dissecting del22q11 syndrome. Nature reviews Genetics *2*, 858-868.

Linsen, S.E., de Wit, E., Janssens, G., Heater, S., Chapman, L., Parkin, R.K., Fritz, B., Wyman, S.K., de Bruijn, E., Voest, E.E., *et al*. (2009). Limitations and possibilities of small RNA digital gene expression profiling. Nature methods *6*, 474-476.

Liu, J., Carmell, M.A., Rivas, F.V., Marsden, C.G., Thomson, J.M., Song, J.J., Hammond, S.M., Joshua-Tor, L., and Hannon, G.J. (2004). Argonaute2 is the catalytic engine of mammalian RNAi. Science *305*, 1437-1441.

Long, D., Lee, R., Williams, P., Chan, C.Y., Ambros, V., and Ding, Y. (2007). Potent effect of target structure on microRNA function. Nature structural & molecular biology *14*, 287-294.

Lu, B. (2003). BDNF and activity-dependent synaptic modulation. Learn Mem *10*, 86-98.

Lumsden, A., Sprawson, N., and Graham, A. (1991). Segmental origin and migration of neural crest cells in the hindbrain region of the chick embryo. Development *113*, 1281-1291.

Lund, E., Guttinger, S., Calado, A., Dahlberg, J.E., Kutay, U. (2004). Nuclear export of microRNA precursors. Science *303*, 95-98.

Lund, E., Liu, M., Hartley, R.S., Sheets, M.D., and Dahlberg, J.E. (2009). Deadenylation of maternal mRNAs mediated by miR-427 in Xenopus laevis embryos. RNA *15*, 2351-2363.

Ma, J., Flemr, M., Stein, P., Berninger, P., Malik, R., Zavolan, M., Svoboda, P., and Schultz, R.M. (2010). MicroRNA activity is suppressed in mouse oocytes. Current biology : CB *20*, 265-270.

Mai, J., Fok, L., Gao, H., Zhang, X., and Poo, M.M. (2009). Axon initiation and growth cone turning on bound protein gradients. The Journal of neuroscience : the official journal of the Society for Neuroscience *29*, 7450-7458.

Makeyev, E.V., Zhang, J., Carrasco, M.A., and Maniatis, T. (2007). The MicroRNA miR-124 promotes neuronal differentiation by triggering brain-specific alternative pre-mRNA splicing. Molecular cell *27*, 435-448.

Malone, C.D., Brennecke, J., Dus, M., Stark, A., McCombie, W.R., Sachidanandam, R., and Hannon, G.J. (2009). Specialized piRNA pathways act in germline and somatic tissues of the Drosophila ovary. Cell *137*, 522-535.

Marcet, B., Chevalier, B., Luxardi, G., Coraux, C., Zaragosi, L.E., Cibois, M., Robbe-Sermesant, K., Jolly, T., Cardinaud, B., Moreilhon, C., *et al*. (2011). Control of vertebrate multiciliogenesis by miR-449 through direct repression of the Delta/Notch pathway. Nature cell biology *13*, 693-699.

Marson, A., Levine, S.S., Cole, M.F., Frampton, G.M., Brambrink, T., Johnstone, S., Guenther, M.G., Johnston, W.K., Wernig, M., Newman, J., *et al*. (2008). Connecting microRNA genes to the core transcriptional regulatory circuitry of embryonic stem cells. Cell *134*, 521-533.

Marszalek, J.R., Ruiz-Lozano, P., Roberts, E., Chien, K.R., and Goldstein, L.S. (1999). Situs inversus and embryonic ciliary morphogenesis defects in mouse mutants lacking the KIF3A subunit of kinesin-II. Proceedings of the National Academy of Sciences of the United States of America *96*, 5043-5048.

Martin, G., and Keller, W. (2007). RNA-specific ribonucleotidyl transferases. RNA *13*, 1834-1849.

Martinez-Arca, S., Coco, S., Mainguy, G., Schenk, U., Alberts, P., Bouille, P., Mezzina, M., Prochiantz, A., Matteoli, M., Louvard, D., *et al*. (2001). A common exocytotic mechanism mediates axonal and dendritic outgrowth. The Journal of neuroscience : the official journal of the Society for Neuroscience *21*, 3830-3838.

Matranga, C., Tomari, Y., Shin, C., Bartel, D.P., and Zamore, P.D. (2005). Passenger-strand cleavage facilitates assembly of siRNA into Ago2-containing RNAi enzyme complexes. Cell *123*, 607-620.

Matteoli, M., Pozzi, D., Grumelli, C., Condliffe, S.B., Frassoni, C., Harkany, T., and Verderio, C. (2009). The synaptic split of SNAP-25: different roles in glutamatergic and GABAergic neurons? Neuroscience *158*, 223-230.

McKee, A.G., Loscher, J.S., O'Sullivan, N.C., Chadderton, N., Palfi, A., Batti, L., Sheridan, G.K., O'Shea, S., Moran, M., McCabe, O., *et al*. (2010). AAV-mediated chronic over-expression of SNAP-25 in adult rat dorsal hippocampus impairs memory-associated synaptic plasticity. Journal of neurochemistry *112*, 991-1004.

Melton, C., Judson, R.L., and Blelloch, R. (2010). Opposing microRNA families regulate self-renewal in mouse embryonic stem cells. Nature *463*, 621-626.

Memczak, S., Jens, M., Elefsinioti, A., Torti, F., Krueger, J., Rybak, A., Maier, L., Mackowiak, S.D., Gregersen, L.H., Munschauer, M., *et al*. (2013). Circular RNAs are a large class of animal RNAs with regulatory potency. Nature *495*, 333-338.

Mishima, Y., Abreu-Goodger, C., Staton, A.A., Stahlhut, C., Shou, C., Cheng, C., Gerstein, M., Enright, A.J., and Giraldez, A.J. (2009). Zebrafish miR-1 and miR-133 shape muscle gene expression and regulate sarcomeric actin organization. Genes & development *23*, 619-632.

Miyoshi, K., Tsukumo, H., Nagami, T., Siomi, H., and Siomi, M.C. (2005). Slicer function of Drosophila Argonautes and its involvement in RISC formation. Genes & development *19*, 2837-2848.

Mooney, M., Bond, J., Monks, N., Eugster, E., Cherba, D., Berlinski, P., Kamerling, S., Marotti, K., Simpson, H., Rusk, T., *et al*. (2013). Comparative RNA-Seq and Microarray Analysis of Gene Expression Changes in B-Cell Lymphomas of Canis familiaris. PloS one *8*, e61088.

Morin, R.D., O'Connor, M.D., Griffith, M., Kuchenbauer, F., Delaney, A., Prabhu, A.L., Zhao, Y., McDonald, H., Zeng, T., Hirst, M., *et al*. (2008). Application of massively parallel sequencing to microRNA profiling and discovery in human embryonic stem cells. Genome research *18*, 610-621.

Murchison, E.P., Stein, P., Xuan, Z., Pan, H., Zhang, M.Q., Schultz, R.M., and Hannon, G.J. (2007). Critical roles for Dicer in the female germline. Genes & development *21*, 682-693.

Myers, P.Z., Eisen, J.S., and Westerfield, M. (1986). Development and axonal outgrowth of identified motoneurons in the zebrafish. The Journal of neuroscience : the official journal of the Society for Neuroscience *6*, 2278-2289.

Napoli, C., Lemieux, C., and Jorgensen, R. (1990). Introduction of a Chimeric Chalcone Synthase Gene into Petunia Results in Reversible Co-Suppression of Homologous Genes in trans. The Plant cell *2*, 279-289.

Newport, J., and Kirschner, M. (1982). A major developmental transition in early Xenopus embryos: I. characterization and timing of cellular changes at the midblastula stage. Cell *30*, 675-686.

Nicoli, S., Standley, C., Walker, P., Hurlstone, A., Fogarty, K.E., and Lawson, N.D. (2010). MicroRNA-mediated integration of haemodynamics and Vegf signalling during angiogenesis. Nature *464*, 1196-1200.

Nie, X., Wang, Q., and Jiao, K. (2011). Dicer activity in neural crest cells is essential for craniofacial organogenesis and pharyngeal arch artery morphogenesis. Mechanisms of development *128*, 200-207.

Nigg, E.A., and Raff, J.W. (2009). Centrioles, centrosomes, and cilia in health and disease. Cell *139*, 663-678.

Ning, G., Liu, X., Dai, M., Meng, A., and Wang, Q. (2013). MicroRNA-92a upholds Bmp signaling by targeting noggin3 during pharyngeal cartilage formation. Developmental cell *24*, 283-295.

Nonaka, S., Tanaka, Y., Okada, Y., Takeda, S., Harada, A., Kanai, Y., Kido, M., and Hirokawa, N. (1998). Randomization of left-right asymmetry due to loss of nodal cilia generating leftward flow of extraembryonic fluid in mice lacking KIF3B motor protein. Cell *95*, 829-837.

O'Farrell, P.H., Stumpff, J., and Su, T.T. (2004). Embryonic cleavage cycles: how is a mouse like a fly? Current biology : CB *14*, R35-45.

Ohnishi, Y., Totoki, Y., Toyoda, A., Watanabe, T., Yamamoto, Y., Tokunaga, K., Sakaki, Y., Sasaki, H., and Hohjoh, H. (2010). Small RNA class transition from siRNA/piRNA to miRNA during pre-implantation mouse development. Nucleic acids research *38*, 5141-5151.

Okada, Y., Nonaka, S., Tanaka, Y., Saijoh, Y., Hamada, H., and Hirokawa, N. (1999). Abnormal nodal flow precedes situs inversus in iv and inv mice. Molecular cell *4*, 459-468.

Okamura, K., and Lai, E.C. (2008). Endogenous small interfering RNAs in animals. Nature reviews Molecular cell biology *9*, 673-678.

Osen-Sand, A., Catsicas, M., Staple, J.K., Jones, K.A., Ayala, G., Knowles, J., Grenningloh, G., and Catsicas, S. (1993). Inhibition of axonal growth by SNAP-25 antisense oligonucleotides in vitro and in vivo. Nature *364*, 445-448.

Osen-Sand, A., Staple, J.K., Naldi, E., Schiavo, G., Rossetto, O., Petitpierre, S., Malgaroli, A., Montecucco, C., and Catsicas, S. (1996). Common and distinct fusion proteins in axonal growth and transmitter release. The Journal of comparative neurology *367*, 222-234.

Ostenson, C.G., Gaisano, H., Sheu, L., Tibell, A., and Bartfai, T. (2006). Impaired gene and protein expression of exocytotic soluble N-ethylmaleimide attachment protein receptor complex proteins in pancreatic islets of type 2 diabetic patients. Diabetes *55*, 435-440.

Osumi-Yamashita, N., Ninomiya, Y., Doi, H., and Eto, K. (1994). The contribution of both forebrain and midbrain crest cells to the mesenchyme in the frontonasal mass of mouse embryos. Developmental biology *164*, 409-419.

Otaegi, G., Pollock, A., Hong, J., and Sun, T. (2011). MicroRNA miR-9 modifies motor neuron columns by a tuning regulation of FoxP1 levels in developing spinal cords. The Journal of neuroscience : the official journal of the Society for Neuroscience *31*, 809-818.

Packer, A.N., Xing, Y., Harper, S.Q., Jones, L., and Davidson, B.L. (2008). The bifunctional microRNA miR-9/miR-9* regulates REST and CoREST and is downregulated in Huntington's disease. The Journal of neuroscience : the official journal of the Society for Neuroscience *28*, 14341-14346.

Parrish, J.Z., Xu, P., Kim, C.C., Jan, L.Y., and Jan, Y.N. (2009). The microRNA bantam functions in epithelial cells to regulate scaling growth of dendrite arbors in drosophila sensory neurons. Neuron *63*, 788-802.

Pasquinelli, A.E., Reinhart, B.J., Slack, F., Martindale, M.Q., Kuroda, M.I., Maller, B., Hayward, D.C., Ball, E.E., Degnan, B., Muller, P., *et al*. (2000). Conservation of the sequence and temporal expression of let-7 heterochronic regulatory RNA. Nature *408*, 86-89.

Pauli, A., Rinn, J.L., and Schier, A.F. (2011). Non-coding RNAs as regulators of embryogenesis. Nature reviews Genetics *12*, 136-149.

Qureshi, I.A., and Mehler, M.F. (2009). Regulation of non-coding RNA networks in the nervous system--what's the REST of the story? Neuroscience letters *466*, 73-80.

Rajasethupathy, P., Antonov, I., Sheridan, R., Frey, S., Sander, C., Tuschl, T., and Kandel, E.R. (2012). A role for neuronal piRNAs in the epigenetic control of memory-related synaptic plasticity. Cell *149*, 693-707.

Rajasethupathy, P., Fiumara, F., Sheridan, R., Betel, D., Puthanveettil, S.V., Russo, J.J., Sander, C., Tuschl, T., and Kandel, E. (2009). Characterization of small RNAs in Aplysia reveals a role for miR-124 in constraining synaptic plasticity through CREB. Neuron *63*, 803-817.

Rand, T.A., Petersen, S., Du, F., and Wang, X. (2005). Argonaute2 cleaves the anti-guide strand of siRNA during RISC activation. Cell *123*, 621-629.

Ratcliff, F.G., MacFarlane, S.A., and Baulcombe, D.C. (1999). Gene silencing without DNA. rna-mediated cross-protection between viruses. The Plant cell *11*, 1207-1216.

Raz, E. (2003). Primordial germ-cell development: the zebrafish perspective. Nature reviews Genetics *4*, 690-700.

Reinhart, B.J., Slack, F.J., Basson, M., Pasquinelli, A.E., Bettinger, J.C., Rougvie, A.E., Horvitz, H.R., and Ruvkun, G. (2000). The 21-nucleotide let-7 RNA regulates developmental timing in Caenorhabditis elegans. Nature *403*, 901-906.

Risinger, C., Salaneck, E., Soderberg, C., Gates, M., Postlethwait, J.H., and Larhammar, D. (1998). Cloning of two loci for synapse protein Snap25 in zebrafish: comparison of paralogous linkage groups suggests loss of one locus in the mammalian lineage. Journal of neuroscience research *54*, 563-573.

Rivas, F.V., Tolia, N.H., Song, J.J., Aragon, J.P., Liu, J., Hannon, G.J., and Joshua-Tor, L. (2005). Purified Argonaute2 and an siRNA form recombinant human RISC. Nature structural & molecular biology *12*, 340-349.

Rodriguez, A., Griffiths-Jones, S., Ashurst, J.L., and Bradley, A. (2004). Identification of mammalian microRNA host genes and transcription units. Genome research *14*, 1902-1910.

Rouget, C., Papin, C., Boureux, A., Meunier, A.C., Franco, B., Robine, N., Lai, E.C., Pelisson, A., and Simonelig, M. (2010). Maternal mRNA deadenylation and decay by the piRNA pathway in the early Drosophila embryo. Nature *467*, 1128-1132.

Ruby, J.G., Jan, C., Player, C., Axtell, M.J., Lee, W., Nusbaum, C., Ge, H., and Bartel, D.P. (2006). Large-scale sequencing reveals 21U-RNAs and additional microRNAs and endogenous siRNAs in C. elegans. Cell *127*, 1193-1207.

Ruby, J.G., Stark, A., Johnston, W.K., Kellis, M., Bartel, D.P., and Lai, E.C. (2007). Evolution, biogenesis, expression, and target predictions of a substantially expanded set of Drosophila microRNAs. Genome research *17*, 1850-1864.

Rupp, R.A., Snider, L., and Weintraub, H. (1994). Xenopus embryos regulate the nuclear localization of XMyoD. Genes and Development *8*, 1311-1323.

Rybak, A., Fuchs, H., Hadian, K., Smirnova, L., Wulczyn, E.A., Michel, G., Nitsch, R., Krappmann, D., and Wulczyn, F.G. (2009). The let-7 target gene mouse lin-41 is a stem cell specific E3 ubiquitin ligase for the miRNA pathway protein Ago2. Nature cell biology *11*, 1411-1420.

Saeed, A.I., Bhagabati, N.K., Braisted, J.C., Liang, W., Sharov, V., Howe, E.A., Li, J., Thiagarajan, M., White, J.A., and Quackenbush, J. (2006). TM4 microarray software suite. Methods Enzymol *411*, 134-193.

Saeed, A.I., Sharov, V., White, J., Li, J., Liang, W., Bhagabati, N., Braisted, J., Klapa, M., Currier, T., Thiagarajan, M.*, et al*. (2003). TM4: a free, open-source system for microarray data management and analysis. Biotechniques *34*, 374-378.

Salmena, L., Poliseno, L., Tay, Y., Kats, L., and Pandolfi, P.P. (2011). A ceRNA hypothesis: the Rosetta Stone of a hidden RNA language? Cell *146*, 353-358.

Santagati, F., and Rijli, F.M. (2003). Cranial neural crest and the building of the vertebrate head. Nature reviews Neuroscience *4*, 806-818.

Sanuki, R., Onishi, A., Koike, C., Muramatsu, R., Watanabe, S., Muranishi, Y., Irie, S., Uneo, S., Koyasu, T., Matsui, R.*, et al*. (2011). miR-124a is required for hippocampal axogenesis and retinal cone survival through Lhx2 suppression. Nature neuroscience *14*, 1125-1134.

Saunders, L.R., Sharma, A.D., Tawney, J., Nakagawa, M., Okita, K., Yamanaka, S., Willenbring, H., and Verdin, E. (2010). miRNAs regulate SIRT1 expression during mouse embryonic stem cell differentiation and in adult mouse tissues. Aging *2*, 415-431.

Schiavo, G., Matteoli, M., and Montecucco, C. (2000). Neurotoxins affecting neuroexocytosis. Physiological reviews *80*, 717-766.

Schiavo, G., Santucci, A., Dasgupta, B.R., Mehta, P.P., Jontes, J., Benfenati, F., Wilson, M.C., and Montecucco, C. (1993). Botulinum neurotoxins serotypes A and E cleave SNAP-25 at distinct COOH-terminal peptide bonds. FEBS letters *335*, 99-103.

Schiavo, G., Stenbeck, G., Rothman, J.E., and Sollner, T.H. (1997). Binding of the synaptic vesicle v-SNARE, synaptotagmin, to the plasma membrane t-SNARE, SNAP-25, can explain docked vesicles at neurotoxin-treated synapses. Proceedings of the National Academy of Sciences of the United States of America *94*, 997-1001.

Schier, A.F. (2007). The maternal-zygotic transition: death and birth of RNAs. Science *316*, 406-407.

Schilling, T.F., and Kimmel, C.B. (1994). Segment and cell type lineage restrictions during pharyngeal arch development in the zebrafish embryo. Development *120*, 483-494.

Schnall-Levin, M., Rissland, O.S., Johnston, W.K., Perrimon, N., Bartel, D.P., and Berger, B. (2011). Unusually effective microRNA targeting within repeat-rich coding regions of mammalian mRNAs. Genome research *21*, 1395-1403.

Schneider, I., Houston, D.W., Rebagliati, M.R., and Slusarski, D.C. (2008). Calcium fluxes in dorsal forerunner cells antagonize beta-catenin and alter left-right patterning. Development *135*, 75-84.

Schneider, T.D., and Stephens, R.M. (1990). Sequence logos: a new way to display consensus sequences. Nucleic acids research *18*, 6097-6100.

Schoch, S., Castillo, P.E., Jo, T., Mukherjee, K., Geppert, M., Wang, Y., Schmitz, F., Malenka, R.C., and Sudhof, T.C. (2002). RIM1alpha forms a protein scaffold for regulating neurotransmitter release at the active zone. Nature *415*, 321-326.

Schratt, G. (2009). microRNAs at the synapse. Nature reviews Neuroscience *10*, 842-849.

Schratt, G.M., Tuebing, F., Nigh, E.A., Kane, C.G., Sabatini, M.E., Kiebler, M., and Greenberg, M.E. (2006). A brain-specific microRNA regulates dendritic spine development. Nature *439*, 283-289.

Schwarz, D.S., Hutvagner, G., Du, T., Xu, Z., Aronin, N., and Zamore, P.D. (2003). Asymmetry in the assembly of the RNAi enzyme complex. Cell *115*, 199-208.

Scott, C.E., Wynn, S.L., Sesay, A., Cruz, C., Cheung, M., Gomez Gaviro, M.V., Booth, S., Gao, B., Cheah, K.S., Lovell-Badge, R.*, et al*. (2010). SOX9 induces and maintains neural stem cells. Nature neuroscience *13*, 1181-1189.

Sempere, L.F., Sokol, N.S., Dubrovsky, E.B., Berger, E.M., and Ambros, V. (2003). Temporal regulation of microRNA expression in Drosophila melanogaster mediated by hormonal signals and broad-Complex gene activity. Developmental biology *259*, 9-18.

Shah, A.S., Ben-Shahar, Y., Moninger, T.O., Kline, J.N., and Welsh, M.J. (2009). Motile cilia of human airway epithelia are chemosensory. Science *325*, 1131-1134.

Sheehy, N.T., Cordes, K.R., White, M.P., Ivey, K.N., and Srivastava, D. (2010). The neural crest-enriched microRNA miR-452 regulates epithelial-mesenchymal signaling in the first pharyngeal arch. Development *137*, 4307-4316.

Shibata, M., Kurokawa, D., Nakao, H., Ohmura, T., and Aizawa, S. (2008). MicroRNA-9 modulates Cajal-Retzius cell differentiation by suppressing Foxg1 expression in mouse medial pallium. The Journal of neuroscience : the official journal of the Society for Neuroscience *28*, 10415-10421.

Shin, C. (2008). Cleavage of the star strand facilitates assembly of some microRNAs into Ago2-containing silencing complexes in mammals. Molecules and cells *26*, 308-313.

Simon, D.J., Madison, J.M., Conery, A.L., Thompson-Peer, K.L., Soskis, M., Ruvkun, G.B., Kaplan, J.M., and Kim, J.K. (2008). The microRNA miR-1 regulates a MEF-2-dependent retrograde signal at neuromuscular junctions. Cell *133*, 903-915.

Sinkkonen, L., Hugenschmidt, T., Berninger, P., Gaidatzis, D., Mohn, F., Artus-Revel, C.G., Zavolan, M., Svoboda, P., and Filipowicz, W. (2008). MicroRNAs control de novo DNA methylation through regulation of transcriptional repressors in mouse embryonic stem cells. Nature structural & molecular biology *15*, 259-267.

Skalsky, R.L., and Cullen, B.R. (2010). Viruses, microRNAs, and host interactions. Annu Rev Microbiol *64*, 123-141.

Smith, R., Klein, P., Koc-Schmitz, Y., Waldvogel, H.J., Faull, R.L., Brundin, P., Plomann, M., and Li, J.Y. (2007). Loss of SNAP-25 and rabphilin 3a in sensory-motor cortex in Huntington's disease. Journal of neurochemistry *103*, 115-123.

Soares, A.R., Pereira, P.M., Santos, B., Egas, C., Gomes, A.C., Arrais, J., Oliveira, J.L., Moura, G.R., and Santos, M.A. (2009). Parallel DNA pyrosequencing unveils new zebrafish microRNAs. BMC genomics *10*, 195.

Soni, K., Choudhary, A., Patowary, A., Singh, A.R., Bhatia, S., Sivasubbu, S., Chandrasekaran, S., and Pillai, B. (2013). miR-34 is maternally inherited in Drosophila melanogaster and Danio rerio. Nucleic acids research *41*, 4470-4480.

Sorensen, J.B., Nagy, G., Varoqueaux, F., Nehring, R.B., Brose, N., Wilson, M.C., and Neher, E. (2003). Differential control of the releasable vesicle pools by SNAP-25 splice variants and SNAP-23. Cell *114*, 75-86.

Sudhof, T.C., and Rothman, J.E. (2009). Membrane fusion: grappling with SNARE and SM proteins. Science *323*, 474-477.

Suh, N., Baehner, L., Moltzahn, F., Melton, C., Shenoy, A., Chen, J., and Blelloch, R. (2010). MicroRNA function is globally suppressed in mouse oocytes and early embryos. Current biology : CB *20*, 271-277.

Sun, A.X., Crabtree, G.R., and Yoo, A.S. (2013). MicroRNAs: regulators of neuronal fate. Current opinion in cell biology *25*, 215-221.

Sun, K., Westholm, J.O., Tsurudome, K., Hagen, J.W., Lu, Y., Kohwi, M., Betel, D., Gao, F.B., Haghighi, A.P., Doe, C.Q., *et al*. (2012). Neurophysiological defects and neuronal gene deregulation in Drosophila mir-124 mutants. PLoS genetics *8*, e1002515.

Sunkar, R., Zhou, X., Zheng, Y., Zhang, W., and Zhu, J.K. (2008). Identification of novel and candidate miRNAs in rice by high throughput sequencing. BMC plant biology *8*, 25.

Supp, D.M., Brueckner, M., Kuehn, M.R., Witte, D.P., Lowe, L.A., McGrath, J., Corrales, J., and Potter, S.S. (1999). Targeted deletion of the ATP binding domain of left-right dynein confirms its role in specifying development of left-right asymmetries. Development *126*, 5495-5504.

t Hoen, P.A., Ariyurek, Y., Thygesen, H.H., Vreugdenhil, E., Vossen, R.H., de Menezes, R.X., Boer, J.M., van Ommen, G.J., and den Dunnen, J.T. (2008). Deep sequencing-based expression analysis shows major advances in robustness, resolution and inter-lab portability over five microarray platforms. Nucleic acids research *36*, e141.

Tabara, H., Sarkissian, M., Kelly, W.G., Fleenor, J., Grishok, A., Timmons, L., Fire, A., and Mello, C.C. (1999). The rde-1 Gene, RNA Interference, and Transposon Silencing in C. elegans. Cell *99*, 123.

Tafoya, L.C., Shuttleworth, C.W., Yanagawa, Y., Obata, K., and Wilson, M.C. (2008). The role of the t-SNARE SNAP-25 in action potential-dependent calcium signaling and expression in GABAergic and glutamatergic neurons. BMC neuroscience *9*, 105.

Taft, R.J., Glazov, E.A., Cloonan, N., Simons, C., Stephen, S., Faulkner, G.J., Lassmann, T., Forrest, A.R., Grimmond, S.M., Schroder, K., *et al*. (2009). Tiny RNAs associated with transcription start sites in animals. Nature genetics *41*, 572-578.

Takeda, S., Yonekawa, Y., Tanaka, Y., Okada, Y., Nonaka, S., and Hirokawa, N. (1999). Left-right asymmetry and kinesin superfamily protein KIF3A: new insights in determination of laterality and mesoderm induction by kif3A-/- mice analysis. The Journal of cell biology *145*, 825-836.

Takimoto, K., Wakiyama, M., and Yokoyama, S. (2009). Mammalian GW182 contains multiple Argonaute-binding sites and functions in microRNA-mediated translational repression. RNA *15*, 1078-1089.

Tam, O.H., Aravin, A.A., Stein, P., Girard, A., Murchison, E.P., Cheloufi, S., Hodges, E., Anger, M., Sachidanandam, R., Schultz, R.M.*, et al*. (2008). Pseudogene-derived small interfering RNAs regulate gene expression in mouse oocytes. Nature *453*, 534-538.

Tanabe, Y., William, C., and Jessell, T.M. (1998). Specification of motor neuron identity by the MNR2 homeodomain protein. Cell *95*, 67-80.

Tang, F., Kaneda, M., O'Carroll, D., Hajkova, P., Barton, S.C., Sun, Y.A., Lee, C., Tarakhovsky, A., Lao, K., and Surani, M.A. (2007). Maternal microRNAs are essential for mouse zygotic development. Genes & development *21*, 644-648.

Tay, Y., Zhang, J., Thomson, A.M., Lim, B., and Rigoutsos, I. (2008). MicroRNAs to Nanog, Oct4 and Sox2 coding regions modulate embryonic stem cell differentiation. Nature *455*, 1124-1128.

Thatcher, E.J., Bond, J., Paydar, I., and Patton, J.G. (2008). Genomic organization of zebrafish microRNAs. BMC genomics *9*, 253.

Thatcher, E.J., Flynt, A.S., Li, N., Patton, J.R., and Patton, J.G. (2007). MiRNA expression analysis during normal zebrafish development and following inhibition of the Hedgehog and Notch signaling pathways. Developmental dynamics : an official publication of the American Association of Anatomists.

Thompson, D.M., Lu, C., Green, P.J., and Parker, R. (2008). tRNA cleavage is a conserved response to oxidative stress in eukaryotes. RNA *14*, 2095-2103.

Thomson, J.M., Newman, M., Parker, J.S., Morin-Kensicki, E.M., Wright, T., and Hammond, S.M. (2006). Extensive post-transcriptional regulation of microRNAs and its implications for cancer. Genes & development *20*, 2202-2207.

Tomari, Y., Du, T., Haley, B., Schwarz, D.S., Bennett, R., Cook, H.A., Koppetsch, B.S., Theurkauf, W.E., and Zamore, P.D. (2004). RISC assembly defects in the Drosophila RNAi mutant armitage. Cell *116*, 831-841.

Tomari, Y., and Zamore, P.D. (2005). MicroRNA biogenesis: drosha can't cut it without a partner. Current biology : CB *15*, R61-64.

Trevarrow, B., Marks, D.L., and Kimmel, C.B. (1990). Organization of hindbrain segments in the zebrafish embryo. Neuron *4*, 669-679.

Trumpp, A., Depew, M.J., Rubenstein, J.L., Bishop, J.M., and Martin, G.R. (1999). Cre-mediated gene inactivation demonstrates that FGF8 is required for cell survival and patterning of the first branchial arch. Genes & development *13*, 3136-3148.

Tsuji, M., Inanami, O., and Kuwabara, M. (2001). Induction of neurite outgrowth in PC12 cells by alpha -phenyl-N-tert-butylnitron through activation of protein kinase C and the Ras-extracellular signal-regulated kinase pathway. The Journal of biological chemistry *276*, 32779-32785.

Tsurudome, K., Tsang, K., Liao, E.H., Ball, R., Penney, J., Yang, J.S., Elazzouzi, F., He, T., Chishti, A., Lnenicka, G., *et al*. (2010). The Drosophila miR-310 cluster negatively regulates synaptic strength at the neuromuscular junction. Neuron *68*, 879-893.

Tuschl, T., Zamore, P.D., Lehmann, R., Bartel, D.P., and Sharp, P.A. (1999). Targeted mRNA degradation by double-stranded RNA in vitro. Genes & development *13*, 3191-3197.

Urbich, C., Kaluza, D., Fromel, T., Knau, A., Bennewitz, K., Boon, R.A., Bonauer, A., Doebele, C., Boeckel, J.N., Hergenreider, E., *et al*. (2012). MicroRNA-27a/b controls endothelial cell repulsion and angiogenesis by targeting semaphorin 6A. Blood *119*, 1607-1616.

Vagin, V.V., Sigova, A., Li, C., Seitz, H., Gvozdev, V., and Zamore, P.D. (2006). A distinct small RNA pathway silences selfish genetic elements in the germline. Science *313*, 320-324.

Verdel, A., Jia, S., Gerber, S., Sugiyama, T., Gygi, S., Grewal, S.I., and Moazed, D. (2004). RNAi-mediated targeting of heterochromatin by the RITS complex. Science *303*, 672-676.

Verhage, M., and Sorensen, J.B. (2008). Vesicle docking in regulated exocytosis. Traffic *9*, 1414-1424.

Visvanathan, J., Lee, S., Lee, B., Lee, J.W., and Lee, S.K. (2007). The microRNA miR-124 antagonizes the anti-neural REST/SCP1 pathway during embryonic CNS development. Genes & development *21*, 744-749.

Vo, N.K., Cambronne, X.A., and Goodman, R.H. (2010). MicroRNA pathways in neural development and plasticity. Current opinion in neurobiology *20*, 457-465.

Vrljic, M., Strop, P., Ernst, J.A., Sutton, R.B., Chu, S., and Brunger, A.T. (2010). Molecular mechanism of the synaptotagmin-SNARE interaction in Ca2+-triggered vesicle fusion. Nature structural & molecular biology *17*, 325-331.

Wang, J., Czech, B., Crunk, A., Wallace, A., Mitreva, M., Hannon, G.J., and Davis, R.E. (2011). Deep small RNA sequencing from the nematode Ascaris reveals conservation, functional diversification, and novel developmental profiles. Genome research *21*, 1462-1477.

Wang, Y., Baskerville, S., Shenoy, A., Babiarz, J.E., Baehner, L., and Blelloch, R. (2008). Embryonic stem cell-specific microRNAs regulate the G1-S transition and promote rapid proliferation. Nature genetics *40*, 1478-1483.

Wang, Y., Medvid, R., Melton, C., Jaenisch, R., and Blelloch, R. (2007). DGCR8 is essential for microRNA biogenesis and silencing of embryonic stem cell self-renewal. Nature genetics *39*, 380-385.

Washbourne, P., Thompson, P.M., Carta, M., Costa, E.T., Mathews, J.R., Lopez-Bendito, G., Molnar, Z., Becher, M.W., Valenzuela, C.F., Partridge, L.D., *et al*. (2002). Genetic ablation of the t-SNARE SNAP-25 distinguishes mechanisms of neuroexocytosis. Nature neuroscience *5*, 19-26.

Wayman, G.A., Davare, M., Ando, H., Fortin, D., Varlamova, O., Cheng, H.Y., Marks, D., Obrietan, K., Soderling, T.R., Goodman, R.H., *et al*. (2008). An activity-regulated microRNA controls dendritic plasticity by down-regulating p250GAP. Proceedings of the National Academy of Sciences of the United States of America *105*, 9093-9098.

Wei, C., Salichos, L., Wittgrove, C.M., Rokas, A., and Patton, J.G. (2012). Transcriptome-wide analysis of small RNA expression in early zebrafish development. RNA.

Wei, C., Thatcher, E.J., Olena, A.F., Cha, D.J., Perdigoto, A.L., Marshall, A.F., Carter, B.D., Broadie, K., and Patton, J.G. (2013). miR-153 regulates SNAP-25, synaptic transmission, and neuronal development. PloS one *8*, e57080.

Wellner, U., Schubert, J., Burk, U.C., Schmalhofer, O., Zhu, F., Sonntag, A., Waldvogel, B., Vannier, C., Darling, D., zur Hausen, A., *et al*. (2009). The EMT-activator ZEB1 promotes tumorigenicity by repressing stemness-inhibiting microRNAs. Nature cell biology *11*, 1487-1495.

Weng, R., and Cohen, S.M. (2012). Drosophila miR-124 regulates neuroblast proliferation through its target anachronism. Development *139*, 1427-1434.

Westerfield, M., McMurray, J.V., and Eisen, J.S. (1986). Identified motoneurons and their innervation of axial muscles in the zebrafish. The Journal of neuroscience : the official journal of the Society for Neuroscience *6*, 2267-2277.

Wheeler, D.A., Srinivasan, M., Egholm, M., Shen, Y., Chen, L., McGuire, A., He, W., Chen, Y.J., Makhijani, V., Roth, G.T., *et al*. (2008). The complete genome of an individual by massively parallel DNA sequencing. Nature *452*, 872-876.

Wickner, W., and Schekman, R. (2008). Membrane fusion. Nature structural & molecular biology *15*, 658-664.

Wienholds, E., Kloosterman, W.P., Miska, E., Alvarez-Saavedra, E., Berezikov, E., de Bruijn, E., Horvitz, H.R., Kauppinen, S., and Plasterk, R.H. (2005a). MicroRNA expression in zebrafish embryonic development. Science *309*, 310-311.

Wienholds, E., Kloosterman, W.P., Miska, E., Alvarez-Saavedra, E., Berezikov, E., de Bruijn, E., Horvitz, H.R., Kauppinen, S., and Plasterk, R.H.A. (2005b). MicroRNA Expression in Zebrafish Embryonic Development. Science *309*, 310-311.

Wienholds, E., and Plasterk, R.H. (2005). MicroRNA function in animal development. FEBS letters *579*, 5911-5922.

Wilkie, A.O. (1997). Craniosynostosis: genes and mechanisms. Human molecular genetics *6*, 1647-1656.

Williams, B.B., Cantrell, V.A., Mundell, N.A., Bennett, A.C., Quick, R.E., and Jessen, J.R. (2012). VANGL2 regulates membrane trafficking of MMP14 to control cell polarity and migration. Journal of cell science *125*, 2141-2147.

Wu, J., and Xie, X. (2006). Comparative sequence analysis reveals an intricate network among REST, CREB and miRNA in mediating neuronal gene expression. Genome biology *7*, R85.

Wu, J.I., Lessard, J., Olave, I.A., Qiu, Z., Ghosh, A., Graef, I.A., and Crabtree, G.R. (2007). Regulation of dendritic development by neuron-specific chromatin remodeling complexes. Neuron *56*, 94-108.

Wulczyn, F.G., Smirnova, L., Rybak, A., Brandt, C., Kwidzinski, E., Ninnemann, O., Strehle, M., Seiler, A., Schumacher, S., and Nitsch, R. (2007). Post-transcriptional regulation of the let-7 microRNA during neural cell specification. FASEB journal : official publication of the Federation of American Societies for Experimental Biology *21*, 415-426.

Wyman, S.K., Knouf, E.C., Parkin, R.K., Fritz, B.R., Lin, D.W., Dennis, L.M., Krouse, M.A., Webster, P.J., and Tewari, M. (2011). Post-transcriptional generation of miRNA variants by multiple nucleotidyl transferases contributes to miRNA transcriptome complexity. Genome research *21*, 1450-1461.

Xu, N., Papagiannakopoulos, T., Pan, G., Thomson, J.A., and Kosik, K.S. (2009). MicroRNA-145 regulates OCT4, SOX2, and KLF4 and represses pluripotency in human embryonic stem cells. Cell *137*, 647-658.

Yamaguchi, K., Nakayama, T., Fujiwara, T., and Akagawa, K. (1996). Enhancement of neurite-sprouting by suppression of HPC-1/syntaxin 1A activity in cultured vertebrate nerve cells. Brain research *740*, 185-192.

Yamasaki, S., Ivanov, P., Hu, G.F., and Anderson, P. (2009). Angiogenin cleaves tRNA and promotes stress-induced translational repression. The Journal of cell biology *185*, 35-42.

Yao, B., Li, S., Lian, S.L., Fritzler, M.J., and Chan, E.K. (2011). Mapping of Ago2-GW182 functional interactions. Methods Mol Biol *725*, 45-62.

Yelick, P.C., and Schilling, T.F. (2002). Molecular dissection of craniofacial development using zebrafish. Crit Rev Oral Biol Med *13*, 308-322.

Yi, R., Pasolli, H.A., Landthaler, M., Hafner, M., Ojo, T., Sheridan, R., Sander, C., O'Carroll, D., Stoffel, M., Tuschl, T.*, et al*. (2009). DGCR8-dependent microRNA biogenesis is essential for skin development. Proceedings of the National Academy of Sciences of the United States of America *106*, 498-502.

Yi, R., Poy, M.N., Stoffel, M., and Fuchs, E. (2008). A skin microRNA promotes differentiation by repressing 'stemness'. Nature *452*, 225-229.

Yi, R., Qin, Y., Macara, I.G., and Cullen, B.R. (2003). Exportin-5 mediates the nuclear export of pre-microRNAs and short hairpin RNAs. Genes & development *17*, 3011-3016.

Yoo, A.S., Staahl, B.T., Chen, L., and Crabtree, G.R. (2009). MicroRNA-mediated switching of chromatin-remodelling complexes in neural development. Nature *460*, 642-646.

Zamore, P.D., Tuschl, T., Sharp, P.A., and Bartel, D.P. (2000). RNAi: double-stranded RNA directs the ATP-dependent cleavage of mRNA at 21 to 23 nucleotide intervals. Cell *101*, 25-33.

Zehir, A., Hua, L.L., Maska, E.L., Morikawa, Y., and Cserjesi, P. (2010). Dicer is required for survival of differentiating neural crest cells. Developmental biology *340*, 459-467.

Zhao, C., Sun, G., Li, S., and Shi, Y. (2009). A feedback regulatory loop involving microRNA-9 and nuclear receptor TLX in neural stem cell fate determination. Nature structural & molecular biology *16*, 365-371.

Zhao, T., Li, G., Mi, S., Li, S., Hannon, G.J., Wang, X.J., and Qi, Y. (2007). A complex system of small RNAs in the unicellular green alga Chlamydomonas reinhardtii. Genes & development *21*, 1190-1203.

Zhou, Q., Xiao, J., and Liu, Y. (2000). Participation of syntaxin 1A in membrane trafficking involving neurite elongation and membrane expansion. Journal of neuroscience research *61*, 321-328.